

https://dspace.org/

Characterisation of Cape Town brown haze

Walton, Nicola Maria

2006-11-16T12:13:23Z
http://hdl.handle.net/10539/1810

Downloaded from a DSpace repository. https://dspace.org/

CHARACTERISATION OF CAPE TOWN BROWN HAZE

Nicola Maria Walton

School of Geography, Archaeology and Environmental Studies

University of the Witwatersrand, Johannesburg

Dissertation submitted to the Faculty of Science

for the degree of Master of Science

October 2005

Declaration

I declare that this dissertation is my own unaided work in fulfillment of the degree of Master of Science in the School of Geography, Archaeology and Environmental Studies at the University of Witwatersrand, Johannesburg. It has not been submitted previously for any degree or examination in any other university.

_____

(Nicola Walton)

_____day of_____2005

In memory of my Grandmother

Jeanette Petronella Fleming

(1925 – 2003)

ABSTRACT

The Cape Town brown haze is a brown-coloured smog that is present over the Cape Town atmosphere during the winter months due to the accumulation of gaseous and particulate pollutants. The main aim of this research was to evaluate the impact of atmospheric pollutants to visibility impairment by the brown haze through visibility modelling of major pollution sources around the City of Cape Town. The screening model, VISCREEN, the Plume Visibility model, PLUVUE II and the CALPUFF Modelling System were employed to model the visual impact of emissions from the major sources. Two point sources, Caltex Oil Refinery and Consol Glass, and three area sources, Cape Town Central Business District (CBD), Cape Town International Airport and the townships of Khayelitsha and Mitchell's Plain were identified as the major sources. An initial screening analysis indicated that emissions from the two industrial sources would be visible and would result in a yellow-brown discolouration of the atmosphere. Detailed modelling using PLUVUE II identified the area sources of Cape Town CBD and the townships to be the significant contributors to visibility impairment over Cape Town. Plume perceptibility is primarily dependant upon particulate emissions while NO_x emissions influence the colouration of the atmosphere. CALPUFF was employed to assess the distribution of NO_x, SO_2 and PM10 concentrations over the area and the associated visibility impairment on a non-haze (13 August 2003) and haze day (22 August 2003). Pollutant concentrations were considerably reduced on the non-haze day compared to the haze day. The Cape Town CBD was an important source of all the major pollutants with the townships contributing significantly to the aerosol loading over Cape Town. Pollutant concentrations are particularly elevated during the late evening and early morning periods, particularly between 7 am and 8 am. Visibility impairment is greatest on the haze day, particularly over the central Cape Town region and the townships. The greatest reduction in visibility is experienced between midnight and 9 am which corresponds with the periods of elevated atmospheric pollutant concentrations.

PREFACE

Deteriorating urban air quality is of considerable concern in many cities around the world. Primary particles, secondary particles and gaseous nitrogen dioxide are considered to be the main contributors to visibility impairment in urban areas (Latimer and Samuelsen, 1978). Elevated levels of pollutants can occur in the form of photochemical smogs or haze which can adversely affect human health, the local environment and the global climate. Smogs can form in regions where certain geographic features, such as hills and mountains, and meteorological factors, such as temperature inversions, promote the accumulation of pollutants (Kumar and Mohan, 2002).

Within South Africa, winter meteorological conditions are conducive to haze formation in cities such as Durban, Johannesburg and Cape Town as well as over the Mpumalanga industrial highveld (Tyson *et al*., 1988; Piketh *et al*., 1999). In Cape Town, the steep topography and stable conditions associated with a high-pressure system during April to September result in the accumulation of atmospheric pollution and subsequent brown haze (Jury *et al*., 1990). However, as limited studies have been undertaken, the haze phenomenon is not very well understood, requiring the need for further detailed studies in this field.

In this dissertation, the visibility impairment by the Cape Town brown haze is discussed. Modelling is undertaken to evaluate the impact that major pollution sources have on pollutant levels and visibility in the City of Cape Town. Particulate and gaseous pollutant levels and their role in visibility impairment over Cape Town's atmosphere are assessed. The meteorological conditions that promote the accumulation of pollutants and the subsequent brown haze episodes are also investigated.

This dissertation is divided into four chapters. **Chapter 1** introduces the basis of this study. A general literature review of urban air pollutants and the meteorological conditions favourable for pollution accumulation are given. The major sources in the City of Cape Town are discussed. **Chapter 2** outlines the Cape Town Brown Haze II

study and gives a description of the models and input data used in this study. **Chapter 3** presents a discussion of the modelling results. **Chapter 4** presents a summary of the findings of this research and provides conclusions to them.

This work forms part of the Cape Town Brown Haze II study funded by the South African Petroleum Industries Association (SAPIA), the City of Cape Town, Tertiary Human Resources in Industry Programme (THRIP) and the National Association for Clean Air (NACA), Western Cape Branch. The South African Weather Service provided the Aerocommander 690A aircraft for the airborne sampling. Sections of this work have been presented at local conferences including the South African Society of Atmospheric Sciences (SASAS), held in Pretoria from 13 - 14 October 2003 and in Cape Town from 24 – 25 May 2004.

I would like to thank the National Research Foundation (NRF), the University of the Witwatersrand, Deutscher Akademischer Austauschdienst (DAAD) and the Climatology Research Group (CRG) for financial support throughout the duration of this research. Thanks to Grant Ravenscroft from the Scientific Services Department of the City of Cape Town (CCT) for emissions data and ambient air quality monitoring network data. A note of appreciation to Jan De Wind at Consol Glass for his quick response in providing emissions data, Judy St Leger at Caltex Oil Refinery for Caltex emissions data and Juliet Mert from Pentech University for CMC vehicular emissions data. Thanks to Roelof Burger for Cape Town International Airport meteorological data and his continuous helpfulness and assistance in all areas. Extended thanks are given to Kristy Ross for her support and encouragement throughout my involvement in the Climatology Research Group. Wendy Job is thanked for her diagrams and Melanie Kneen for her valuable advice and assistance with the CALPUFF Modelling System and TNT Mips. This research was done under the guidance of Dr Stuart Piketh, who is thanked for the opportunities given to me and his continuous supervision and guidance throughout my duration in the Climatology Research Group and this project. A special thank you my Christopher.

CONTENTS

Declaration....ii

Dedication....iii

Abstract....iv

Preface....v

Contents....vii

Abbreviations....xi

CHAPTER 1 OVERVIEW 1

Introduction....1

Literature review....4
Components influencing air quality....4
Meteorological influences on air pollution....8
Previous haze studies....11
Cape Town Brown Haze 1 study....13
Sources of emission....15
Air quality legislation and monitoring....20
Meteorological controls on air pollution in Cape Town....23
Air pollution sources in the City of Cape Town....25

Research goals....30

CHAPTER 2 DATA AND METHODOLOGY 31

Overview of field campaign....31

Visibility Modelling....33
Plume Visual Impact Screening Model (VISCREEN)....33
Plume Visibility Model (PLUVUE II)....35
CALPUFF Lagrangian Puff Dispersion Model....39

Meteorology of study region....42

CHAPTER 3 VISIBILITY IMPAIRMENT BY THE BROWN HAZE 46

Brown haze episodes in August 2003....46

Modelling results....49
VISCREEN model output....49
PLUVUE II model output....53
CALPUFF model output....64

CHAPTER 4 SUMMARY AND CONCLUSIONS 90

REFERENCES 93

List of figures

Chapter 1

Figure 1. Source contributions to the Cape Town brown haze. 14
Figure 2. Location of ambient air quality monitoring stations in the City of Cape Town 22
Figure 3. Atmospheric stable layers over Cape Town at midnight (top) and midday (bottom) for August 2003. 24
Figure 4. Wind directions over Cape Town at midnight (top) and midday (bottom) for August 2003. 25
Figure 5. Map of Cape Town showing location of major emission sources identified for modelling. 26
Figure 6. The Consol Glass plant in Bellville showing visible white plumes emitted from the plant. 27
Figure 7. Aerial photograph of Cape Town CBD showing the N1 and N2 highways. 28
Figure 8. The townships of Khayelitsha (left) and Mitchell's Plain (right). 29

Chapter 2

Figure 9. The South African Weather Service Aerocommander 690A. 32
Figure 10. Geometry of plume and observer lines of sight used in VISCREEN. 34
Figure 11. Flow diagram of the Plume Visibility Model, PLUVUE II. 36
Figure 12. PLUVUE II output of the four visibility impairment parameters. 38
Figure 13. Surface wind roses for Goodwood on non-brown haze days (left) and brown haze days (right). 43
Figure 14. Temperature and relative humidity on 13 August (top) and 22 August (bottom). 44
Figure 15. Surface wind roses for Goodwood on 13 August (left) and 22 August (right). 45

Chapter 3

Figure 16. Synoptic conditions on 22 August 2003. 48
Figure 17. Synoptic conditions on 13 August 2003. 48
Figure 18. Plume perceptibility (ΔE) for Caltex (top) and Consol Glass (bottom). 51
Figure 19. Blue-red ratio for Caltex (top) and Consol Glass (bottom). 52
Figure 20. Visual effects calculated using PLUVUE II for all emission sources versus downwind distance for a) visual range, b) blue-red ratio, c) plume contrast and d) ΔE. 53
Figure 21. Reduction of visual range with downwind distance for all sources with reduced NO_x emissions (top) and reduced particulate matter emissions (bottom). 56

Figure 22. Change in blue-red ratio with downwind distances for all sources with reduced NO_x emissions (top) and reduced particulate matter emissions (bottom). 58
Figure 23. Change of ΔE with downwind distance for all sources with reduced NO_x emissions (top) and reduced particulate matter emissions (bottom).....59
Figure 24. SO_2 to SO_4^{2-} conversion rate with downwind distance for all emission sources. 61
Figure 25. NO_x to NO_3^- conversion rate with downwind distance for all emission sources. 63
Figure 26. Comparison of the City of Cape Town's ground-based (left) and modelled NO_x concentrations (right) for City Hall (blue) and Goodwood (purple).....65
Figure 27. Comparison of the City of Cape Town's ground-based (left) and modelled SO_2 concentrations (right) for City Hall (blue), Goodwood (purple) and Khayelitsha (yellow). 66
Figure 28. Comparison of the City of Cape Town's ground-based (left) and modelled PM10 concentrations (right) for City Hall (blue), Goodwood (purple), Khayelitsha (yellow) and Table View (green). 67
Figure 29. Spatial comparison of aircraft (left) and modelled NO_x concentrations (ppb) (right) over the Cape Town region for August 2003.....68
Figure 30. Spatial comparison of aircraft (left) and modelled SO_2 concentrations (ppb) (right) over the Cape Town region for August 2003.....69
Figure 31. Spatial comparison of aircraft (left) and modelled aerosol concentrations (right) over the Cape Town region for August 2003. 70
Figure 32. Spatial distribution of NO_x concentrations on 13 August (top) and 22 August (bottom) for the worst 1-hour, 3-hour and 24-hour averages.....71
Figure 33. Spatial distribution of SO_2 concentrations on 13 August (top) and 22 August (bottom) for the worst 1-hour, 3-hour and 24-hour averages.....72
Figure 34. Spatial distribution of PM10 concentrations on 13 August (top) and 22 August (bottom) for the worst 1-hour, 3-hour and 24-hour averages.....73
Figure 35. Nitrogen oxide concentration time series (00 – 12 hours) for 22 August 2003. 75
Figure 36. Nitrogen oxide concentration time series (12 – 24 hours) for 22 August 2003. 76
Figure 37. Sulphur dioxide concentration time series (00 – 12 hours) for 22 August 2003. 78
Figure 38. Sulphur dioxide concentration time series (12 – 24 hours) for 22 August 2003. 79
Figure 39. Aerosol concentration time series (00 – 12 hours) for 22 August 2003. 81
Figure 40. Aerosol concentration time series (12 – 24 hours) for 22 August 2003. 82
Figure 41. Visibility on 13 August (top) and 22 August (bottom) for the worst 1-hour, 3-hour and 24-hour averages. 84
Figure 42. Visibility time series (00 – 12 hours) for 22 August 2003. 85
Figure 43. Visibility time series (12 – 24 hours) for 22 August 2003. 86
Figure 44. PM10 versus SO_2 at Khayelitsha for measured (top) and modelled (bottom) concentrations. 88
Figure 45. PM10 versus NO_x at Cape Town CBD for measured (top) and modelled (bottom) concentrations. 89

List of Tables

Chapter 1

Table 1. International and local air pollution standards/guidelines. 21

Chapter 3

Table 2. The United Kingdom air pollution banding system as adopted by the City of Cape Town.....23
Table 3. Air pollution episodes identified by the City of Cape Town during the Cape Town Brown Haze II study.....47
Table 4. Summary of maximum visual effects for Caltex Oil Refinery emissions ... .49
Table 5. Summary of maximum visual effects for Consol Glass emissions.....50

ABBREVIATIONS

APPA	Air Pollution Prevention Act
CBD	Central Business District
CCT	City of Cape Town
CH_4	Methane
CO	Carbon monoxide
CO_2	Carbon dioxide
CRG	Climatology Research Group
DEAT	Department of Environmental Affairs and Tourism
ENPAT	Environmental Potential Atlas
ESP	Electrostatic Precipitator
FCC	Fluidized-bed Catalytic Cracking
FSSP	Forward Scattering Spectrometer Probe
GC	Gas Chromatography
HC	Hydrocarbons
H_2O	Water Vapour
H_2S	Hydrogen sulphide
H_2SO_4	Sulphuric acid gas
HNO_3	Nitric acid
NaOH	Sodium hydroxide
Na_2SO_4	Sodium sulphate
NH_3	Ammonia
NO	Nitrogen oxide
NO_2	Nitrogen dioxide
NO_x	Nitrogen oxides
NO_3^-	Nitrate
NH_4HSO_4	Ammonium bisulphate
$(NH_4)_2SO_4$	Ammonium sulphate
NH_4NO_3	Ammonium nitrate
N_2O_5	Nitric pentoxide
O_2	Oxygen
O_3	Ozone
OH	Hydroxyl radical
PAN	Peroxyacetyl nitrate
PM2.5	Particulate matter with an aerodynamic diameter of less than 2.5μm
PM10	Particulate matter with an aerodynamic diameter of less than 10μm
SAWS	South African Weather Service
SO_2	Sulphur dioxide
SO_4^{2-}	Sulphate
SO_x	Suphur oxides
TCC	Thermafor Catalytic Cracking
USEPA	United States Environmental Protection Agency
VOC	Volatile Organic Compounds
WHO	World Health Organisation

CHAPTER 1 OVERVIEW

Chapter one gives an overview of urban air quality in an international and local context. The components contributing to air pollution will be highlighted and the meteorological controls on air pollution in the atmosphere and specifically over Cape Town will be introduced. The major sources of air pollution in Cape Town will be identified. An outline of the research goals will be given.

Introduction

Deteriorating urban air quality within many major cities around the world has implications for climate, health and visibility. Trace gases and aerosols impact climate through their effect on the radiative balance of the earth. Trace gases such as greenhouse gases absorb and emit infrared radiation which raises the temperature of the earth's surface. Aerosol particles have a direct effect by scattering and absorbing solar radiation and an indirect effect by acting as cloud condensation nuclei. Atmospheric aerosol particles range from dust and smoke to mists, smogs and haze (IPCC, 2001). Smogs and haze are common in regions where certain geographic features, such as mountains, and weather conditions, such as temperature inversions, contribute to the trapping of air pollutants (Kumar and Mohan, 2002). The accumulation of pollutants for extended periods can induce cardiovascular and respiratory diseases, exacerbate asthma, bronchitis and emphysema and lead to increased morbidity and mortality (WHO, 2000). Smogs and haze also contribute to visibility degradation through the absorption and scattering of radiation by gases and particulates (Elsom, 1996).

In South Africa, the winter meteorological conditions are conducive to the formation of haze in urban areas such as Cape Town, Durban and Johannesburg and the industrial Highveld region of Mpumalanga (Tyson *et al*., 1988; Piketh *et al*., 1999). These winter smogs occur during cold anticyclonic conditions when surface temperature inversions prevent the vertical dispersion of pollutants. Smogs have been associated with unpleasant odours, health effects and visibility impairment (Wicking-Baird *et al*., 1997). The term 'smog' has been historically been used to describe a

combination of smoke and fog but is used here to describe a brown-coloured haze formed primarily of ozone and other secondary pollutants (Elsom, 1996).

Primary particles, secondary particles and nitrogen dioxide (NO_2) gas are considered to be the main contributors to visibility impairment (Latimer and Samuelsen, 1978). Primary particles are emitted directly by sources and their atmospheric concentrations are proportional to the quantities which are emitted. Secondary particles are formed in the atmosphere by chemical reactions of gases sometimes with existing particles. Their concentrations are dependant upon a number of factors other than the concentration of the precursor gas (Watson *et al*., 1990) such as temperature, humidity and time (Manahan, 1991). Sulphates (SO_4^{2-}) and nitrates (NO_3^-) are the most common secondary particles and result from the emissions of sulphur dioxide (SO_2) and nitrogen oxides (NO_x), respectively. In urban areas, sulphates and nitrates exist primarily as ammonium sulphates ($(NH_4)_2SO_4$) and nitrates (NH_4NO_3) since ammonium is a product of the nitrogen cycle. Sulphates tend to be smaller in size than nitrates and therefore play the major role in reducing visibility in urban areas (Elsom, 1987). The two most prevalent oxides of nitrogen are nitric oxide (NO) and nitrogen dioxide. Nitric oxide is emitted from high temperature combustion, and later partially converted to NO_2 by photochemical reactions (Derwent and Hertel, 1998). Gaseous NO_2 strongly absorbs blue light and may cause a brownish discoloration of the atmosphere (Haas and Fabrick, 1981; Latimer and Samuelsen, 1978).

Cape Town is located at 34 °S at the south-western tip of Africa. Cape Town is bordered by the Table Mountain range along the west coast, which together with its position between False Bay and Table Bay, influence air flow within the region. During winter, Cape Town experiences high pollution levels with the occurrence of a brown-coloured smog or ‘brown haze’. The brown haze is evident from April to September, due to strong temperature inversions and calm conditions that are experienced during this period. The haze extends over most of the City of Cape Town (CCT) and shifts according to the prevailing wind direction (Wicking-Baird *et al*., 1997).

The Cape Town Brown Haze I study was undertaken from July 1995 to June 1996 to determine the contribution of all major sources to the brown haze and to obtain a better understanding of the mechanism of haze formation. The study focused on PM2.5 which is known to be a major cause of visibility impairment in urban areas (Watson *et al*., 1990). The study found that vehicles, in particular diesel vehicles to be the main contributor of PM2.5 to the brown haze with wood-burning and industrial boilers also being important (Wicking-Baird *et al*., 1997). However, the study was limited as it did not adequately address aerosol characteristics of the haze, the vertical distribution of aerosols in the atmosphere or emissions from informal settlements. A more comprehensive study, the Cape Town Brown Haze II study, was undertaken in July and August 2003. Objectives of this study included identifying and quantifying the contribution of sources to the brown haze as well as characterizing the temporal, spatial, chemical and physical profiles of the brown haze. This includes an analysis of the contribution of both gases and particulates to visibility impairment over Cape Town.

Under the Clean Air Act (1990), visibility impairment is defined as "…any humanly perceptible change in visibility (visual range, contrast, colouration) from that which would have existed under natural conditions." Visibility impairment can occur either through a change in the contrast or colour of a section of the atmosphere when viewed against a background or through an alteration in the appearance of the background features. For the first case, the contrast (|C|) and the colour difference parameter (ΔE) of the plume and the viewing background are calculated. For the second case, the change in the atmospheric light extinction (Δb_{ext}) compared to the background natural conditions is calculated (FLAG, 2000). Different thresholds of perceptibility are applied to the different visibility parameters. If the plume is viewed against a background, contrast values of $\pm$ 0.01 to $\pm$ 0.05 indicate that the plume will be perceptible (NAPAP, 1990) while for a change in ΔE of less than 1 to 4, the plume will be visible. Thresholds of perceptibility for b_{ext}, where a just noticeable change occurs, correspond to a change in extinction of 2% under ideal conditions and 5% in most landscapes (NAPAP, 1990; Pitchford and Malm, 1994).

The screening model, VISCREEN (USEPA, 1992a) and the visibility model, PLUVUE II (USEPA, 1992b) can be used to model potential plume impacts on

visibility. VISCREEN and PLUVUE II calculate the change in ΔE and plume contrast, with threshold values of $\Delta E \geq 2$ and $|C| \geq 0.05$ for VISCREEN and $\Delta E \geq 1$ and $|C| \geq 0.02$ for PLUVUE II (FLAG, 2000). The CALPUFF Modelling System (CALPUFF, CALMET AND CALPOST) is suitable for deriving the long range transport of pollutants as well as for use on a case-by-case basis for near-field applications involving complex meteorological conditions. CALPUFF calculates Δb_{ext} compared to the natural background extinction. The model can also be used to model visibility impacts which will be its primary function for this study (Scire *et al*., 2000).

The aims of this study are to quantify the visibility impairment of the Cape Town brown haze through an evaluation of major source contributions, and to determine the chemical, physical, spatial and temporal profiles of both particulates and gases on brown haze and non-brown haze days through visibility modelling.

Literature review

Components influencing air quality

Nitrogen oxides and nitrates

Nitrogen oxides are produced by natural processes such as lightning and volcanic eruptions and by human activities such as fossil fuel combustion in stationary sources and motor vehicles. Nitric oxide and nitrogen dioxide are the most important oxides of nitrogen that contribute to air pollution (Elsom, 1987). Nitrogen dioxide is soluble, reddish-brown in colour and a strong oxidant (Maroni *et al*., 1995). Nitrogen dioxide is an important atmospheric gas as it absorbs visible light and contributes to visibility impairment as well as playing an important role in determining ozone (O_3) concentrations in the atmosphere (WHO, 2000).

Nitrogen oxide converts to NO_2 via a reaction with O_3. Nitrogen dioxide can then follow several pathways: 1) it can be reduced to NO in the presence of ultraviolet radiation, 2) it can change to short-lived radical species such as NO_3^- and nitric pentoxide (N_2O_5), 3) it can form organic nitrates such as peroxyacetyl nitrate (PAN)

and 4) it can oxidize to form nitric acid (HNO_3). The major pathway to form nitrates involves the gas phase reaction of NO_2 with the hydroxyl radical to produce nitric acid (Calvert *et al*., 1985). Conversion rates for NO_2 to HNO_3 occur equally significantly during the day and night (Calvert and Stockwell, 1983). Nitric acid can also be formed in aqueous phase reactions in fogs and clouds. Nitric acid dissolves in the droplet and reacts with ammonia (NH_3) to form NH_4NO_3 which is a common component of urban aerosols (Watson *et al*., 1990). These secondary formed aerosols occur in the fine fraction, PM2.5 (Monn, 2002) which has implications for human health.

In terms of visibility and health, NO_2 is the most important NO_x compound. Nitrogen dioxide results in a yellow-brown discolouration of the atmosphere at high concentrations (Latimer and Samuelsen, 1978). Nitrates, in the form of NH_4NO_3, are responsible for light extinction in urban areas (Elsom, 1987). Health effects associated with exposure to NO_2 include respiratory irritations such as coughs and sore throats and reduced lung function (Frampton *et al*., 1991). Nitrogen dioxide can be very irritating to the mucous membranes of the lung (Spengler, 1993). Due to its high solubility in water, it can react with water in the lungs to form HNO_3 and may react with lipids and proteins to form nitrite anions and hydrogen ions (Postlethwait and Bidani, 1990). Nitrogen dioxide can aggravate diseases such a bronchitis, asthma and emphysema (Elsom, 1996). The health effects of NO_2 may be greatest amongst children and asthmatics (Li *et al*., 1994).

Ozone

Ozone is a secondary pollutant, created through photochemical reactions between NO_x and hydrocarbons in the presence of sunlight. Motor vehicles are the dominant source of ozone precursor emissions although other stationary sources such as power stations and chemical plants also contribute to NO_2 levels (Elsom, 1996). The atmospheric concentrations of O_3 are related to the amount of solar insolation and the precursor concentrations. Increased solar insolation together with high concentrations of NO_2 and VOCs will promote O_3 formation. Ozone levels are at a minimum in the early morning, and will increase during the day as a result of photochemical processes, reaching a peak in the early afternoon. During the night,

ozone is scavenged by NO (Seinfeld and Pandis, 1998) so that O_3 concentrations will remain low until the next morning when sunlight begins to promote O_3 formation.

Ozone is the major constituent of photochemical smog and is known to have adverse effects on human health, vegetation, materials and visibility (Stevens, 1987). Human exposure to O_3 can cause irritations of the respiratory system, reduce lung function, worsen bronchitis, emphysema and asthma and cause inflammation of the cells lining the lungs (USEPA, 1999).

Sulphur oxides and sulphates

Sulphur dioxide is a colourless gas that is emitted from natural sources, industrial activities and combustion processes, especially from the combustion of coal and oil (Elsom, 1987). Once emitted, SO_2 can react with various oxidants in the atmosphere to form sulphate particles. Sulphate particles are predominantly composed of sulphuric acid (H_2SO_4) and its salts, ammonium sulphate ($(NH_4)_2SO_4$) and ammonium bisulphate (NH_4HSO_4) (Seinfeld and Pandis, 1998). The atmospheric conversion processes involved in the oxidation of SO_2 to sulphate influence the chemical composition and size distribution of the particulate sulphate, which in turn affect the impact of the resultant fine particles on visibility and human health. Conversion of SO_2 to particulate sulphate is one of the main contributors to both PM2.5 and PM10 concentrations, of which PM2.5 contributes to visibility degradation (Eatough *et al.*, 1994).

Sulphur dioxide can be oxidized to sulphate in the gas phase, in the liquid phase and in heterogeneous reactions (Pienaar and Helas, 1996). In the gas-phase pathway, SO_2 reacts with hydroxyl radicals (OH) in the atmosphere to form hydrogen sulphide (H_2S), which in turn reacts rapidly with oxygen (O_2) and water vapour (H_2O) to form sulphuric acid gas (H_2SO_4). In the presence of water, sulphuric acid gas forms sulphuric acid droplets. Gas-to-particle transformation rates are controlled by the presence or absence of the hydroxyl radical and other gas reactions. Since the hydroxyl radical is closely related to photochemistry, the SO_2 to sulphate transformation rate is at a maximum during the day and minimum at night (Watson *et al.*, 1990) and occurs more rapidly during summer than winter. The gas-phase

conversion process ranges from less than 1% per hour to 10% per hour at high temperatures and relative humidities (Eatough *et al*., 1994).

In the presence of water droplets (fog or clouds), SO_2 can be dissolved in the droplet where it undergoes liquid-phase reactions. The major oxidants are O_3 and hydrogen peroxide (H_2O_2) which are the secondary products formed in the gas-phase reactions. When these compounds are dissolved in the droplet, SO_2 is oxidized to sulphuric acid. When the droplet evaporates, a small, solid sulphate particle remains (Watson *et al*., 1994). The oxidation of SO_2 in water droplets is faster in the presence of NH_3, which reacts with SO_2 to produce bisulfite ion and sulfite ion in solution (Pienaar and Helas, 1991).

Sulphur dioxide can be oxidized to sulphate in heterogeneous reactions on fly ash, soot particles and oxides of metals (aluminum, iron, lead). These particles act as catalysts and grow in size by the accumulation of reaction products (Manahan, 1991).

Visibility impacts of SO_2 are associated with the conversion of SO_2 to sulphate particles which, due to their small size, contribute to visibility extinction in urban areas (Elsom, 1987), Health effects associated with SO_2 are associated with the respiratory system. Due to its aqueous solubility, SO_2 can be absorbed in the mucous membranes of the nose and upper respirator tract (Maroni *et al*., 1995). Exposure to extreme concentrations can severely reduce lung function (Islam and Ulmer, 1979).

Particulates (PM2.5 and PM10)

Particulates originate from a variety of sources that includes natural sources such as windblown dust and fires; combustion sources such as motor vehicles and industries; and the interaction of gases with other compounds to form particulate matter (Dracoulides, 2002). Particulate air pollution is a mixture of solid and/or liquid particles suspended in the air which vary in size, composition and origin. Particles can be classified by their aerodynamic properties into coarse particles, PM10 (particulate matter with an aerodynamic diameter of less than 10μm) and fine particles, PM2.5 (particulate matter with an aerodynamic diameter of less than 2.5μm) (Harrison and van Grieken, 1998). The fine particles contain the secondarily formed aerosols such as

sulphates and nitrates, combustion particles and recondensed organic and metal vapours. The coarse particles contain earth crust materials and fugitive dust from roads and industries (Fenger, 2002).

The effects of particles on visibility and health depend on the size of the particles. Fine particles (PM2.5) are the most significant influence on visibility because their size allows them to scatter or absorb light. It also allows them to remain airborne for long periods and can be transported over long distances. Coarse particles (PM10) can scatter visible light and can affect visibility when present in high concentrations. However, these particles are usually quickly deposited on the ground or washed out from the atmosphere (Ministry of the Environment, 2001). In terms of health effects, particulate air pollution is associated with complaints of the respiratory system (WHO, 2000). Particle size is important for health because it controls where in the respiratory system a given particle deposits. Fine particles are thought to be more damaging to human health than coarse particles as larger particles are less respirable in that they do not penetrate deep into the lungs compared to smaller particles (Manahan, 1991). Larger particles are deposited into the extrathoracic part of the respiratory tract while smaller particles are deposited into the smaller airways leading to the respiratory bronchioles (WHO, 2000).

Meteorological influences on air pollution

The accumulation and dispersion of pollution in the atmosphere is strongly dependant upon the state of the atmosphere. Controls of air pollution in the vertical occur in the form of absolutely stable layers and temperature inversions associated with atmospheric subsidence or surface cooling. Transport of air pollution in the horizontal is controlled largely by the wind field patterns which occur on slopes or along coastlines.

Subtropical, semi-permanent anticyclones

Over southern Africa, the general atmospheric circulation is anticyclonic throughout much of the year. These subtropical, semi-permanent anticyclones are associated with subsidence of air which produces clear, dry, stable conditions. These

conditions are conducive to the formation of absolutely stable layers in the troposphere that prevent the vertical transport of pollution. Over the interior plateau, three stable layers occur at 700 hPa, 500 hPa, 300 hPa respectively with another layer at 800 hPa between the plateau and the coast. On days when these stable layers occur, dense haze layers are evident (Tyson *et al*., 1996). Absolutely stable layers at the surface in the form of surface inversions develop due to cooling during the night. Surface inversions prevent the vertical distribution of pollutants in the atmosphere which can reduce visibility during the early morning. During the day, the stable boundary layer is eroded away by heating and a mixing layer develops which may erode away the surface inversion (Tyson *et al*., 1988). Pollutants trapped below the surface inversion are then able to rise and disperse. Over the west coast of southern Africa, surface inversions occur with a high frequency and strength due to the strong controlling influence of the South Atlantic anticyclone and the cold Benguela current (Tyson *et al*., 1977). In Cape Town, brown haze episodes are experienced when anticyclonic conditions persist. Strong temperature inversions trap the pollutants in the lower levels of the atmosphere, producing the characteristic brown haze which can result in visibility impairment in the early morning (Wicking-Baird *et al*., 1997).

Thermally-induced local winds

On slopes, differential heating and cooling of the air produces local baroclinic fields. During the day, the absorption of radiation by the slopes warms the air near the surface, initiating low-level, up-slope anabatic flow with an upper-level return flow to complete the closed circulation. During the night, the mechanism and the circulation are reversed as surface cooling produces down-slope katabatic flow and its return flow. The formation of frost hollows and the accumulation of fog and pollutants are associated with down-slope flow (Atkinson, 1981).

Within valleys, local airflow is dependant on the geometry (depth and orientation) of valleys and the time of day or night (Tyson and Preston-Whyte, 2000). In valleys whose slopes are equally heated (east-west valleys), early morning circulations are up-slope and down-slope in the evening. During the day, up-valley valley winds occur with an upper-level anti-valley wind to complete the closed circulation. During the night, down-valley mountain winds and the return anti-

mountain wind occur. In valleys at right angles to the rising and setting sun (north-south valleys), the flow patterns are similar except that a unicellular circulation is set up at sunrise and sunset. These wind fields control the transport and dispersion of low-level pollutants within valleys (Tyson *et al*., 1988).

Across shorelines, land-sea breezes form due to uneven heating and cooling of the land and sea. During the day, the land heats up faster than the sea and so a sea breeze starts to develop. The sea breeze and its return current blow in a closed circulation with convergence and ascent of air over the land and divergence and descent over the ocean. With a strengthening of the system during the day, the sea-breeze advances inland. By the late afternoon, the system has weakened along the coastline. During the night, the land cools more rapidly than the sea and so a land breeze and its return current develops (Tyson and Preston-Whyte, 2000). Land-sea breezes exert important controls on the distribution of pollution in coastal areas (Atkinson, 1981). Land-sea breezes are common along the west coast of southern Africa due to the strong temperature gradient between the cold Benguela Current and the hot desert regions (Tyson and Preston-Whyte, 2000). In Cape Town, land-breezes dominate the wind field pattern during the night by transporting pollutants seaward while during the day, weak sea-breezes trap pollutants within the Cape Town basin (Keen, 1979).

Berg winds

Berg winds are common along the coastal regions and are responsible for abrupt changes in temperature, humidity and wind speed (Atkinson, 1981). They are associated with large-scale, pre-frontal divergence and warming of subsiding air with an offshore component. Berg winds are common in late winter and early spring and are most frequent on the west coast. These winds may blow for only a few hours or for extended periods of a few days (Tyson and Preston-Whyte, 2000). In Cape Town, berg winds occur when a high-pressure system over Kwazulu-Natal is associated with a high-pressure system over the Western Cape with an approaching cold front. Brown haze episodes can be associated with warm north-easterly berg winds as they reduce dew point temperatures during the night (Jury *et al*., 1990).

Cold fronts

Cold fronts occur together with westerly waves, depressions or cut-off lows. Cold fronts occur most frequently in winter and bring cool weather due to airflow from the south and south-west. Ahead of the front, northerly airflow is associated with divergence and subsidence that brings stable, clear conditions. Behind the front, southerly airflow, associated with low-level convergence causes cool conditions and rain (Tyson and Preston-Whyte, 2000). With the passage of a cold front, wind direction changes from north-west to west and south-west. Most winter rain in the South-Western Cape is associated with north-westerly, pre-frontal winds (Jackson and Tyson, 1971). These north-westerly winds and rain will cleanse the atmosphere of any accumulated pollutants (Jury *et al*., 1990).

Previous haze studies

Urban haze studies have been conducted in the United States, China, Japan, Mexico, London and Hong Kong, since the late 1970's. The urban haze experienced in Los Angeles in the United States of America and Mexico City in Mexico will be discussed. Los Angeles is a coastal site in the western United States and experiences humid conditions characteristic of a coastal environment. Los Angeles experiences air pollution in the form of photochemical smog during the summer season. Mexico City is an urban area within a developing country and experiences winter smogs under similar meteorological conditions to South Africa. Within South Africa, the Cape Town Brown Haze I study undertaken in 1996 will discussed.

Los Angeles haze

Photochemical smog was first identified in Los Angeles in the late 1940's. Los Angeles is situated along the Pacific coastline in the state of California and is characterised by a mild, sunny, semi-arid, Mediterranean coastal climate. Airflow into the Los Angeles basin is predominantly from the west which transports relatively clean, unpolluted air from the Pacific Ocean. The air flows into a large basin which is surrounded by mountains that prevent transport to the east. Stable air conditions with low level inversions, together with the blocking effect of the mountains, prevents the

dispersion of pollutants and promotes the subsequent formation of the well known Los Angeles smog (Elsom, 1996). The haze can appear yellow-brown in colour, although at times it is also distinctly white or grey coloured (Husar and White, 1976). These pollution episodes can last for up to four days and are common during the late summer and early autumn period (Hidy *et al*., 1978).

Studies undertaken in the Los Angeles basin (Hidy and Friedlander, 1971; Miller *et al*., 1972; Heisler *et al*., 1973; Hidy *et al*., 1974; Gartrell and Friedlander, 1975) have identified the chemical composition of atmospheric aerosols to consist predominantly of sulphates, nitrates and organic compounds. These secondary-generated aerosols are the most important visibility-reducing species in the basin. Sulphates in particular were show to be much more effective light scatters per unit mass than any other particulate compound and may be responsible for over half of the light scattering in downtown Los Angeles (Hidy *et al*., 1974; White and Roberts, 1977). Origins of the precursors of these pollutants are petrol sources from motor vehicles as well as fuel and crude oil sources from power plants, industries, oil refining and mobile sources such as ships, trains, airplanes and diesel vehicles (White and Roberts, 1977).

Mexico City haze

Mexico City is one the world's largest metropolitan areas. The basin of Mexico City has an area of approximately 1300 km^2 and is surrounded by mountains to the south, east and west. Over 20% of Mexico's population is located within Mexico City while the industrial area comprises more than 30% of the whole national industry and is located in the northern parts of the city (Edgerton *et al*., 1999). A combination of numerous emission sources, topography and subtropical climate result in very poor air quality within the city (Elsom, 1996). During the cold season (December to February), low temperatures cause frequent temperature inversions that trap pollutants in the basin. Intense periods of sunshine, together with calm conditions, promote the formation of photochemical smog in the area. Despite efforts to reduce emissions, a persistent haze blankets the city, especially during winter (Vega *et al*., 2002).

Aerosols that contribute to this visibility degradation are a combination of primary and secondary aerosols (Edgerton *et al*., 1997). Mexico City experiences very high O_3 and particulate levels as well as elevated SO_2, NO_x, and CO concentrations. Emissions in Mexico are dominated by mobile sources contributing approximately 80% of PM2.5 and NO_x, 45% of VOCs and 30% of SO_2 emissions in 2000. Area sources, particularly the use of solvents and Liquid Petroleum Gas, are significant sources of VOCs while point sources, such as the chemical, textile and paper industries, contribute 70% of SO_2 emissions (McKinley *et al*., 2005). Efforts to reduce emissions have included the introduction of unleaded fuel, the use of catalytic converters after 1990 and many old diesel vehicles have been replaced. Despite these controls, particulate concentrations remain high and hourly PM10 concentrations often exceed 500 $\mu g/m^3$ (Vega *et al*., 2002). Edgerton *et al* (1997) characterised particulate matter concentrations in Mexico City during winter. They observed that secondary ammonium nitrate and ammonium sulphate constituted about 10 – 20% of the PM10 and 15 -30% of the PM2.5. Carbon-containing aerosols accounted for 20 – 35% of the PM10 and 25 – 50% of the PM2.5. Geological material was the major contributor to PM10 (40 – 55%) concentrations (Edgerton *et al*., 1997).

Cape Town Brown Haze 1 study

In the 1950s and 1960s, Cape Town experienced the presence of a thick smog caused by three power stations in the area, coal-burning locomotives and tugs, industrial incinerators and heavy fuel burning appliances. In 1968, steps were taken by the City Council to reduce air pollution which was successfully achieved by the late 1970s through the termination of the use of coal-burning locomotives and tugs, the closure of two of the power stations and the enforcement of standards for fuel burning appliances. However, a brown-coloured smog or 'brown haze' began to emerge as a major pollution problem, particularly during the winter months (Wicking-Baird *et al*., 1997).

In order to obtain a better understanding of the brown haze, a pilot study was conducted by the Energy Research Institute in 1992. The ground-based study concluded that Cape Town does have a serious air pollution problem comparable to other heavily polluted international cities and that the air quality was likely to

deteriorate. It was recommended that a second study be undertaken to determine the major contribution of all major sources to the brown haze, and to obtain a better understanding of the mechanism of haze formation. The Brown Haze I study focused on a source apportionment of PM2.5 using the Chemical Mass Balance Model. The brown haze was sampled from July 1995 to June 1996 at City Hall, Goodwood, Table View and Wynberg (Wicking-Baird *et al.*, 1997).

The study found that vehicles, most notably diesel vehicles, are the principal source of Cape Town's brown haze, which cause over half (65%) of the brown haze experienced. Industries, in particular low-level emitting industries, are the next most significant cause (22%) of the brown haze followed by the use of wood (11%) by a large sector of the population. Natural sources such as wind-blown dust and sea salt contribute very little (2%) towards the brown haze (Wicking-Baird *et al.*, 1997) (Figure 1).

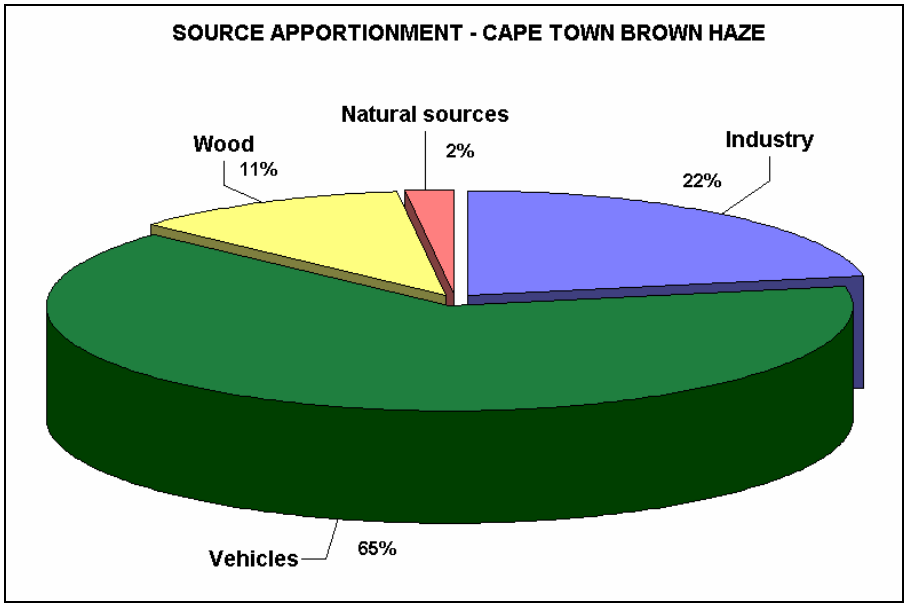

Figure 1. Source contributions to the Cape Town brown haze (Wicking-Baird *et al.*, 1997).

Sources of emission

Atmospheric emissions released within the CCT originate from a variety of combustion and non-combustion sources. Combustion-related sources include transportation, industrial activities, fuel-burning appliances, domestic fuel burning, wild fires and tyre burning. Emissions from non-combustion sources include fugitive emissions from wind erosion and agriculture, evaporative losses and landfill operations and waste water treatment (Scorgie, 2003). Of these sources, transportation-related emissions from vehicles and aircraft, industrial-related emissions from petroleum refining and glass manufacturing processes and emissions from the domestic burning of wood and paraffin in the townships and informal settlements will be discussed due to their significant contribution to air pollution in the CCT. Sources that have not been included in this study are recognized to contribute to air pollution in Cape Town and their omission from this modelling study is expected to influence the distribution and levels of pollutant concentrations that can potentially be experienced in Cape Town.

Transportation

One of the major contributors to urban air pollution is vehicular emissions. Atmospheric pollutants emitted from motor vehicles include hydrocarbons, CO, NO_x, SO_2 and particulates. Hydrocarbon emissions, such as benzene, result from the incomplete combustion of fuel molecules in the engine. Carbon monoxide is a product of incomplete combustion and occurs when carbon in the fuel is only partially oxidized to carbon dioxide. Nitrogen oxides are formed by the reaction of nitrogen and oxygen under high pressure and temperature conditions in the engine. Sulphur dioxide is emitted due to the high sulphur content of the fuel. Particulates such as lead originate from the combustion process as well as from brake and clutch linings wear. With the introduction of unleaded fuel, lead emissions have been reduced. However, compared to petrol-fuelled vehicles, diesel engines are a significant source of particulate emissions. Vehicle emission rates are affected by specific vehicle-related factors such as vehicle class, model, fuel-delivery system, vehicle speed and maintenance history; fuel-related factors such as fuel type, oxygen, sulphur, benzene

and lead content and environmental factors such as altitude, humidity and temperature (Samaras and Sorensen, 1999).

Airports are important generators of air pollution due to airport operations, vehicle traffic, on-site fuel storage facilities and aircraft maintenance and operation (Dracoulides, 2002). On a local level, commercial aircraft are a significant contributor to urban air pollution. Airports produce large amounts of air pollution, emitted from aircraft activity, ground service equipment, vehicular activity (motor vehicles, taxis and buses), fueling facilities and other stationary sources such as airport power sources. Aircraft engines produce CO_2, H_2O, NO_x, CO, SO_x, VOCs, particulates and other trace elements. About 10% of all aircraft emissions, except hydrocarbons and CO, are produced during ground level activities and during landing and takeoff. The majority of aviation emissions (90%) occur at higher altitudes (FAA, 2005).

Petroleum Refining

Petroleum refineries convert crude oil, coal, or natural gases into fuels such as petrol, diesel, paraffin and kerosene. Oil refineries perform three refinery processes: separation, conversion and treatment. The first phase is the separation of crude oil into its major components in distillation towers through atmospheric distillation, vacuum distillation and light ends recovery (gas processing) (USEPA, 1995). Within the towers, liquids and vapours are separated into components according to weight and boiling point. The lightest fractions (gasoline and liquid petroleum gas) vapourise and rise to the top, where they condense back to liquids. Medium weight liquids (kerosene and diesel oil distillates) remain in the middle while the heavier liquids or gas oils separate lower down. The heaviest fractions, called residuum, settle at the bottom of the tower (Caltex, 2003). Emissions released during this first process are from the steam ejectors or vacuum pumps associated with the vacuum distillation column as well as from the combustion products from the process heater (furnace). Fugitive hydrocarbon emissions are also released from leaking seals and fittings of the vacuum distillation column (USEPA, 1995).

The second phase is the conversion of large petroleum molecules into smaller ones. The most common method is cracking which uses heat and pressure to ‘crack’

heavy hydrocarbon molecules into lighter ones. Catalytic cracking processes can be classified as either fluidized-bed (FCC) or moving-bed units characterised by Thermafor Catalytic Cracking Units (TCC). Emissions from catalytic cracking processes are due to combustion from process heaters and in the flue gas from catalyst regeneration. Hydrocarbons, SO_x, NH_3, aldehydes, NO_x, cyanides, CO and particulates are emitted from the catalyst regenerator. FCC particulate emissions can be controlled by using cyclones and ESP which have collection efficiencies of 80 - 85%. Carbon monoxide waste heat boilers are used to reduce CO and hydrocarbon emissions from FCC units. Particulate emissions from a TCC unit are controlled by high-efficiency cyclones while CO and hydrocarbon emissions are reduced by passing the flue gas through a process heater firebox or smoke plume burner. Sulphur oxides can be removed by passing the regenerator flue gases through a water or caustic scrubber (USEPA, 1995). Other methods of thermal cracking include visbreaking and coking which use heat and pressure to convert residiuum into lighter products (Caltex, 2003). Emissions include coke dust from coking operations, combustion gases from the visbreaking and coking process heaters and fugitive emissions. Particulates are emitted when the coke is removed from the coke drum while hydrocarbon emissions occur during the cooling and venting of the coke drum before coke removal. Particulate emissions are controlled by wetting down the coke during the decoking operation (USEPA, 1995).

The final phase involves the treatment of petroleum products which stabilize and upgrade the fuel by removing impurities such as sulphur, nitrogen and oxygen through hydrodesulphurization, hydrotreating, chemical sweetening and acid gas removal processes. Hydrocarbon emissions are released during the sweetening process (USEPA, 1995).

Atmospheric emissions are also released from other sources within the refinery. Sulphur emissions are released from sulphur recovery plants which convert H_2S into elemental sulphur. The most common conversion method is the Claus method which has a sulphur recovery efficiency of 90 - 95%. Sulphur emissions released from the Claus process can be reduced by adding a scrubber at the tail end of the plant or incinerating the sulphur-containing tailgases to form SO_2. Process heaters are used in refineries to supply the heat necessary to raise the temperature of the feed materials to

reaction or distillation level. Hydrocarbons, NO_2, SO_2, PM, CO and CO_2 are released from process heaters. Sulphur oxides can be controlled by flue gas desulphurization or flue gas treatment. Flue gas desulphurization methods include limestone scrubbers, sodium scrubbers and dual alkali scrubbers which have a sulphur removal efficiency of over 95% (USEPA, 1995).

Glass manufacturing

The raw materials needed for glass manufacturing include silica sand, soda ash and limestone. The raw materials are crushed and stored in silos from which they are transferred through a gravity feed system and automatically weighed out from computerized control rooms before being transported to batch mixers. The material is mixed with cullet (recycled glass) and the batch is transported to a batch storage bin at the furnace. The batch is then continuously fed into the melting furnace through the feeder where it is converted to molten glass and maintained at temperatures greater than 1500°C. The molten glass flows through a submerged throat leading to the refiner and cooled to about 1200ºC. After refining, the molten glass is transported to the bottle-making machines through forehearths and the bottle goes to be shaped by blowing. The bottle is coated with a thin layer of tin oxide to strengthen it before entering the annealing oven where it is slowly cooled (Consol Glass, 2004).

The main pollutants released during the manufacturing process are particulates, SO_x and NO_x. The main pollutant emitted by the batch plant is particulate dust. The melting furnace is responsible for 99% of the total emissions of both particulates and gases. Particulate emissions result from the volatilization of materials in the melt that combine with gases and for particulate condensates. Other sources of particulate emissions are from a) the ash in fuel which generates 150 kg of fly-ash per day, contributing to about 70 mg/m^{-3} in exhaust, b) the evaporation of soda from the glass surface in the presence of moisture (as NaOH) which combines with SO_3 from fuel to form sodium sulphate (Na_2SO_4). This condenses to form fine dust below 880 °C and contributes to about 100 mg/m^{-3} in exhaust and c) batch carry over of some fine raw materials which contributes to about 5 mg/m^{-3} in exhaust (J. de Wind, personal communication, 2004). These particulate emissions can be controlled by primary means such as reducing the fly ash content and sulphur content of the fuel, converting

to gas firing and minimizing batch carry over by presintering, briquetting, palletizing or liquid alkali treatment. Secondary means include the installation of an ESP and bag filters which have an efficiency of up to 99% in the collection of particulates (USEPA, 1995).

In the melting furnance, SO_x emissions result from the decomposition of the sulphates in the batch and fuel sulphur content. Emissions from the forming and finishing phases occur as a visible dense white cloud that can have over 40% opacity. These emissions are generated by flash vapourization of hydrocarbon greases and oils (USEPA, 1995). Primary means to reduce SO_x emissions include a reduction in the sulphur content of the fuel as well as minimizing the sulphate in batch composition. Secondary means include hydrated lime or soda ash scrubbing followed by the use of an ESP and bag filters (J. de Wind, personal communication, 2004).

Nitrogen oxides form in the melting furnace when nitrogen and oxygen react at high temperatures. Also, higher specific melting rates require higher operating temperatures which result in higher NO_x emissions. Methods to reduce NO_x emissions include a) an increase in electrostatic boosting to reduce the operating temperature, b) an increase in the use of cullet c) special burner design, d) staged or delayed combustion, e) reduction of excess air/excess gas injection, f) ammonia injection, g) oxy-fuel combustion and h) cold top electric melting of glass (J. de Wind, personal communication, 2004).

Domestic fuel burning

Within townships and informal settlements, lack of basic services such as electricity and waste removal, require the use of wood, coal and paraffin for cooking and heating purposes (CCT, 2002). Pollutants released from these fuels include CO, NO_2, SO_2, particulates and polycyclic aromatic hydrocarbons. CO is produced by the incomplete combustion of fuel. Nitrogen dioxide is formed from the combination of nitrogen and oxygen during combustion at high temperatures (Maroni *et al*., 1995). SO_2 is produced by the oxidation of sulphur impurities during the burning of coal and other sulphur containing fuels (Burr, 1997). Particulates are the dominant source of emissions from the burning of wood. Smoke from wood burning contains respirable

particles that are small enough in diameter to enter and deposit in the lungs. These particles are comprised of a mix of inorganic and organic substances including aromatic hydrocarbon compounds, trace metals, nitrates and sulphates. Polycyclic aromatic hydrocarbons are produced as a result of incomplete combustion and are potentially carcinogenic in woodsmoke (Maroni *et al*., 1995). The burning of these fuels occurs on a much larger scale during winter when the need for space heating increases. Under inversion conditions these pollutants will accumulate in the area, forming a 'blanket' of air pollution that is often visible over the townships in the early morning.

Air quality legislation and monitoring

To protect the public and environment from the adverse effects of air pollution, ambient air quality guidelines/standards are established. Guidelines provide a basis for protecting the public from the adverse effects of air pollution and aim to eliminate or reduce air pollutants that are or will be hazardous to human health and well being (Van Niekerk, 2001). An ambient standard is a description of a level of air quality that is adopted by a regulatory authority as enforceable (WHO, 2000) to protect people and the environment from harm.

The World Health Organization (WHO) and the United States Environmental Protection Agency (USEPA) are two of the main international organizations for publishing air quality guidelines/standards. Table 1 shows the guidelines/standards that have been proposed by the USEPA and WHO as well as the South African guidelines established by the Department of Environmental Affairs and Tourism (DEAT) and the United Kingdom standards which have been adopted by the CCT. Currently, South Africa lacks any legally binding air pollution regulations, only having non-binding guidelines that are applied in the discretion of the Chief Air Pollution Control Officer. Sulphur dioxide is the only pollutant for which an ambient standard has been set in South Africa with other pollutants remaining at the basic guideline levels (Country Analysis Briefs, 2002). South Africa's guidelines are currently under review as South Africa has recently replaced the outdated Atmospheric Pollution Prevention Act (APPA) with the National Air Quality Management Act.

Table 1. International and local air pollution standards/guidelines (ppb) (USEPA, 2005; WHO, 2000; CCT, 2005; Scorgie, 2003).

Pollutant	Averaging Time	EPA Standard	WHO Guidelines	DEAT Guidelines	UK Limits
NO_2	1 year	53	20	50	21
	1 month			80	
	24 hours			100	
	1 hour	128	100	200	105
SO_2	1 year	30	20	19	8
	1 month			50	
	24 hours	140	40	48	47
	1 hour			300	132
O_3	8 hours	80			50
	1 hour		60	120	
PM2.5 ($\mu g/m^3$)	1 year	15	Dose-response		
	24 hours	65			
PM10 ($\mu g/m^3$)	1 year	50	Dose-response	60	40
	24 hours	150		180	50

Monitoring of air quality in Cape Town began in 1958 with the monitoring SO_2 and smoke. With the introduction of the APPA in 1965, the Cape Town local authority was able to make provision for the control of smoke, dust and vehicle emissions although this was limited to the control of diesel vehicles. In 2001, the CCT undertook to update and promulgate its own Air Pollution Control By-Law to control air pollution in the CCT area. The By-Law, which came into effect in 2003, declares the entire municipal area as an air pollution control zone, reduces the permissible smoke emission from industries, controls smoke from all diesel-driven vehicles, controls smoke from residential premises and adds a nuisance section to control air pollution related nuisances (Linde and Ravenscroft, 2002). Cape Town is the first local authority to promulgate its own By-Law on air pollution.

Cape Town has an established air quality monitoring network at 10 sites around the CCT (Figure 2). These instruments measure the concentration of ambient air pollutants in 20 second scans which can either be expressed over 10-minute, 1-hour, 24-hour, monthly or annual averaging periods. Pollutants measured at these sites include SO_2, NO_x, O_3, CO, H_2S, PM10 and PM2.5. The CCT also has 2 mobile monitoring stations to determine 'hotspots' within the area (Linde and Ravenscroft, 2002).

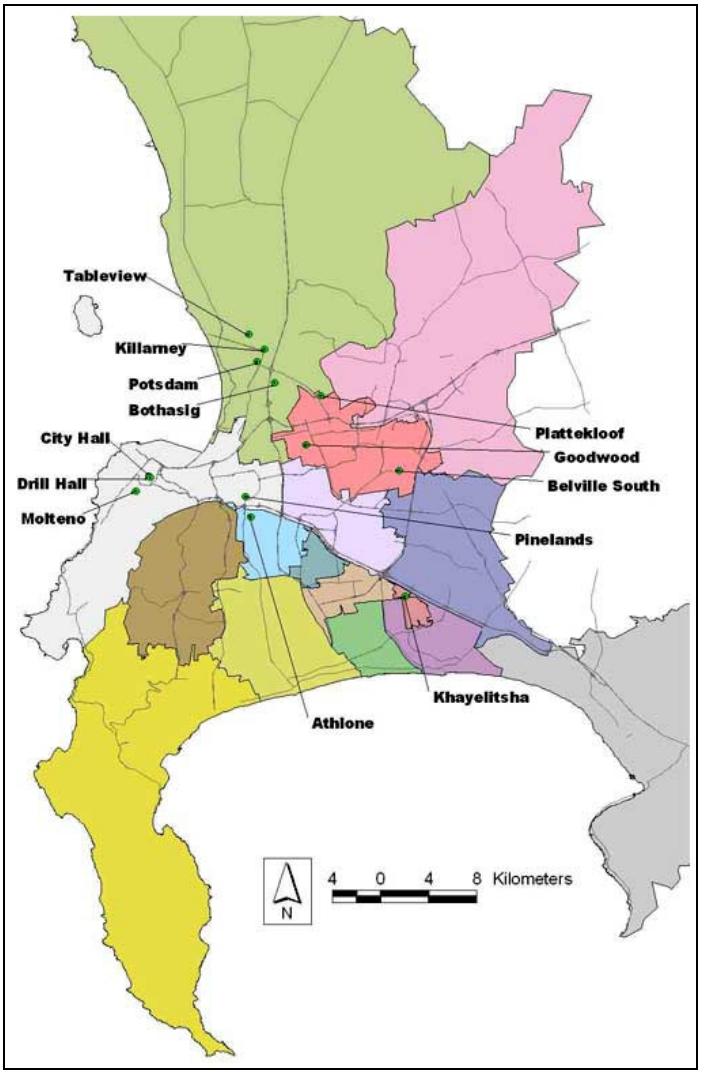

Figure 2. Location of ambient air quality monitoring stations in the City of Cape Town *(www.capetown.gov.za).*

In 1998 the Cape Metropolitan Council implemented the guidelines and air quality banding system as adopted by the Department of the Environment, Transport and the Regions in the United Kingdom (CCT, 2005). This system classifies air quality into four banding levels for NO_2, SO_2, O_3, PM10 and CO (Stedman *et al*., 1998) (Table 2).

Table 2. The United Kingdom air pollution banding system as adopted by the City of Cape Town (ppb).

Pollutant	Low	Moderate	High	Very High
SO_2	<100	100 - 199	200 – 399	> 400
O_3	< 50	50 – 89	90 – 179	> 180
CO	< 10	10 – 14	15 – 19	> 20
NO_2	< 150	150 - 299	300 - 399	> 400
$PM10_{(\mu g/m^3)}$	< 50	50 - 74	75 - 99	> 100

Low pollution levels are associated with effects which are unlikely to be noticed even by individuals who know they are sensitive to air pollutants. Moderate pollution levels are associated with mild effects that are unlikely to require action, but may be noticed amongst sensitive individuals. High pollution levels are associated with significant effects which will be noticed by sensitive individuals. Action to avoid or reduce these effects may be needed. Very high pollution levels will exacerbate the effects experienced by individuals susceptible to high pollution levels (Stedman *et al*., 1998).

Meteorological controls on air pollution in Cape Town

In Cape Town, previous studies undertaken (Keen, 1979; Redding *et al*., 1982; Jury, 1987) have identified meteorological conditions such as sea-breezes, urban heat islands and topographically induced flows during summer to be important controls on air pollution dispersion. In autumn, sea breezes advect cool air from the cold Benguela Current over Cape Town (Jury and Spencer-Smith, 1988; Comrie, 1988). In winter, the passage of cold fronts over the region brings north-westerly winds and rain which has a cleansing effect on the atmosphere. Between periods of rain, cold anticyclones ridge eastward over Cape Town and bring stable conditions that promote the accumulation of pollutants (Jury *et al*., 1990). Brown haze episodes are often associated with berg winds and strong temperature inversions (Wicking-Baird *et al*., 1997).

During the Cape Town Brown Haze II project in August 2003, stable layers can be identified over Cape Town from an analysis of vertical radiosonde soundings from Cape Town International Airport. Absolute stability occurs when the environmental lapse rate is smaller than or equal to the saturated lapse rate (Tyson and Preston-Whyte, 2000). The stable layer that is evident between 900 hPa and 750 hPa is perhaps the most important layer as it is the layer responsible for preventing the vertical dispersion of pollution. Due to night time cooling, surface inversions are also evident in the lower atmosphere over Cape Town. Clear skies, low relative humidity and low wind speeds associated with anticyclones promote the formation of these nocturnal inversions. These inversions reach their maximum depth before sunrise and break down after sunrise due to convective mixing of surface air (Tyson *et al*., 1977). By noon, surface heating has eroded away the surface inversions and a high degree of instability occurs from 1000 hPa to 900 hPa (Piketh *et al*., 2004) (Figure 3).

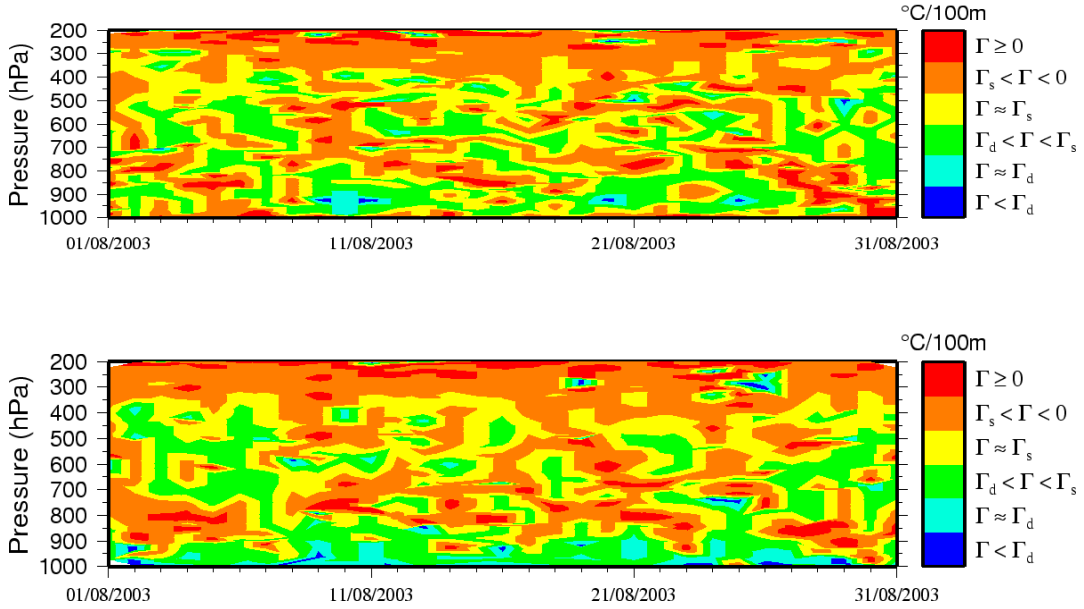

Figure 3. Atmospheric stable layers over Cape Town at midnight (top) and midday (bottom) for August 2003. Stability is classified in terms of the atmospheric lapse rates. Absolute stability is represented by orange and red on the colour scale.

The local wind field in Cape Town also exerts a dominant control on pollution dispersion. Between the surface (1000 hPa) and 700 hPa, the wind direction is variable with distinct changes from a northerly and north westerly flow to a south westerly flow (Figure 4). This change in wind pattern can be attributed to the passing

of a cold front over the region. Westerly flow is observed in the upper levels as noted by Jury *et al* (1990). At the surface, airflow with a north easterly component, similar to that under berg wind conditions, is also evident (Piketh *et al*., 2004). Berg winds lower the dewpoint and bring about cooling at the surface (Jury *et al*., 1990) which promotes brown haze episodes.

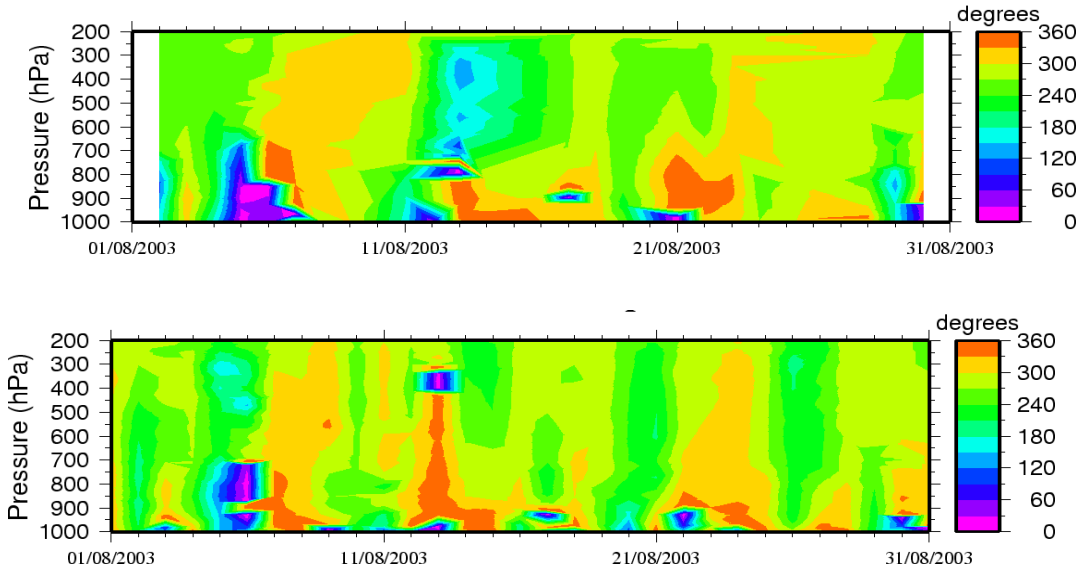

Figure 4. Wind directions over Cape Town at midnight (top) and midday (bottom) for August 2003.

Air pollution sources in the City of Cape Town

Air pollution sources contributing to visibility degradation within the CCT were identified and modelled. Identified sources of emissions within the CCT include transportation (vehicles, aircraft and shipping), domestic fuel burning of wood and paraffin and industrial activities (petroleum refining, glass manufacturing). Two industrial sources, Caltex Oil Refinery in Table View and Consol Glass in Bellville and three area sources, Cape Town Central Business District (CBD), the townships of Khayelitsha and Mitchell's Plain and Cape Town International Airport, were selected for modelling (Figure 5). This modelling is limited to the above mentioned sources, although it is recognised that emissions from other sources such as smaller industrial sources, landfill sites and agriculture will influence the local air quality.

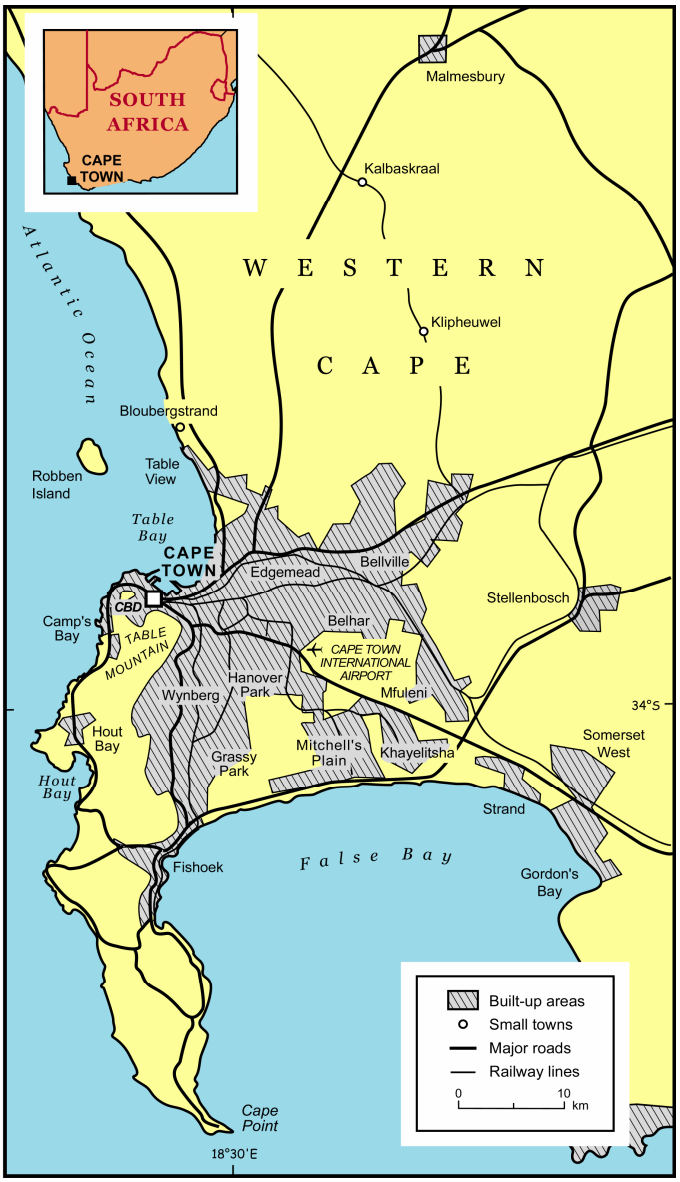

Figure 5. Map of Cape Town showing location of major emission sources identified for modelling.

The Caltex Oil Refinery has previously been identified as an important emission source (Wicking-Baird *et al.*, 1997; Jury *et al.*, 1990) of SO_2. The Caltex Oil Refinery (33.85°S; 18.53°E) is situated in Table View, 10 km to the NNE of Cape Town (Jury *et al.*, 1990). The Caltex Oil Refinery uses coal to produce a range of fuels as well as sulphur, gas and paving asphalt. Consol Glass in Bellville South (33.93°S; 18.65°E) is situated in a major industrial area within the region and was identified based on the visible white plumes released during the forming and finishing processes (Figure 6). Consol Glass is the largest glass container manufacturer in South Africa. The factory

in Bellville has four furnaces of ten lines, with a production capacity of 800 tons per day. Consol Glass has recently commissioned an Electrostatic Precipitator plant to reduce emissions from the four melting furnaces (J. de Wind, personal communication, 2004).



Figure 6. The Consol Glass plant in Bellville showing visible white plumes emitted from the plant.

The three area sources, Cape Town CBD, the townships of Khayelitsha and Mitchell's Plain and Cape Town International Airport were also modelled. The Cape Town CBD is the dominant area of business, legal and governmental activity within the Cape region (Dewar, 2004). It is also the main transport centre in the city, with approximately 240 000 commuters arriving daily into the area (Dewar, 2004). In Cape Town, an increase in urban areas and expansion of the previously urbanized areas has resulted in a larger number of people in the area and therefore a higher number of potential users of public (taxis, rail and buses) and especially, private transport. In 2002, there were 825 000 registered vehicles in all classes in the Cape Metropolitan Area of which 570 000 are motor vehicles, a 50% increase in 25 years. Cape Town CBD experiences huge volumes of traffic entering and leaving the area, resulting in congestion particularly during the peak periods (CCT, 2002). Commuters enter the CBD on two main highways, the N1 and N2 to the south and south-east (Figure 7). Approximately 60% of all traffic flow from around the Cape Metropolitan Area is

into the CBD (J. Mert, personal communication, 2004). Other activities such as shipping and industry were not accounted for in the CBD.



Figure 7. Aerial photograph of Cape Town CBD showing the N1 and N2 highways.

Insufficient housing as a result of rapid urbanization within Cape Town has resulted in the formation of 71 informal settlements in the region. These areas are often characterised by poverty, extreme density and lack of basic services such as electricity and waste removal (Muzondo *et al*., 2004). The major townships of Khayelitsha and Mitchell's Plain still use wood for space heating and cooking purposes which release significant amounts of particulates, especially during the winter months. Khayelitsha and Mitchell's Plain are located on the Cape Flats, to the south-east of Cape Town (Figure 8). Khayelitsha, meaning 'Our Home' was formed in 1983 (Muzondo *et al*., 2004) and has an estimated population of over 400 000 people. Khayelitsha is characterised by high levels of unemployment, a shortage of housing and infrastructure and low income levels (Dyantyi and Frater, 1998).

Mitchell's Plain was founded in 1947 and has an estimated population of 300 000 people. Mitchell's Plain is predominantly developed with formal housing and a small informal component in Tafelsig (DPLG, 2004).



Figure 8. The townships of Khayelitsha (left) and Mitchell's Plain (right).

Cape Town International Airport (33.96°S; 18.60°E) is South Africa's second largest airport, covering an area of approximately 700 ha (ACSA, 2004). There has been a significant increase in international and domestic flights to and from Cape Town International Airport since 2001/2. The airport is capable of accommodating up to one million passengers a year (CCT, 2002).

Dracoulides (2002) modelled annual emissions of CO, HC, SO_2, NO_x and PM10 from Cape Town International Airport. Modelled emissions in 2002 were estimated at 1791 tons of CO, 210 tons of HC, 634 tons of NO_x, 44 tons of SO_2 and 3 tons of PM10 from both ground based sources and aircraft activity. Aircraft operations accounted for the highest percentage of NO_x and SO_2 emissions. Projected emissions for 2015 show an increase to 3332 tons of CO, 410 tons of HC, 848 tons of NO_x, 66 tons of SO_2 and 7 tons of PM10. Aircraft activity is again a significant contributor to NO_x emissions (Dracoulides, 2002).

Research goals

The aim of this research is to determine the influence of atmospheric pollutants to visibility impairment by the brown haze through visibility modelling of known pollution sources around the City of Cape Town using the visibility models, VISCREEN, PLUVUE II and the CALPUFF Modelling System.

The main objectives are as follows:

- Evaluate the impact that major point and area sources in Cape Town have on pollutant levels and visibility impairment.
- Identify the influence of particulates and NO_x on plume visibility and relative colouration of the brown haze.
- Evaluate the relative contribution of primary and secondary particles to the development of the brown haze.
- Investigate the meteorological conditions that are necessary for the accumulation of pollutants in the atmosphere and subsequent brown haze formation.

****

Urban air quality, and the pollutants and meteorology contributing to its degradation have been discussed. Sources of air pollution and those specific to the City of Cape Town have been highlighted and the research goals outlined. Data and methodology will be discussed in Chapter 2.

CHAPTER 2 DATA AND METHODOLOGY

Chapter 2 gives an overview of the Cape Town Brown Haze II study. The models used in this research and the input data are described. The meteorology of the study region is discussed.

Overview of field campaign

The unattractive brown haze that is present over Cape Town during the winter months was the focus of the Cape Town Brown Haze II study which was carried out over a period of five weeks from 22 July to 28 August 2003. The study was undertaken by the Climatology Research Group (CRG) from the University of the Witwatersrand, in collaboration with the CCT and the South African Weather Service (SAWS). The study employed both ground-based and airborne measurements through the use of a fully equipped research aircraft (Aerocommander 690A) (Figure 9). Particulates were measured with two Condensation Nuclei counters, a Passive Capacity Aerosol Spectrometer Probe (PCASP-100), a Forward Scattering Spectrometer Probe (FSSP-100) and an airborne streaker sampler. Trace gases measured included NO, NO_2, SO_2, O_3, CO and CO_2 respectively. Volatile Organic Compounds (VOCs) and methane (CH_4) canister samples were also taken, to be later analysed by Gas Chromatography on the ground. Ground-based measurements included a network of 18 haze meters around the CCT and a CIMEL sun photometer to measure aerosol loading of the atmosphere. A 10 m meteorological station was set up at Goodwood to measure wind speed and direction, solar radiation, temperature, relative humidity, pressure and precipitation at three levels; 5 m, 8 m and 10 m.



Figure 9. The South African Weather Service Aerocommander 690A.

The aircraft was based at a local landing strip in Malmesbury, north of Cape Town. Every morning, synoptic charts obtained from the South African Weather Service were consulted to determine whether brown haze conditions would occur before a flight plan was drawn up. A total of 17 flights were conducted over the study period, with about 22 hours of flight time.

Flights were undertaken predominantly during brown haze episodes when conditions were clear and sunny, often after the passage of a cold front. Background samples were taken on non-haze days for comparison with the haze days. Flight duration was on average 1 – 2 hours, although in some instances it was extended to three hours under good brown haze conditions. Flights were undertaken early in the morning during the peak traffic, when the brown haze starts to form, and in the afternoon to investigate the temporal transformation of the haze. Flights were also done on week days and on weekends to investigate the influence of vehicles on the haze. Vertical and horizontal profiles of the brown haze over Cape Town were undertaken to determine the spatial extent of the haze.

Visibility Modelling

Plume Visual Impact Screening Model (VISCREEN)

Overview of the model

An initial screening analysis was undertaken to evaluate the potential emissions impact on visibility. The USEPA VISCREEN model was used to assess the impact that plumes from two major point sources, Consol Glass and Caltex, have on visibility over the Cape Town region.

VISCREEN is a conservative screening model used to determine the visual impact parameters for a plume from a single source at a given receptor point. The model calculates three main parameters: the colour difference parameter (ΔE) between the plume and the background, plume contrast at three wavelengths (0.4, 0.55, 0.7 μm) and the blue-red ratio for plumes against a sky background and a terrain background. A detailed explanation of these parameters can be found later in the text. VISCREEN calculates lines of sight for every 5° increments of azimuth, starting from the emission source. The lines of sight are described by phi (φ), the angle between the source and the observer and the line of sight and alpha (α), the angle between the line of sight and plume centerline (USEPA, 1992a). The model uses two scattering angles to calculate potential plume visual impacts for cases where the plume is likely to be brightest (10° azimuth for the forward scatter) and darkest (140° azimuth for the backward scatter) (Figure 10). At these angles, the light that scatters plume particles is at a maximum. Because particles mainly scatter light in the forward scatter direction, the forward scatter case will produce a very bright plume when the sun is directly in front of the observer, while the backward scatter case will produce a dark plume when the sun is directly behind the observer (USEPA, 1992a).

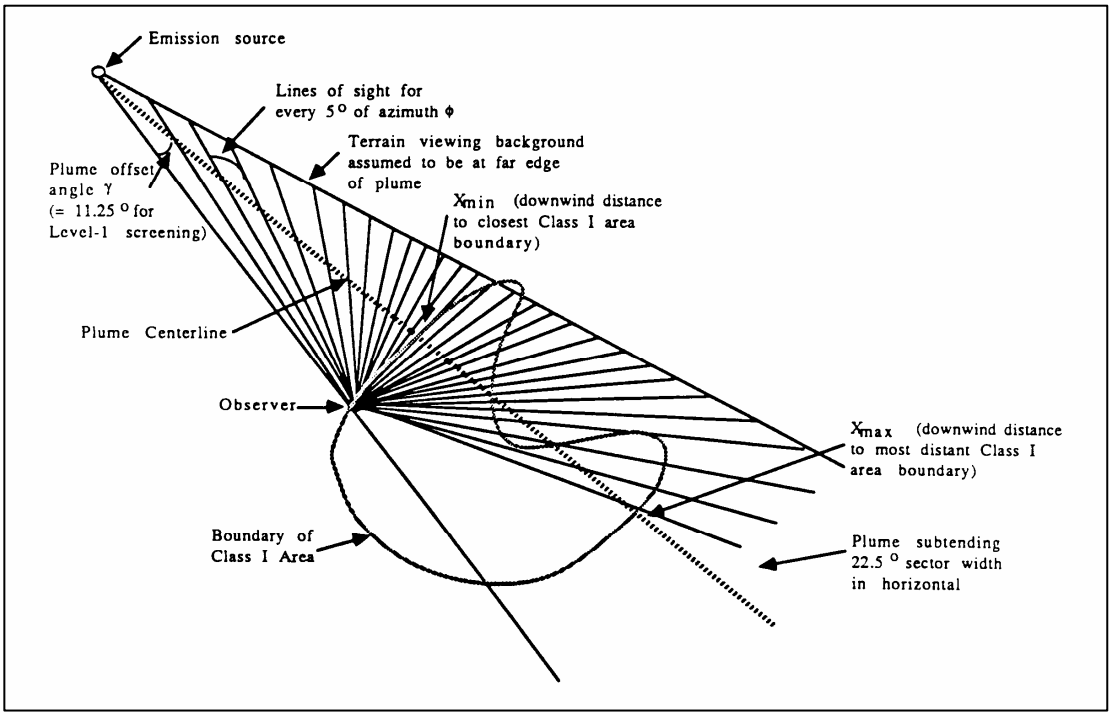

Figure 10. Geometry of plume and observer lines of sight used in VISCREEN (USEPA, 1992a).

A screening threshold of 2.0 for ΔE and 0.05 for green contrast is used for comparison with the modelled results. These values represent the threshold at which a plume would be perceptible to an untrained human observer. If screening calculations indicate that during worst-case meteorological conditions a plume would not have any adverse effect, further analysis would not be required. However, if the screening criteria are exceeded, a more detailed plume visual impact analysis would need to be undertaken to determine the magnitude, frequency, location and timing of plume visual impacts. Such an analysis can be undertaken using PLUVUE II (USEPA, 1992a).

Model input data

Emissions from two industrial point sources, Consol Glass in Bellville and Caltex Oil Refinery in Table View were initially assessed to determine if the emitted plumes have any visual impact. Input data into the model includes emission rates of particulates, NO_x, primary NO_2, soot and primary sulphate with the latter three modelled as zero. A default worst-case meteorological condition of Class F

atmospheric stability and very low wind speed of 1.0 m/s is assumed to persist for a 12-hour period. The wind direction is modelled so that the plume will be transported directly adjacent to the observer. An observer was positioned in the Strand which was identified during the Cape Town Brown Haze II study as an important pollution receptor region, particularly during the afternoon. The distance between the emission source and the observer was measured. Plume centerlines offset by 11.25° were drawn on either side of the observer. The downwind distance (along the assumed plume centerlines) to the closest (X_{min}) and furthest (X_{max}) receptor region boundaries was measured (Figure 10). A background visual range of 50 km was assumed to be representative of the Cape Town region, based on previously measured sulphate and nitrate concentrations during the Cape Town Brown Haze I study. Visual range is defined as the distance at which a large black object would no longer be perceptible. The greater the background visual range, the clearer the background visibility. Within the United States, natural background visual ranges have been estimated to be between 100 – 130 km in the east and 182 – 193 km in the west (Malm, 1999).

Plume Visibility Model (PLUVUE II)

Overview of the model

The Plume Visibility Model (PLUVUE II) is a model used to calculate the visual impact (visual range reduction and atmospheric discoloration) caused by plumes resulting from the emissions of sulphur oxides, nitrogen oxides and particulate matter from a point or area source. PLUVUE II predicts the transport, dispersion, chemical reactions, optical effects and surface deposition of point and area source emissions (USEPA, 1992b). The general flow of the visibility model is shown in Figure 11.

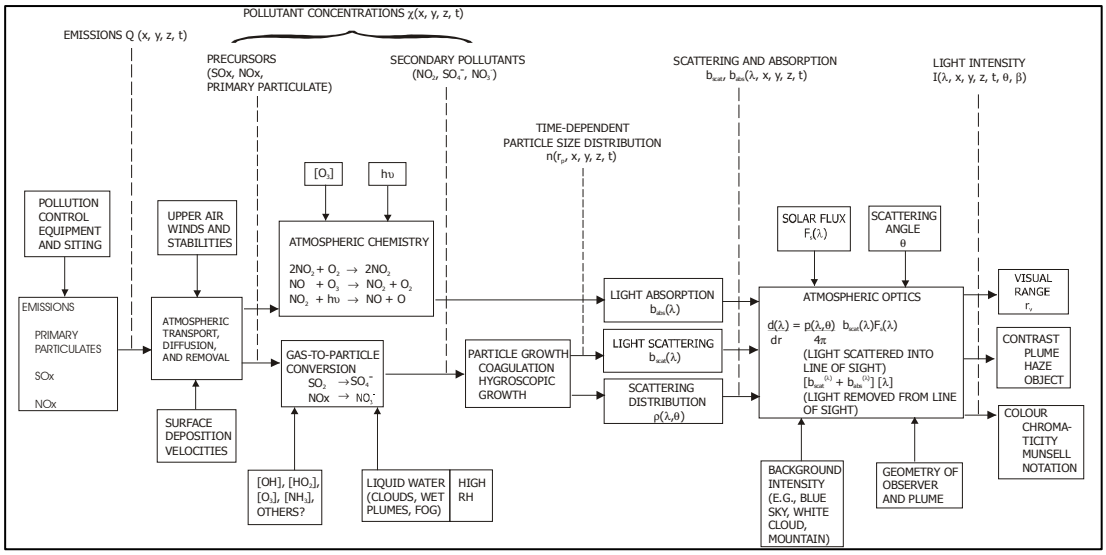

Figure 11. Flow diagram of the Plume Visibility Model, PLUVUE II (Latimer *et al*., 1978).

Transport of pollutants and their subsequent dispersion is determined using a Gaussian diffusion parameter. Plume rise is calculated according to the Briggs formula (1975).

The chemistry component of the model involves nine reactions among NO, NO_2, O_3, O_2, SO_2 and OH^- and applies to clean background atmospheres. This includes the oxidation of NO to NO_2 by O_3 in the flue gases, reactions between NO, NO_2 and O_3, the formation of OH radicals by photolysis of O_3 and the conversion of NO_2 to nitrates and SO_2 to sulphates (Seigneur *et al*., 1984). The aerosol size distribution consists of an accumulation mode and a coarse mode that have a log-normal distribution of mass (USEPA, 1992b).

In the optics module, the light scattering and absorption properties of aerosols and the resultant light intensity for various illumination angles and views are calculated. The spectral light intensity or radiance I (λ) at 39 visible wavelengths is calculated for views with and without the plume. The radiance values are then used to determine visibility impairment parameters. The main parameters calculated by the model to predict visual impact are; a) reduction in visual range; b) contrast of the plume; c) blue-red ratio of the plume and d) colour contrast parameter, ΔE (USEPA, 1992b) (Figure 12).

a) Visual Range Reduction

This parameter indicates the percentage reduction in visual range caused by the emitted plume. It gives an indication of the haziness or loss of contrast of the viewing background by the plume (USEPA, 1992b).

b) *Plume Contrast*

Plume contrast is the relative brightness of the plume as viewed against a sky background or terrain background. A positive contrast indicates a bright plume and a negative contrast indicates a dark plume, viewed against the background sky. The plume is perceptible if the contrast values are greater than 0.02. Plume contrast calculations in PLUVUE II are evaluated at one wavelength, 0.55μm, which is the green colour in the middle of the spectrum and corresponds to the wavelength of peak human visual response (USEPA, 1992b).

c) *Blue-Red ratio*

The blue-red ratio or 'luminance ratio' is a measure of the relative colouration of the plume as viewed against a sky or terrain background. A blue-red ratio less than one is indicative of a plume that is yellow, red or brown in colour compared to the viewing background. A blue-red ratio greater than one indicates a plume that is blue, white or grey in colour. A plume will be perceptible for blue-red ratio values less than 0.9 or greater than 1.1 (USEPA, 1992b).

d) *Colour Contrast Parameter (ΔE)*

Delta E is a measure of the perceived difference in brightness and colour between a plume and the background over a range of colours in the visible spectrum (Wagner *et al*., 2004). A ΔE of 1 corresponds to a 'just noticeable change" or the threshold of the human ability to distinguish between an object and the background. Plumes will be perceptible for ΔE values of 1 if the viewing background is uniform and sharp-edged (USEPA, 1992b). A ΔE of 2 at 55 μm wavelength is the established threshold value for a diffuse edged plume or haze layer. Higher ΔE values indicate

greater colour and brightness differences between the plume and the background while lower ΔE values indicate that the plume will not be visible to the casual observer (Wagner *et al*., 2004).

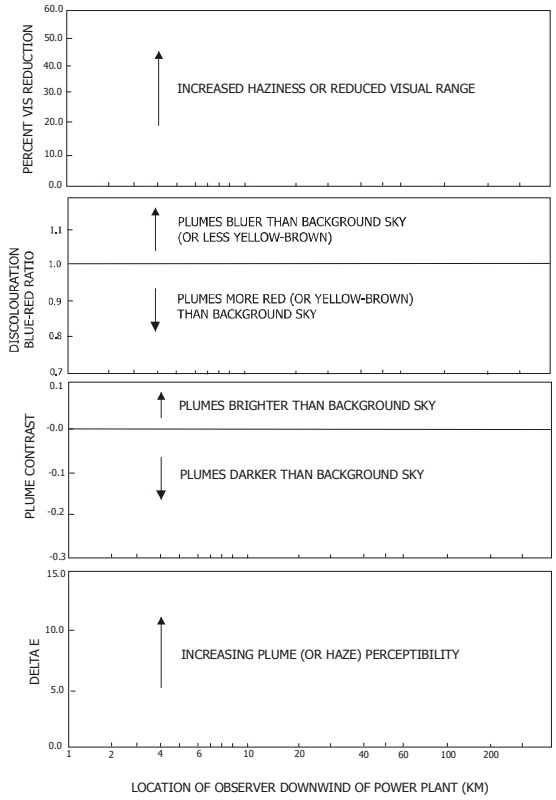

Figure 12. PLUVUE II output of the four visibility impairment parameters (Latimer *et al*., 1978).

Model limitations

Previous evaluations of the model (Seigneur *et al*., 1984) show the accuracy of the model to be limited when modelling visual impacts in receptor areas greater than 50 km from the emission source due to mesoscale wind speed, wind direction and stability variability. The chemical mechanism with which the conversion of sulphur to sulphates and nitrogen oxides to nitrates is predicted is only valid for applications in non-urban or clean environments and not for urban areas. Terrain viewing backgrounds are idealized as white, gray and black objects. The background atmosphere is divided into two layers; a homogenous, surface mixed layer and a relatively clean upper-atmosphere layer (USEPA, 1992b).

Model input data

Visibility modelling was undertaken for Consol Glass in Bellville and Caltex in Table View respectively as well as for three area sources, namely Cape Town International Airport, Cape Town CBD and the townships of Khayelitsha and Mitchell's Plain. The observer was positioned at the Strand and downwind distances from each source to the Strand region were determined from topographic maps. Input data into the model for each source includes emissions data (emissions rate of SO_2, NO_x and primary particulates); stack height and flue gas characteristics (exit temperature, exit velocity and flow rate); aerosol characteristics of background and emitted aerosols in accumulation, coarse and carbonaceous aerosol size modes and deposition velocities for SO_2, NO_x, coarse-mode aerosol and accumulation mode aerosol. Meteorological data was obtained from the South African Weather Service for August 2003. Input data includes wind speed, wind direction, lapse rate, mixing depth and relative humidity. Atmospheric stability was calculated using the six Pasquill-Gifford stability classes.

CALPUFF Lagrangian Puff Dispersion Model

Overview of the model

The CALPUFF modelling system consists of three major components: CALMET, CALPUFF and CALPOST. CALMET is a meteorological model for generating hourly three-dimensional wind and temperature fields on a gridded modelling domain. Other two-dimensional fields such as mixing height, surface characteristics and dispersion properties are also calculated by CALMET. The meteorological fields generated by CALMET are used as input into CALPUFF. CALPUFF is a non-steady state puff model that calculates hourly pollutant concentrations and deposition fluxes at pre-determined receptors. The files generated by CALPUFF are then processed by CALPOST which summarizes visibility impacts, deposition amounts and pollutant concentration levels (Scire *et al*., 2000).

The CALPUFF modelling system can be used for regional visibility impairment studies. CALPUFF calculates hourly concentrations of sulphates (as ammonium

sulphate), nitrates (as ammonium nitrate) and other particles emitted from pollutant sources while CALPOST computes and summarizes the corresponding light extinction coefficient (b_{ext}) relative to the background light extinction (Scire *et al*., 2000).

The change of extinction due to the emission source can be calculated as follows:

$$\text{Extinction change } (\%) = \frac{b_{ext,s}}{b_{ext,b}} \times 100$$

Where $b_{ext,s}$ is the extinction coefficient due to the emission source and $b_{ext,b}$ is the background extinction coefficient under natural conditions (Scire *et al*., 2000).

The light extinction coefficient is a measure of the attenuation of light per unit distance due to scattering (b_{scat}) and absorption (b_{abs}) by gases and particles (USEPA, 1998). Light extinction is expressed in inverse megameters (Mm^{-1}). The extinction coefficient can be calculated as the sum of its parts:

$$b_{ext} = b_{scat} + b_{abs}$$

Where b_{scat} and b_{abs} are the light scattering and absorption coefficients respectively.

The light scattering and absorption coefficients can be further broken down by their respective components. The scattering coefficient can be broken down into light scattering by gases or Rayleigh scattering (b_{Ray}) and scattering by coarse particles and fine particles (b_{sp}). The absorption coefficient can be broken down into light absorption by gases (b_{ag}), especially NO_2 and absorption by particles (b_{ap}), particularly by elemental carbon (FLAG, 2000).

Particulate scattering can be broken down into scattering by fine particles (PM2.5) and coarse particles (PM10). The fine particle scattering coefficient (b_{fine}) can be further defined by the sum of the scattering coefficient due to sulphates (b_{SO4}),

nitrates (b_{NO3}), organic aerosols (b_{OC}) and soil (b_{Soil}). The coarse particle scattering coefficient (b_{Coarse}) cannot be defined any further. Therefore:

$$b_{sp} = b_{SO4} + b_{NO3} + b_{OC} + b_{Soil} + b_{Coarse}$$

Therefore, the total atmospheric light extinction, due to scattering and absorption, can be expressed as:

$$b_{sp} = b_{SO4} + b_{NO3} + b_{OC} + b_{Soil} + b_{Coarse} + b_{ap} + b_{ag} + b_{Ray}$$

Model input data

Input data into CALMET includes climate data and geophysical data. Surface and upper air data for the month of August 2003 was obtained from the South African Weather Service. Surface data included hourly observations of wind speed, wind direction, temperature, cloud cover, ceiling height, surface pressure and relative humidity. Upper air data included twice-daily observations of wind speed, wind direction, temperature, pressure and elevation. Geophysical data included surface elevations and land-use categories which was obtained from the Environmental Potential Atlas (ENPAT) database developed by DEAT. The modelling domain used in the CALMET simulation consisted of 4 vertical, 210 west-east and 210 south-north grid cells. Each grid cell covered a 0.4 km × 0.4 km horizontal area. Total domain coverage was 84 km × 84 km. Three meteorological files were created by CALMET for input into CALPUFF. NO_x, SO_2 and PM10 emissions as well as source characteristics such as stack height, stack diameter, gas exit velocity and gas exit temperature were input into the CALPUFF model. CALPOST postprocessing computations involved 1-hour, 3-hour, 24-hour and 720-hour averaging periods for the month of August and for 13 and 22 August respectively. Time series calculations were performed for 22 August for each pollutant. Visibility impacts were also computed for each of the averaging periods and an hourly time series was run for 22 August.

Meteorology of study region

Brown haze and non-brown haze days

Cape Town is located at 34°S at the south-western tip of Africa and experiences a Mediterranean climate. Summers are warm and dry and winters are cool and wet (Levey, 1996). During summer, a ridging anticyclone over the south-Atlantic Ocean predominates, causing a south-easterly air flow. As a result, pollutants are diluted and dispersed effectively over Cape Town due to high wind velocity and high atmospheric turbulence. During winter, the passage of pre-frontal systems promotes north-westerly winds which result in the ventilation of the area. Between late winter and early spring, the occurrence of north-easterly berg winds together with strong low level inversions, are conducive to the formation of brown haze in the Cape Town region (Jury *et al.*, 1990).

During 2003, the Western Cape experienced below average rainfall during its winter rainfall period. During August 2003, a total of 11 cold fronts passed over Cape Town (Piketh *et al*., 2004), bringing rain and cold temperatures to the region every few days. On these unpolluted, non-brown haze days, wind direction is predominantly north to north-west-north. The shift in wind direction from northerly to south westerly is mainly associated with the influence of the passage of the cold fronts. Elevated wind speeds are experienced on these days which transport pollutants out of the region (Figure 13 left) resulting in clear conditions. Between the passage of the cold fronts, the South Atlantic high pressure system persists resulting in highly stable conditions that are conducive to the formation of brown haze episodes. Prior to the onset of brown haze episodes, strong nocturnal surface inversions form which effectively trap pollutants in the lower levels. The dominant wind direction during brown haze days is also northerly to north-westerly due to the influence of approaching cold fronts to the south-west of Cape Town. Wind speeds are low so that pollutants accumulate within the region and a brown haze episode occurs (Figure 13 right).

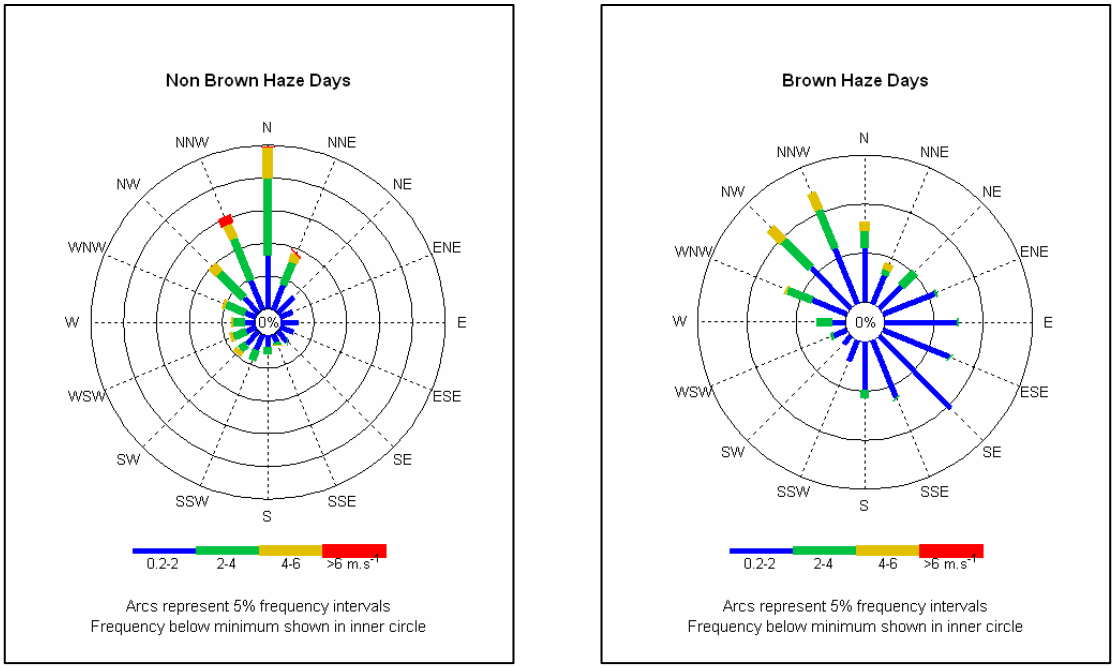

Figure 13. Surface wind roses for Goodwood on non-brown haze days (left) and brown haze days (right).

Meteorology on 13 August and 22 August 2003

13 August 2003 has been chosen to represent a non-brown haze day for this study. 22 August 2003 has been identified by the CCT as a brown haze day and has been chosen as a representative brown haze day for this study.

On 13 August, a cold front persisted over parts of the country bringing cold temperatures and humid conditions to Cape Town (Figure 14 top). Onshore airflow behind the low pressure system resulted in winds with a predominantly northerly component. Wind speeds were strong (Figure 15 left) thereby promoting the mixing and dispersion of pollutants and preventing the formation of haze over the region. On 22 August, a high-pressure system prevailed over the country causing warm temperatures and dry conditions in Cape Town (Figure 14 bottom). Calm, stable conditions persisted so that wind speeds were low and pollutants were able to accumulate, forming the characteristic brown haze. Winds were mainly north-westerly due to the approaching cold front (Figure 15 right).

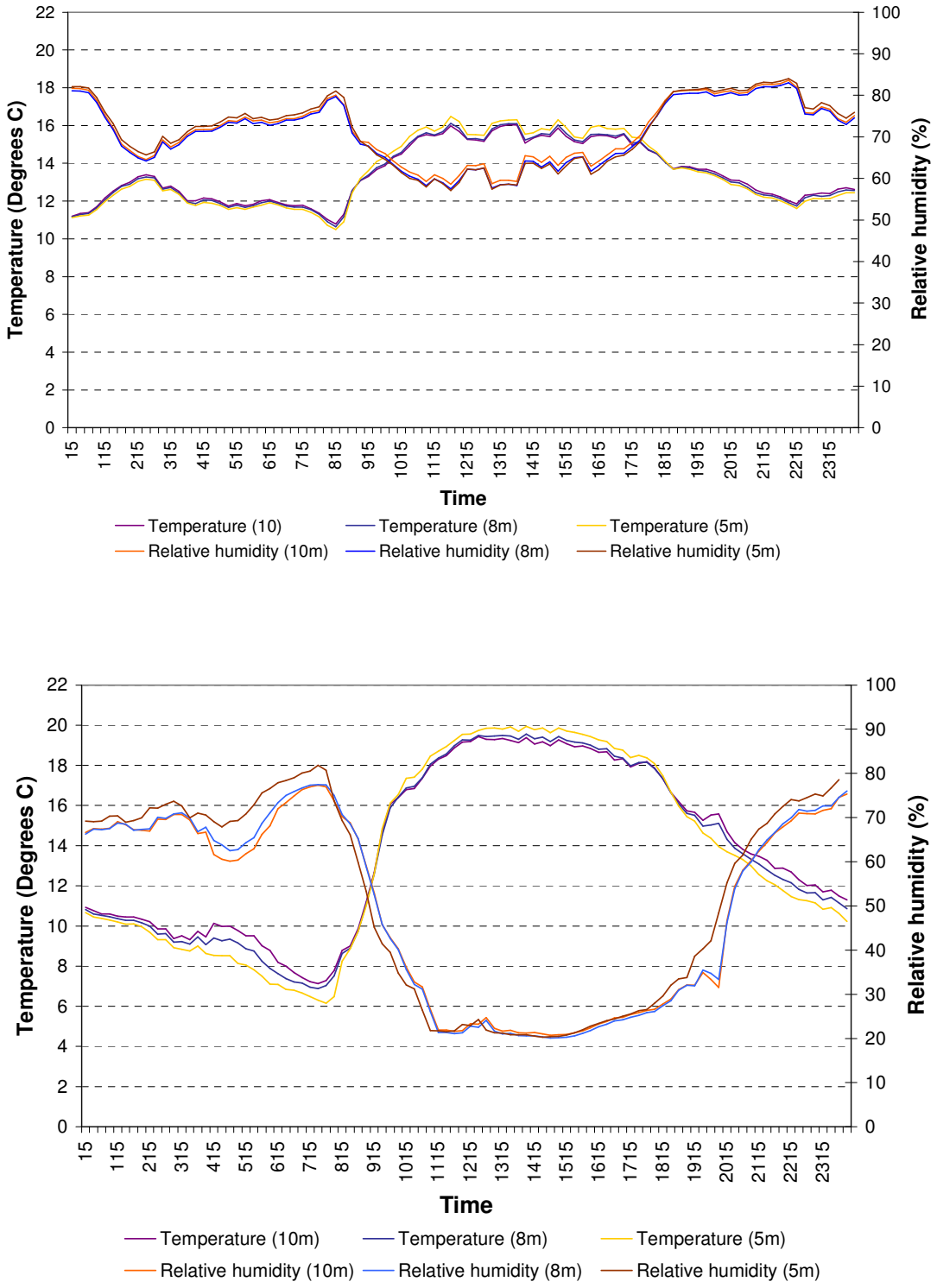

Figure 14. Temperature and relative humidity on 13 August (top) and 22 August (bottom).

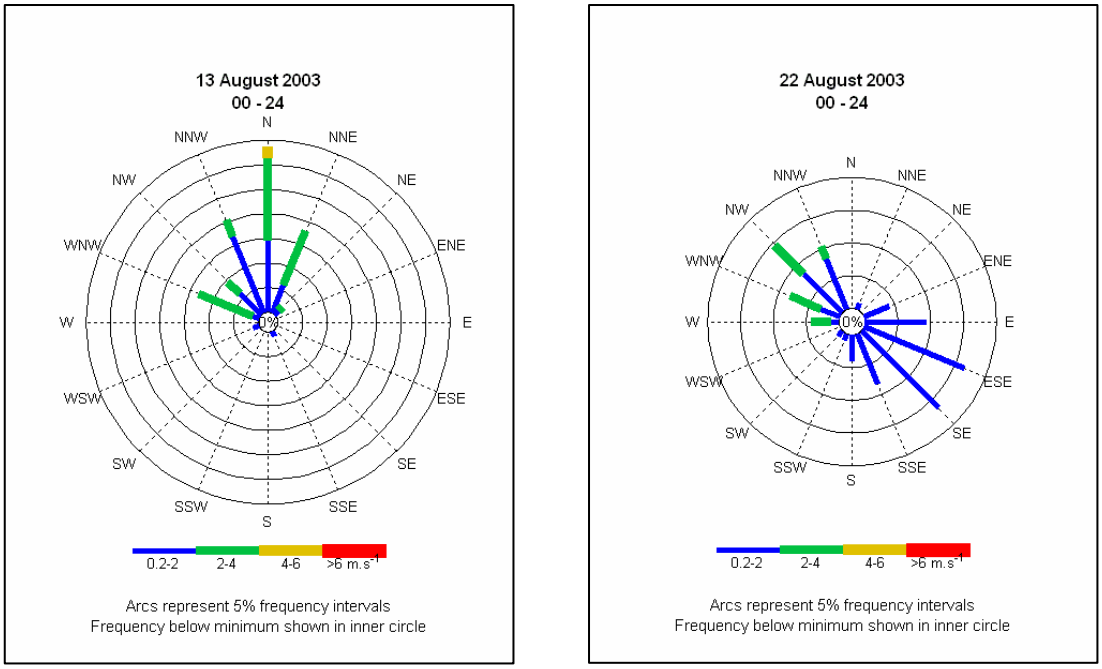

Figure 15. Surface wind roses for Goodwood on 13 August (left) and 22 August (right).

****

Chapter 2 gives an overview of the Cape Town Brown Haze II study. An overview of the models, VISCREEN, PLUVUE II and CALPUFF and the input data into the models has been given. The meteorological conditions in Cape Town have been discussed.

CHAPTER 3 VISIBILITY IMPAIRMENT BY THE BROWN HAZE

Chapter 3 outlines the modelling results from VISCREEN, PLUVUE II and CALPUFF for a non-brown haze day and brown haze day. An initial screening analysis is carried out using VISCREEN. PLUVUE II is used to assess the visual impact of plumes from individual sources while CALPUFF is used for a regional haze analysis over Cape Town.

Brown haze episodes in August 2003

Brown haze episodes identified by the CCT and the associated pollutant concentrations in Cape Town during August 2003 are shown in Table 3. An episode occurs when the CCT air pollution guidelines are exceeded. Brown haze episodes were recorded on 7 days during August. On average, moderate pollution levels characterised the episodes at all the sampling sites during August. The Khayelitsha site experienced 3 high pollution days on 5, 10 and 21 August. Very high pollution levels were recorded at Khayelitsha on 6 August and 22 August.

Table 3. Air pollution episodes identified by the City of Cape Town during the Cape Town Brown Haze II study (CCT, 2005).

Date	Pollutant	Site	Guideline Value ($\mu g/m^3$)	Averaging period	Recorded value ($\mu g/m^3$)
03/08/2003	PM10	Khayelitsha	50	Daily	62
05/08/2003	PM10	Khayelitsha	50	Daily	80
06/08/2003	PM10	Athlone	50	Daily	61
	PM10	Bellville S	50	Daily	56
	PM10	Goodwood	50	Daily	56
	PM10	Khayelitsha	50	Daily	123
07/08/2003	PM10	Khayelitsha	50	Daily	66
10/08/2003	PM10	Khayelitsha	50	Daily	77
21/08/2003	PM10	Khayelithsa	50	Daily	86
22/08/2003	PM10	Bellville S	50	Daily	54
	PM10	Cape Town	200	Hourly	287
	PM10	Goodwood	50	Daily	53
	PM10	Khayelitsha	50	Daily	107

Based on recorded pollutant concentrations by the CCT and observations made during the Cape Town Brown Haze II field campaign, conditions on 22 August 2003 have been chosen to be representative of a brown haze day for modelling purposes. On this brown haze day, a high-pressure system dominated over parts of the country with an approaching cold front to the south-west of Cape Town (Figure 16). The resultant sunny and mild conditions in Cape Town were conducive to the formation of brown haze. 13 August 2003 has been identified as a clear, unpolluted day and will be representative of a non-brown haze day. Conditions on this day were influenced by the presence of a cold front extending across the country which resulted in cold and cloudy conditions in Cape Town (Figure 17).

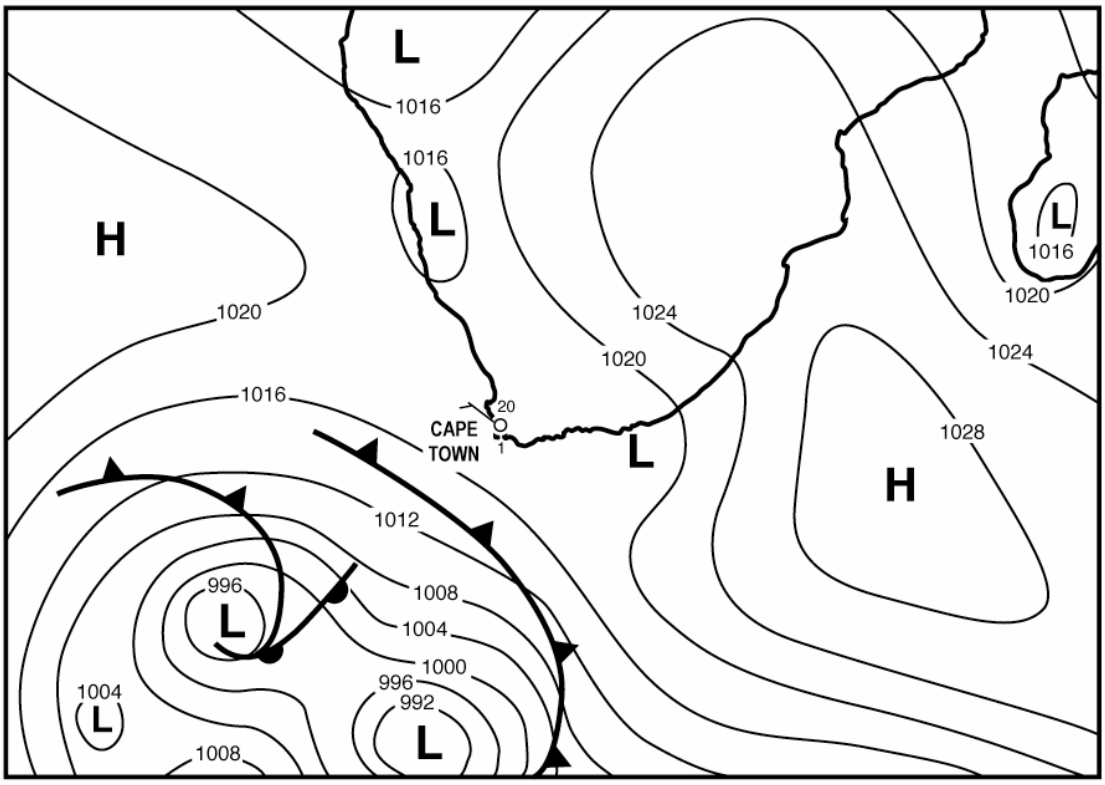

Figure 16. Synoptic conditions on 22 August 2003.

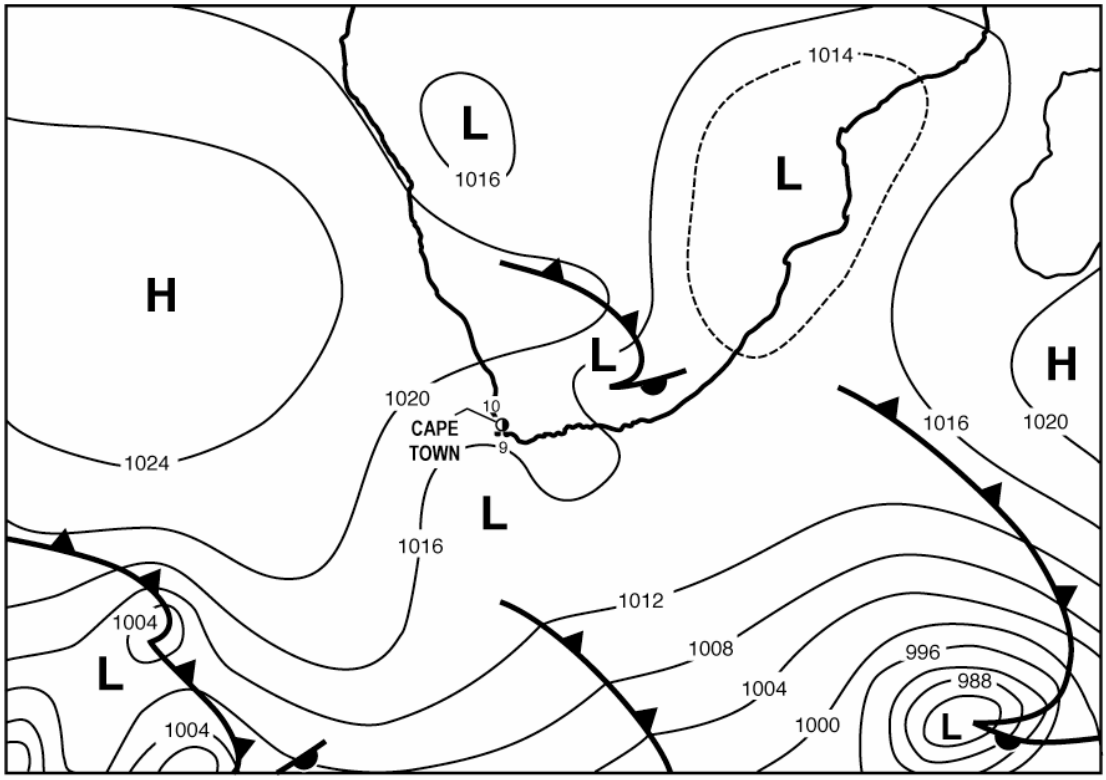

Figure 17. Synoptic conditions on 13 August 2003.

Modelling results

In the forward scatter, the sun is in front of the observer such that the scattering angle (θ) is 10° in this case. The plume is in shadow relative to the observer. The plume contrasts more strongly with the background and hence is more easily visible, but the detail in the plume is less visible because it is in shadow. In the backward scatter, the sun is behind the observer such that the scattering angle is 140°. The sun shines on the plume, making it brighter so that it contrasts less with the background. This makes it less visible, but more detail can be seen (Ministry of the Environment, 2001).

VISCREEN model output

The screening criteria, ΔE and contrast, are exceeded for both emission sources, especially from the oil refinery, as shown in Table 4 and Table 5. When over the Strand, the plumes from Caltex and Consol Glass are most perceptible (ΔE) when there is forward scatter and when viewed against a sky background at downwind distances of 40 km and 29 km respectively. When the plume is not advected over the Strand even larger visual impacts are predicted when viewed against both the sky and terrain although it needs to be considered that at times the observer is looking directly towards a plume located close to the emission source (φ = 0 or 1).

Table 4. Summary of maximum visual effects for Caltex Oil Refinery emissions (* indicates that screening criteria have been exceeded).

Receptor	Bckgrnd	Theta (Θ)	Azimuth (Φ)	Distance (km)	Alpha (ά)	Delta E (ΔE)	Contrast
Over Strand	Sky	10	84	40	84	7.836*	0.006
	Sky	140	84	40	84	3.061*	-0.05*
	Terrain	10	84	40	84	2.960*	0.039
	Terrain	140	84	40	84	0.822	0.024
Outside Strand	Sky	10	50	35	119	8.016*	0.006
	Sky	140	50	35	119	3.056*	-0.055*
	Terrain	10	0	1	168	4.052*	0.041
	Terrain	140	0	1	168	1.259	0.041

Table 5. Summary of maximum visual effects for Consol Glass emissions (* indicates that screening criteria have been exceeded).

Receptor	Bckgrnd	Theta (Θ)	Azimuth (Φ)	Distance (km)	Alpha (ά)	Delta E (ΔE)	Contrast
Over Strand	Sky	10	135	28.6	34	3.477*	-0.001
	Sky	140	135	28.6	34	1.374	-0.020
	Terrain	10	84	22.5	84	1.469	0.015
	Terrain	140	84	22.5	84	0.396	0.007
Outside Strand	Sky	10	10	10.8	159	4.382*	-0.001
	Sky	140	10	10.8	159	1.621	-0.030
	Terrain	10	1	1	168	5.163*	0.063*
	Terrain	140	1	1	168	1.333	0.054*

Colour Difference Parameter (ΔE)

The plume from Caltex is visible against the viewing background, particularly when viewed against the sky in the forward scatter. The plume from Consol Glass is not as visible against the viewing background in both the forward and backward scatter compared to the plume from Caltex (Figure 18). This can be attributed to the higher emission rates of particulates and NO_x from Caltex compared to Consol Glass.

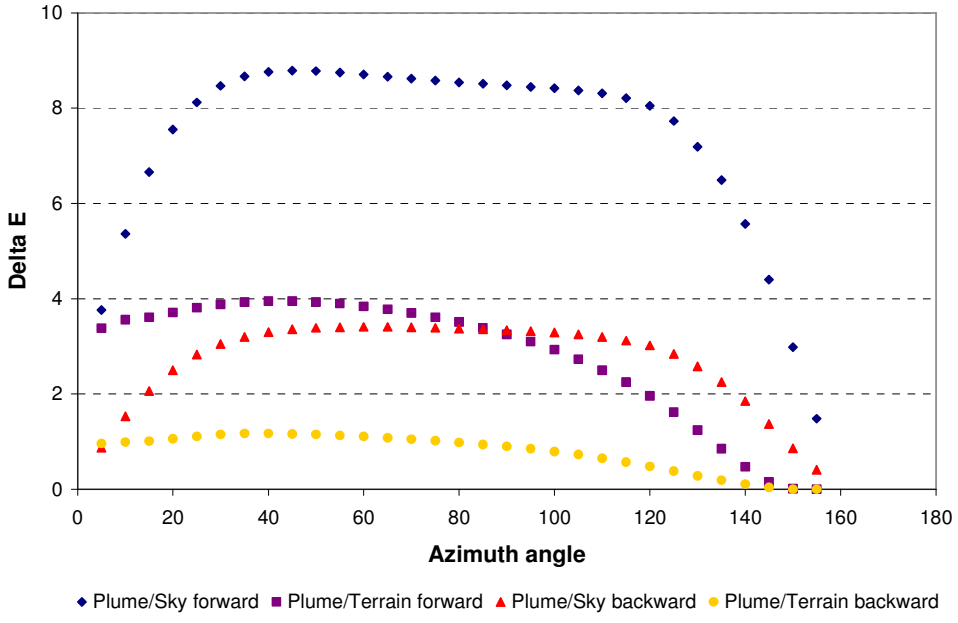

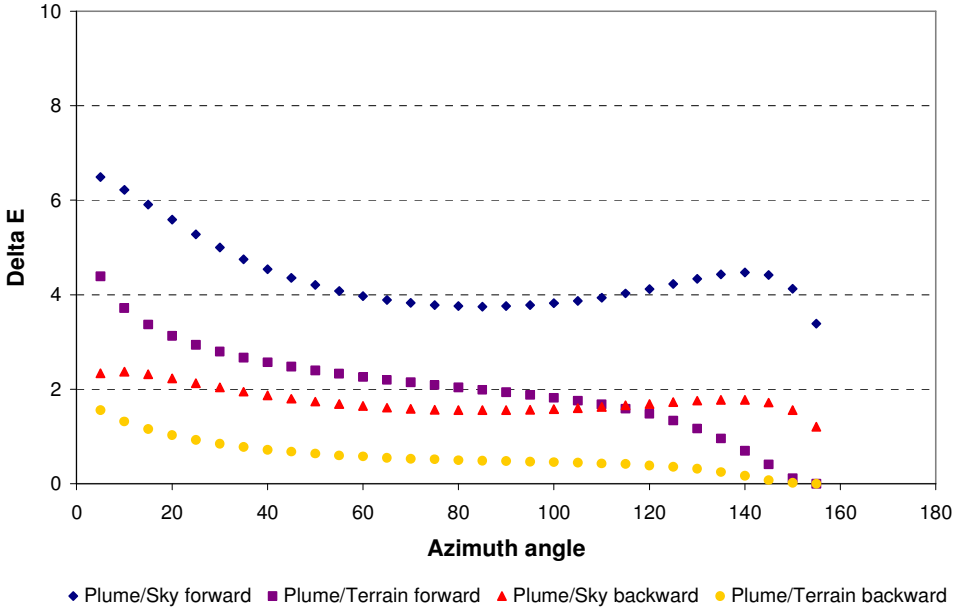

Figure 18. Plume perceptibility (ΔE) for Caltex (top) and Consol Glass (bottom).

Blue-red ratio

Both the plumes from Caltex and Consol Glass appear yellow, red or brown in colour compared to the viewing background as both have a blue-red ratio less than 1. However, based on field observations, a white plume is clearly emitted from Consol Glass (Figure 6) which would suggest a modelled blue-red ratio greater than 1. Blue-red ratios less than 0.9 are indicative of perceptible plumes (USEPA, 1992b). The plume from Caltex will be perceptible between azimuth angles of 25° and 105° when viewed against the sky in both the backward and forward scatter. These angles correspond with the maximum plume perceptibility for ΔE when viewed against the sky in the forward scatter. With blue-red ratios of greater than 0.9, the plume from Consol Glass will not be visible to the observer (Figure 19).

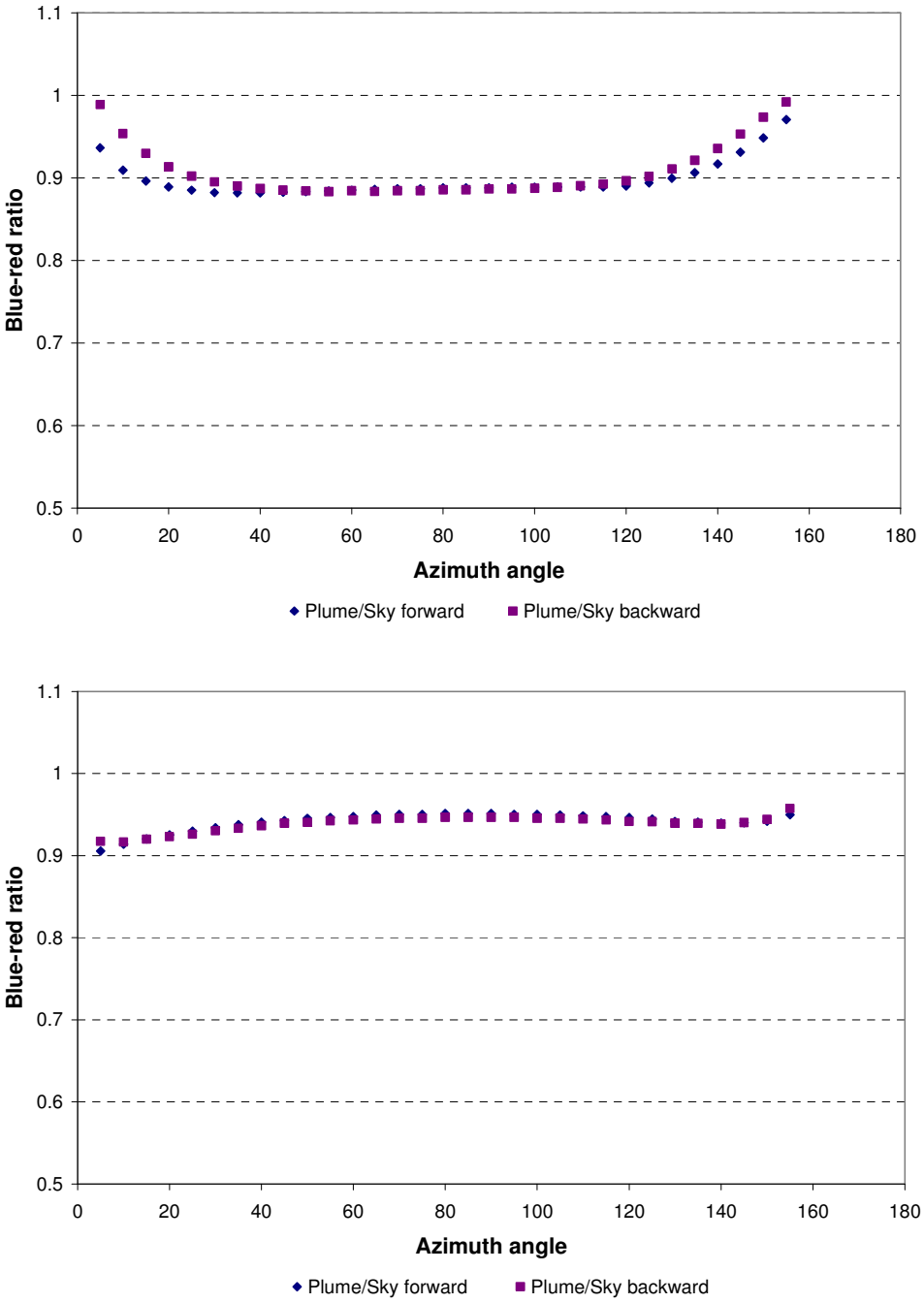

Figure 19. Blue-red ratio for Caltex (top) and Consol Glass (bottom).

The modelled results do not indicate conclusively that the plumes from Consol Glass and Caltex will have any significant visual impact despite an exceedance of the threshold values for certain cases inside and outside the Strand. However, this is not in agreement with observations made during the Cape Town Brown Haze II field campaign which identified visible plumes that were emitted from these sources. This suggests that emissions from these sources may have been underestimated. Since this

is a conservative model, further detailed modelling will be undertaken using the visibility model, PLUVUE II, to address this issue further.

PLUVUE II model output

Contribution of sources to visibility impairment

Model runs are carried out for Caltex Oil Refinery, Cape Town CBD, Cape Town International Airport, Consol Glass and the townships of Khayelitsha and Mitchell's Plain for a brown haze day (22 August 2003). An observer is positioned at the Strand and distances between the observer and plumes from each source are determined. The four visibility parameters are calculated and plotted as a function of downwind distance from the source.

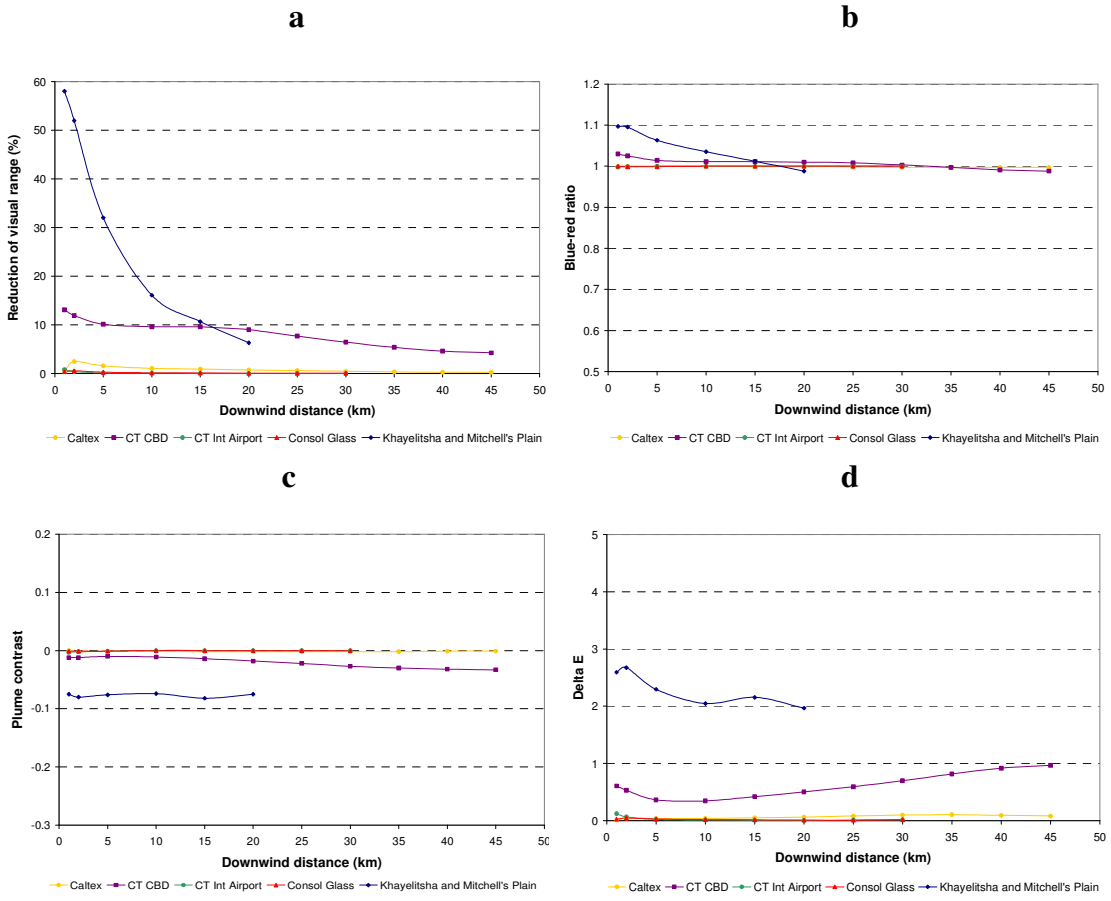

Figure 20. Visual effects calculated using PLUVUE II for all emission sources versus downwind distance for a) visual range, b) blue-red ratio, c) plume contrast and d) ΔE.

Emissions from Consol Glass, Caltex and Cape Town International Airport do not result in any significant reduction of visual range. However, emissions from the two area sources, Cape Town CBD and Khayelitsha and Mitchell's Plain, do result in a reduction of visual range. Visibility is particularly poor near the source of Khayelitsha and Mitchell's Plain with an approximately 60% reduction of visual range. The elevated particulate emissions from this area account for the large reduction in visibility (Figure 20a).

The plumes from Cape Town CBD and Khayelitsha and Mitchell's Plain appear bluer, greyer or whiter than the viewing background while the other sources show no discolouration with a blue-red ratio of 1 (Figure 20b). This is not in agreement with the results modelled by VISCREEN which predicts a plume that is yellow, red or brown for Caltex and Consol Glass. However, this lack of discolouration could be attributed to high emission of particulates from these industries. Prior to particulate emission control, an early study by Latimer and Samuelsen (1978) noted that high particulate emission rates from power plants can have a masking effect on plume colouration caused by NO_2. If aerosols scatter light into the sight path of the observer, the scattered light from the blue end of the visible spectrum will increase the blue-red ratio, making the plume appear less coloured. Blue-red ratios less than 0.9 or greater than 1.1 are indicative of perceptible plumes (USEPA, 1992b). The only plume that would be perceptible less than 5 km from the source is the plume from the townships.

The negative number for plume contrast indicates that the plumes from Cape Town CBD and Khayelitsha and Mitchell's Plain appear darker than the sky. A contrast between the plume and background with an absolute value greater than 0.02 is considered to be perceptible (USEPA, 1992b). For all sources, PLUVUE II predicts that the plumes are not perceptible downwind (Figure 20c).

Only the plume from Khayelitsha and Mitchell's Plain is predicted to be perceptible with ΔE greater than 1. PLUVUE II also predicts lower ΔE value for Caltex and Consol Glass compared to those predicted by the more conservative model, VISCREEN. The plume would be most perceptible for the source of Khayelitsha and Mitchell's Plain in close proximity (Figure 20d). The relative importance of the CBD and the townships as indicated by the model can be attributed

to the higher particulate emissions from these two sources compared to the other sources. However, the visibility effects predicted for Consol Glass are not in agreement with observations, since a white plume was clearly visible when flights were undertaken over the industry and on the ground within Cape Town and surrounding areas. This suggests that the contribution of particulate emissions from this source has been underestimated. The emissions data was obtained directly from the industry and it is therefore difficult to determine the accuracy of the data.

Contribution of sources to NO_x and aerosol emissions

In order to evaluate the relative contribution of NO_x and aerosols to visibility impairment over the Cape Town region, sensitivity simulations were run for each of the five sources with a reduction of a) NO_x emissions and b) particulate emissions to 0.01 tons per day. Gaseous NO_2 absorbs light selectively and may discolour the atmosphere while primary particulate emissions can scatter and absorb light (Latimer and Samuelsen, 1978).

According to the modelled results, particulate matter contributes significantly to visibility impairment over the Cape Town region compared to NO_x emissions which, except for the Cape Town CBD, result in less than a 1% reduction in overall visibility (Figure 21). Sources with reduced NO_x emissions produce a similar reduction of visual range to that observed in Figure 20a.

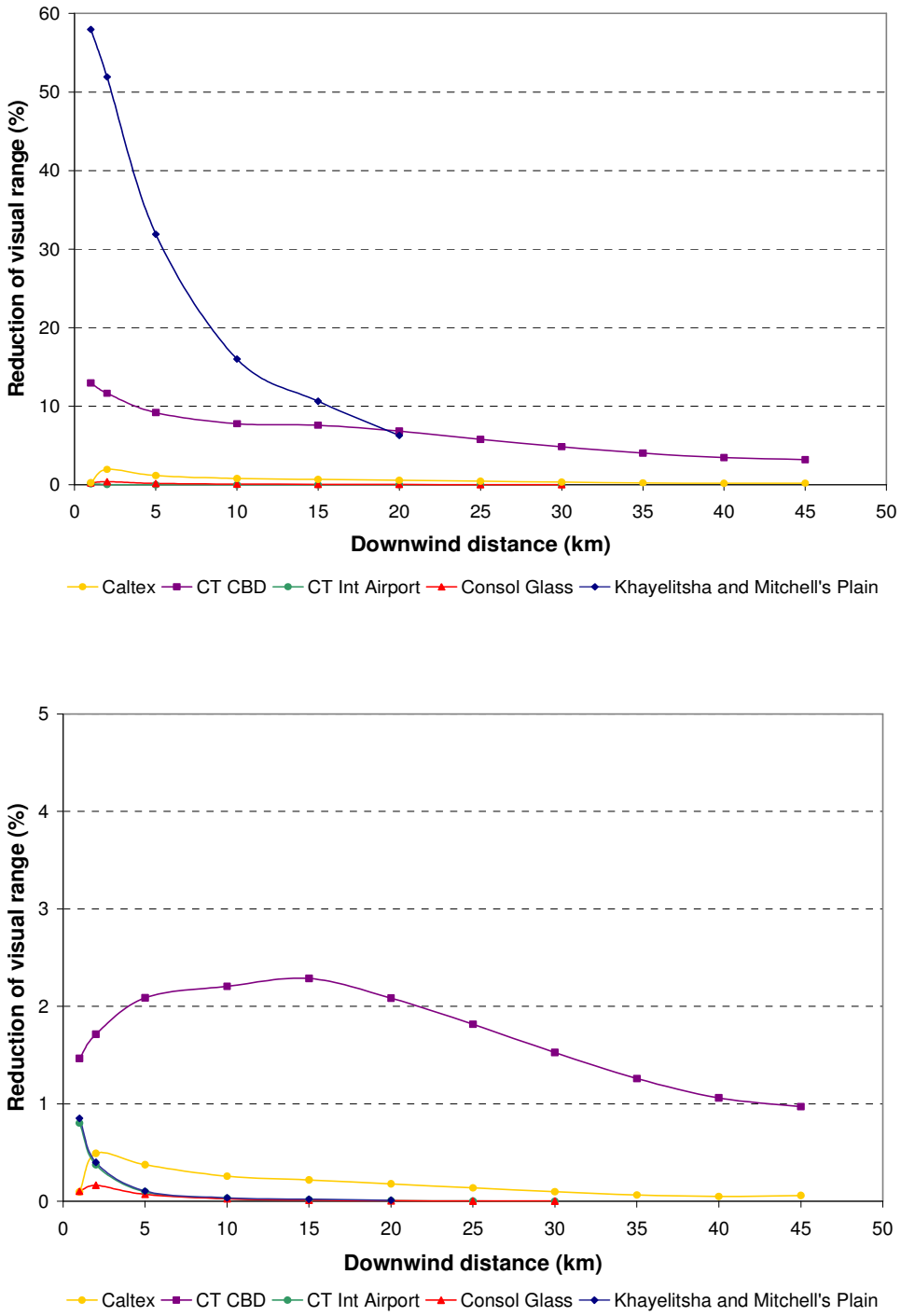

Figure 21. Reduction of visual range with downwind distance for all sources with reduced NO_x emissions (top) and reduced particulate matter emissions (bottom).

Reduced emissions of NO_x result in a plume that is whiter, greyer or bluer than the viewing background due to the influence of the particulates. A similar blue-red ratio to that observed in Figure 20b is modelled for all the sources with reduced NO_x

emissions. With a reduction in particulate emissions, the plumes from the CBD and the townships show a decrease in blue-red ratio. A reddish-brown discolouration in the plume from the CBD is evident from about 25 km downwind. This is expected since NO_2 can cause atmospheric discolouration by producing a plume that is yellow, brown or red in colour. Additionally, the reduced particulate emissions have a decreased masking effect on the colouration of the plume by NO_x. However, for both cases, the plumes from all the sources are not perceptible against the background sky (Figure 22).

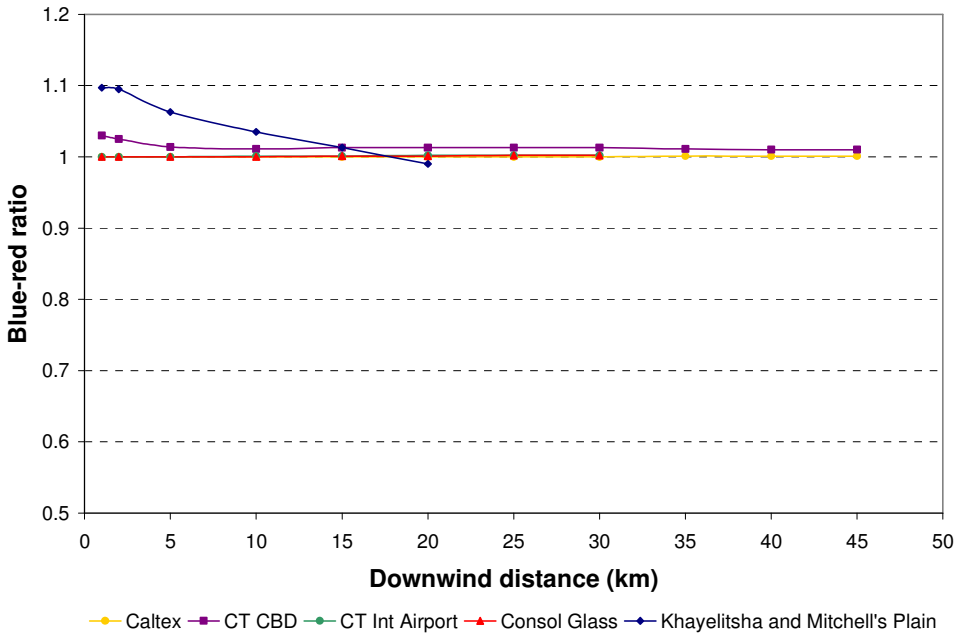

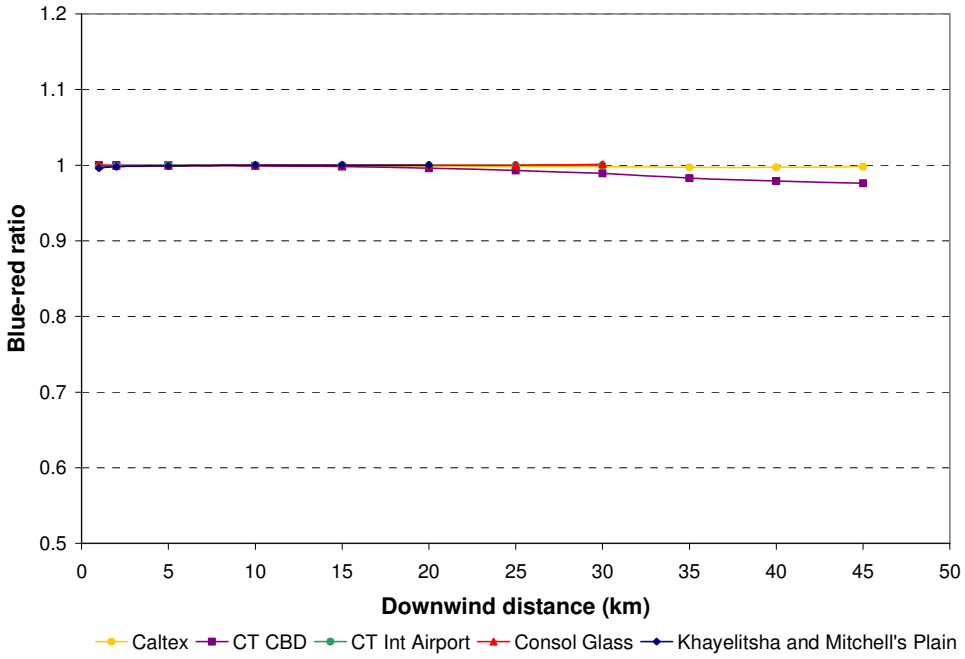

Figure 22. Change in blue-red ratio with downwind distances for all sources with reduced NO_x emissions (top) and reduced particulate matter emissions (bottom).

According to the modelled results, the contribution of NO_x to plume perceptibility is insignificant, as the plume from Khayelitsha and Mitchell's Plain is visible despite reduced NO_x emissions. With reduced particulate emissions, the plumes from the sources are not perceptible (ΔE less than 1) as would be expected (Figure 23). Sources with reduced NO_x emissions have slightly lower ΔE values to those modelled in Figure 20d.

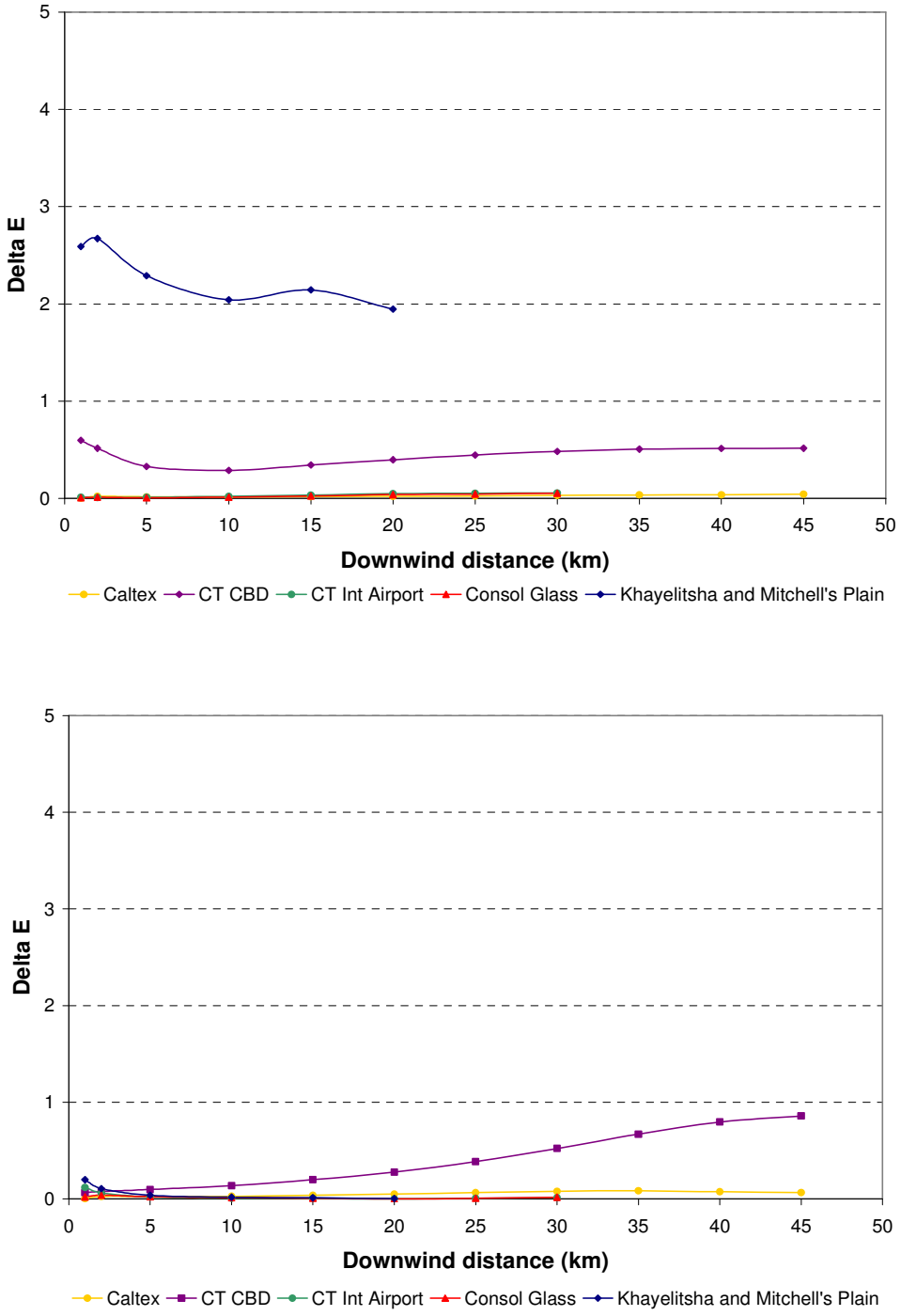

Figure 23. Change of ΔE with downwind distance for all sources with reduced NO_x emissions (top) and reduced particulate matter emissions (bottom).

This sensitivity analysis indicates that visibility impairment is mainly due to emissions of primary particulates with reduced NO_x emissions having little to no impact on plume perceptibility. NO_x emissions influence plume colouration by decreasing the blue-red ratio and producing a reddish-brown plume.

In general, the modelled results by PLUVUE II do not correspond to observations during the Cape Town Brown Haze II field campaign. Studies undertaken by Haas and Fabrick (1981) using the plume visibility model found inconsistencies between the different visual impairment indices. They noted that plumes which are invisible according to one index, such as the contrast index, are visible according to another, such as the blue-red ratio. They suggested that a possible reason for this is that the plume contrast index only measures monochromatic radiance differences whereas the blue-red ratio index effectively compares plume contrast at two different points in the spectrum. Also, there is uncertainty regarding the perception threshold values used for each index (Haas and Fabrick, 1981).

Secondary sulphate and nitrate aerosol formation

Although SO_2 and NO_x do not scatter light significantly, these gases react in the atmosphere to form secondary sulphate and nitrate particles which contribute to visibility impairment. PLUVUE II considers secondary aerosol formation by introducing pseudo-first-order rate constants for the chemical conversion of SO_2 and NO_x (Latimer and Samuelsen, 1978). The model also considers the removal of pollutants from the atmosphere by dry deposition. Deposition on ground surfaces is increased by good mixing, lower stack heights and terrain characteristics. The conversion-removal processes determine the amount of secondary pollutants available for transport and dispersion in the atmosphere (USEPA, 1979).

Sulphur dioxide to sulphate conversion rate

The conversion rate of SO_2 to SO_4^{2-} is dependant upon primary SO_2 emissions (Miller, 1978), NO_x and hydrocarbon concentrations (Isaksen *et al*., 1978), sunlight intensity, water vapour concentrations, background O_3 levels and the extent to which the plume has mixed with background air (Husar *et al*., 1978).

In gas-phase oxidation, the hydroxyl radical is considered to be the main oxidant responsible for the conversion of SO_2 to SO_4^{2-} during the day. The conversion of SO_2 to SO_4^{2-} occurs more rapidly during the day than the night, and more rapidly during summer than winter (Cass, 1981; Meagher *et al*., 1983; Wilson, 1981) due to increased solar radiation. In aqueous-phase oxidation, conversion of SO_2 to SO_4^{2-}

occurs more efficiently than gas-phase reactions (Eatough *et al.*, 1982; Hegg and Hobbs, 1982; Gillani *et al.*, 1983; Schwartz and Newman, 1983; Dittenhoefer, 1984; Seigneur and Saxena, 1988; Husain *et al.*, 1991; Klemm *et al.*, 1992; Pienaar and Helas, 1996).

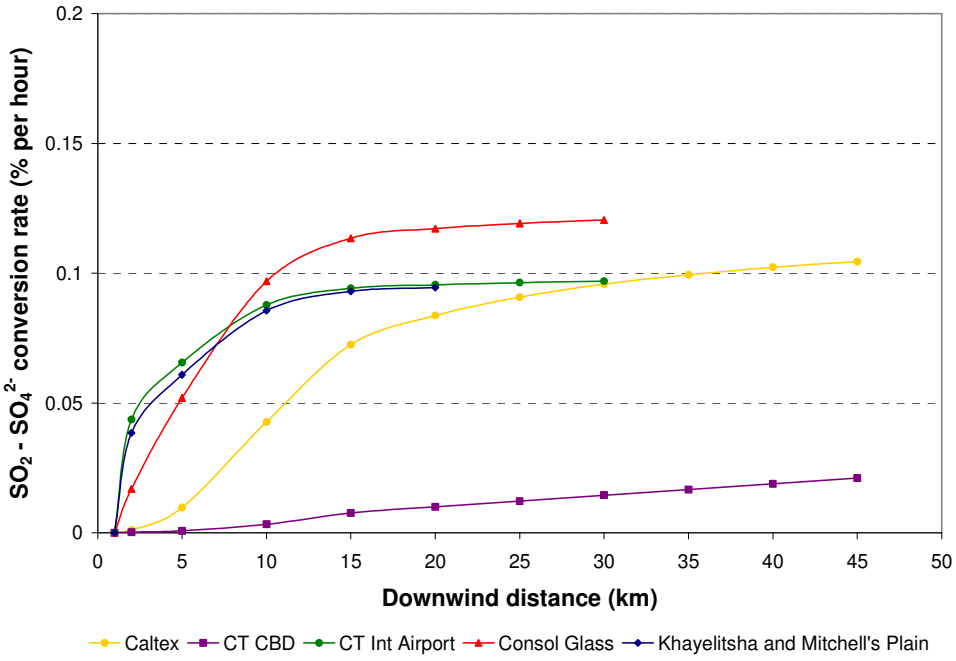

Figure 24. SO_2 to SO_4^{2-} conversion rate with downwind distance for all emission sources.

The conversion rate of SO_2 to SO_4^{2-} in the emitted plumes is initially slow near the emissions source, with a slight increase with downwind distance for all five sources. As ambient air mixes with the plume, the rate of conversion increases until it remains level at just over 0.1% per hour In concentrated plumes, such as the plumes from Cape Town CBD and Caltex, sulphate formation is very slow as OH production is reduced (Figure 24) (USEPA, 1992b). SO_2 emissions from tall stacks become diluted before reaching the ground so that dry deposition is reduced. This increases the atmospheric residence time for SO_2 which promotes SO_2 to SO_4^{2-} conversion (Wilson, 1978). When SO_2 is emitted at low levels, as from the residential wood stoves in Khayelitsha and Mitchell's Plain, the SO_2 can be removed by dry deposition (Wilson, 1978) thereby reducing sulphate formation.

Overall, the SO_2 to SO_4^{2-} conversion rate appears to be underestimated by the model. This is a limitation of PLUVUE II in that the chemical mechanism used in the model to predict the conversion of sulphur and nitrogen oxides is not valid for applications in polluted urban environments (USEPA, 1992b). Eatough *et al* (1994) have estimated the rate of conversion of SO_2 to sulphate by OH to range from less than 1% per hour to 10% per hour at high temperatures and relative humidities. In Los Angeles, during smog episodes, the oxidation rate of SO_2 ranges between 5 and 10% (Manahan, 1991). The model also only considers the gas-phase conversion of SO_2 to SO_4^{2-}. Since Cape Town is a coastal region and is subject to humid conditions, sulphate conversion will also occur in the aqueous-phase. Aqueous-phase reactions dominate daytime sulphate formation for relative humidities greater than 75% (McMurry and Wilson, 1983). Additionally, in winter, the contribution of aqueous-phase reactions to overall sulphate formation will be more significant due to slower daytime SO_2 oxidation by OH radicals (Saxena and Seigneur, 1987). Gillani and Wilson (1983) observed aqueous-phase transformation rates to range between 0.3 – 8% when power station plumes interacted with clouds and light rain.

Nitrogen oxide to nitrate conversion rate

In the gas-phase conversion, the reaction between NO_2 and the OH radical is the principal mechanism of nitrate formation (Pienaar and Helas, 1996). The conversion rate of NO_x to nitrates by OH is approximately 10 times faster than sulphate formation (Hewitt, 2002). Variations in temperature and humidity influence the oxidation rate of nitrates. With a decline in temperature and increase in humidity during the night, particulate nitrate formation is at a maximum. In summer, conversion rates are high due to the increase in the production rate of OH radicals (Warneck, 1988). Modelling studies (Seinfeld, 1986) have indicated an oxidation rate of up to 20% per hour in cloud-free, summer conditions.

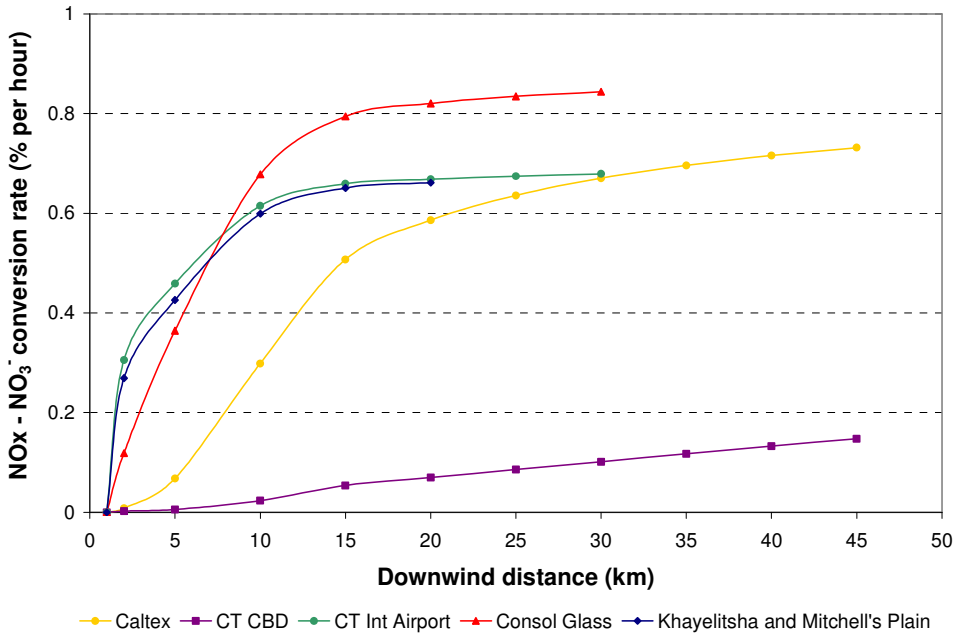

Figure 25. NO_x to NO_3^- conversion rate with downwind distance for all emission sources.

The NO_x to NO_3^- conversion rate showed an increase with distance downwind for all sources. As observed for the sulphate conversion rate, nitrate formation is reduced in concentrated plumes as evident in the plume from the CBD which does not exceed 0.2% per hour (Figure 25). Overall, the NO_x to NO_3^- conversion rate was underestimated by the model at less than 1% per hour due to the previously mentioned model limitation.

Aqueous-phase reactions of nitrate formation are not as significant as those that form sulphates. Aqueous-phase reactions are also much slower than in the gas phase when exposed to solar radiation (Pienaar and Helas, 1996) and hence, will have a reduced role in nitrate formation.

On the basis of the values for SO_2 to SO_4^{2-} and NO_x to NO_3^- conversion rates, it appears that visibility impairment caused by particulates is a result of primary particulates and not secondary particulates. Sulphate and nitrate conversion rates have been underestimated by the model, as seen by comparisons with observed conversion rates. However, it is necessary to consider that these modelled sulphate and nitrate conversion rates are representative of a clean background environment and that

aqueous-phase reactions would also be significant in Cape Town due to the frequent occurrence of clouds and fog.

The PLUVUE II model has been used to model the potential visual impacts that the individual plumes from the five sources have if viewed against the background sky. However, PLUVUE II does not account for regional haze which is an important aspect of air pollution over Cape Town. Therefore, the importance of these sources to visibility impairment needs to be viewed in terms of their contribution to regional haze over the area. An attempt to do this will be undertaken using the CALPUFF Modelling System in order to determine the spatial distribution and temporal variation of the emissions from these sources. An analysis of visibility over Cape Town will also be carried out.

CALPUFF model output

The CALPUFF model was run to evaluate the spatial and temporal distribution and visibility impacts that NO_x, SO_2 and PM10 emissions from the above five sources have over the Cape Town area.

Comparison with ground-based measurements

The CCT has established a comprehensive ground-based monitoring network which consists of 10 continuous monitoring stations which measure concentrations of PM10, PM2.5, SO_2, NO_x, O_3, CO and H_2S. Modelled NO_x, SO_2 and PM10 concentrations on 22 August (haze day) are compared with available ground-based data from the CCT's air quality monitoring network. Modelled concentrations are based on a constant source emission rate and are so influenced by the prevailing meteorological conditions for each hour. Modelled pollutant concentrations within the lowest 500 m of the atmosphere are compared to the ambient concentrations measured on the ground. During SAFARI-92, Diab *et al* (1996a and b) observed that a sharp increase in O_3 concentrations is experienced between the surface and the lowest 1 km layer over southern Africa. Due to this, it is recognised that some variation in pollutant concentrations will be observed when comparing the surface concentrations with the modelled concentrations.

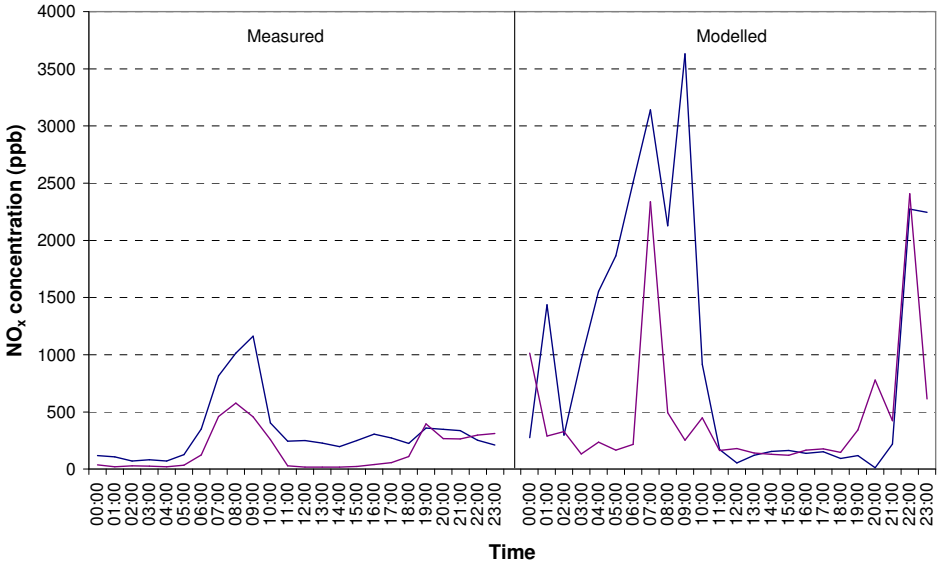

Figure 26. Comparison of the City of Cape Town's ground-based (left) and modelled NO_x concentrations (right) for City Hall (blue) and Goodwood (purple).

Modelled NO_x concentrations have been overpredicted by a factor of 4. This could be a result of high source emission rates that were input into the model. Despite this, CALPUFF has modelled the peak in concentrations between 06:00 to 10:00 in the morning which corresponds with peak hour traffic volumes as people depart for work. Measured values show that City Hall has particularly elevated concentrations as a large proportion of people work in the CBD. Goodwood, a residential area situated centrally in the Cape Town area, also experienced elevated concentrations (Figure 26). Nitrogen oxide concentrations have only been measured at Khayelitsha since September 2004. However, NO_x concentrations are similar to the levels measured at City Hall and higher than those at Goodwood (G. Ravenscroft, personal communication, 2005). The influence of low wind speeds in the morning, coupled with a surface inversion is evident in the high NO_x concentrations during the morning rush hour. By the afternoon rush hour, faster wind speeds effectively disperse traffic emissions resulting in reduced concentrations. CALPUFF models a much sharper peak in the late evening than is observed.

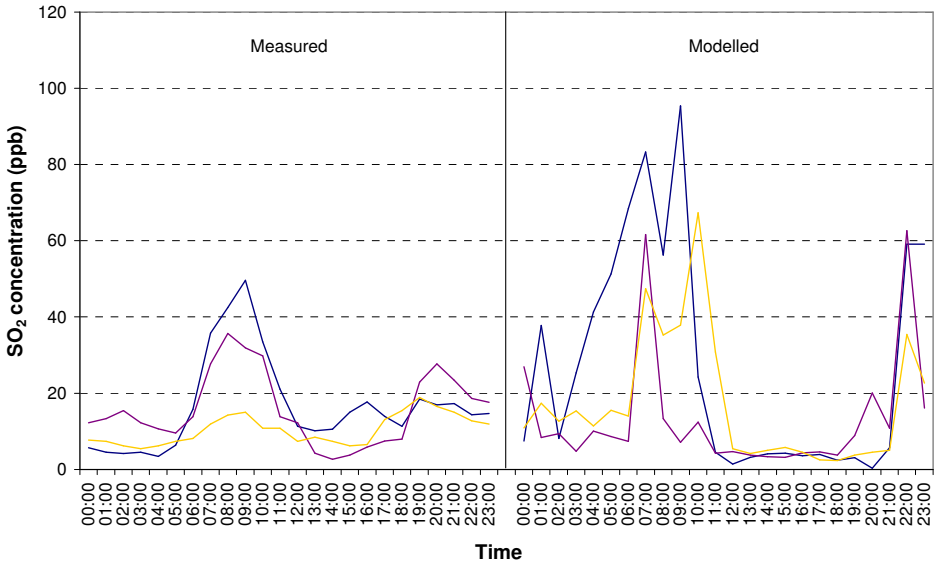

Figure 27. Comparison of the City of Cape Town's ground-based (left) and modelled SO_2 concentrations (right) for City Hall (blue), Goodwood (purple) and Khayelitsha (yellow).

Modelled SO_2 concentrations have been overpredicted by a factor of 2. CALPUFF has again identified the morning peak between 06:00 and 11:00 with a much sharper peak in the late evening between 21:00 and 24:00 than is measured (Figure 27). The elevated concentrations are due to high traffic volumes, particularly at City Hall and Goodwood.

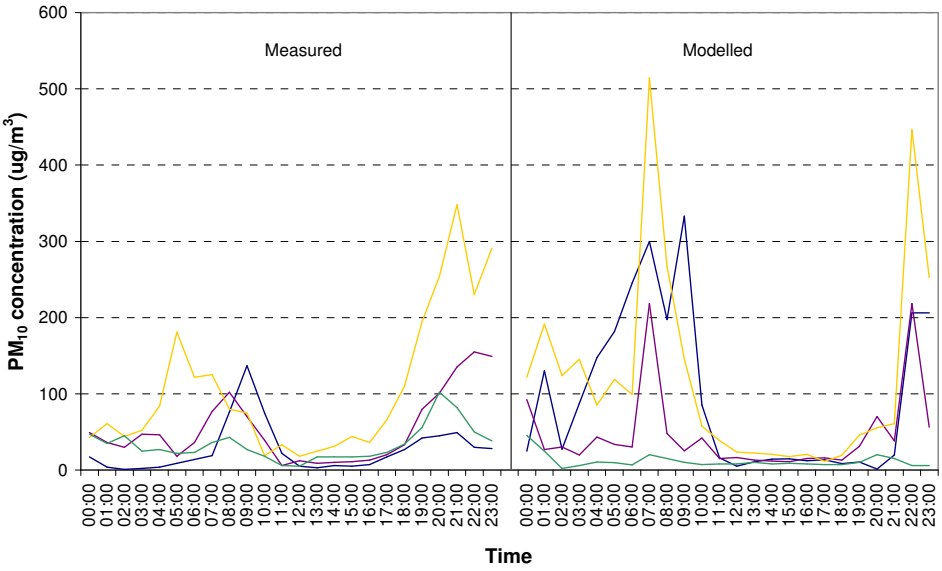

Figure 28. Comparison of the City of Cape Town's ground-based (left) and modelled PM10 concentrations (right) for City Hall (blue), Goodwood (purple), Khayelitsha (yellow) and Table View (green).

Modelled PM10 concentrations have been overpredicted by a factor of 1 to 2. The elevated concentrations in the early morning between 07:00 and 10:00, and again after 19:00 in the late evening have been modelled (Figure 28). The concentration of aerosols in the early morning and evening is due to the surface inversion which effectively traps the pollutants in the lower atmosphere. Aerosol concentrations in Khayelitsha were especially elevated, reaching 350 $\mu g/m^3$ in the late evening of the haze day. The peaks experienced in Khayelitsha are due to the burning of wood for space heating and cooking in the early morning and late evening. The peaks at City Hall, Goodwood and Table View are due to high traffic volumes at these times as people depart to and from work, respectively.

Comparison with aircraft measurements

Modelled NO_x, SO_2 and PM10 concentrations are compared with aircraft data for the month of August. In the diagrams below, the aircraft data is presented as an average of all the flights undertaken during the Cape Town Brown Haze II field campaign while the modelled data is an average for the month.

Nitrogen oxides

Elevated NO_x concentrations over 100 ppb are measured over most of the Cape Town region. Reduced concentration levels are observed over Stellenbosch, Somerset West, Strand and False Bay. CALPUFF has modelled elevated concentrations over the Cape Town CBD and the immediate surrounding areas. Reduced concentrations are modelled over the rest of Cape Town. CALPUFF has not identified the elevated concentrations over Table View suggesting that the NO_x emissions input into the model for Caltex may have been underestimated (Figure 29). However, it should be recognised that the aircraft concentrations are representative of all sources in the CCT while the modelled concentrations are attributed only to the selected sources, therefore, this difference in the spatial distribution of NO_x concentrations can be expected.

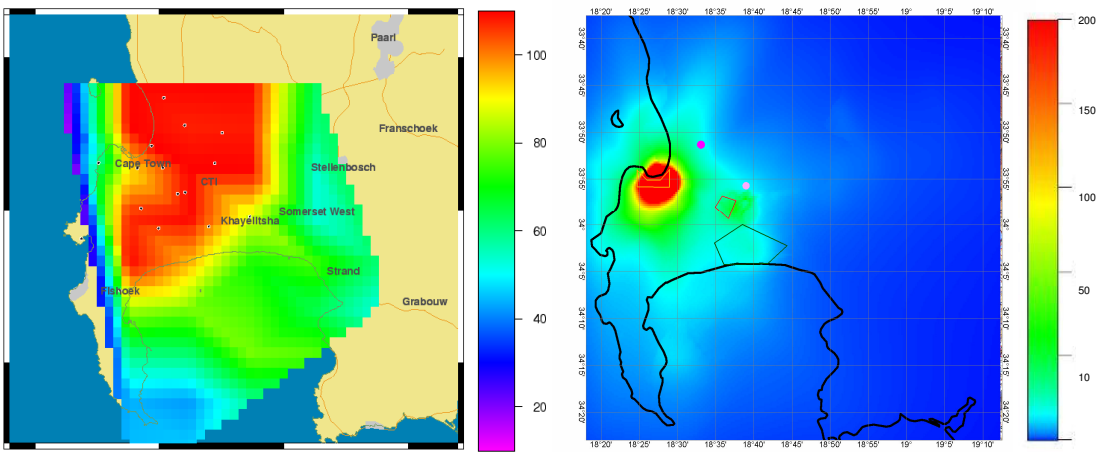

Figure 29. Spatial comparison of aircraft (left) and modelled NO_x concentrations (ppb) (right) over the Cape Town region for August 2003.

Sulphur dioxide

During August, elevated SO_2 concentrations are only measured over Table View with very low concentrations over most of Cape Town. Elevated concentrations are not observed in the Cape Town CBD as would be expected due to the influence of

diesel vehicles. CALPUFF has modelled reduced concentrations over the Cape Town CBD and the townships as well as identifying emissions from Caltex Oil Refinery in Table View. Emissions from Caltex are transported a large distance downwind from the source within the Cape Town area (Figure 30).

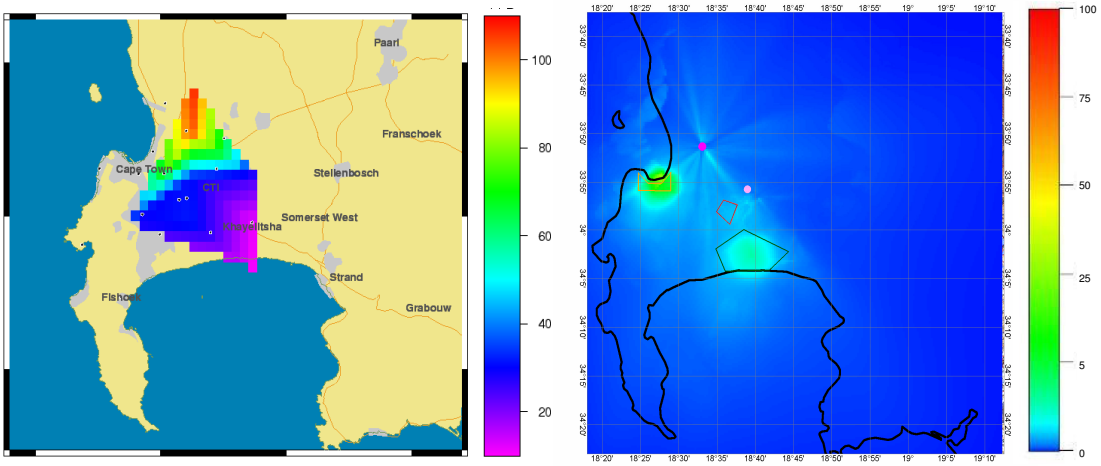

Figure 30. Spatial comparison of aircraft (left) and modelled SO_2 concentrations (ppb) (right) over the Cape Town region for August 2003.

Aerosols

High aerosol loading is measured over a large part of the Cape Town region, including the suburban area of Table View, the industrial area of Bellville and the townships of Khayelitsha and Mitchell's Plain. Elevated concentrations are also observed over the Strand as pollutants are trapped within the basin. CALPUFF has modelled elevated aerosol concentrations over two areas, the Cape Town CBD and the townships. Reduced aerosol concentrations are predicted over the rest of Cape Town. The Strand has not been identified by CALPUFF to have elevated concentrations (Figure 31). The difference in the spatial distribution of aerosol concentrations reflects the discrepancy between the number of measured and modelled sources.

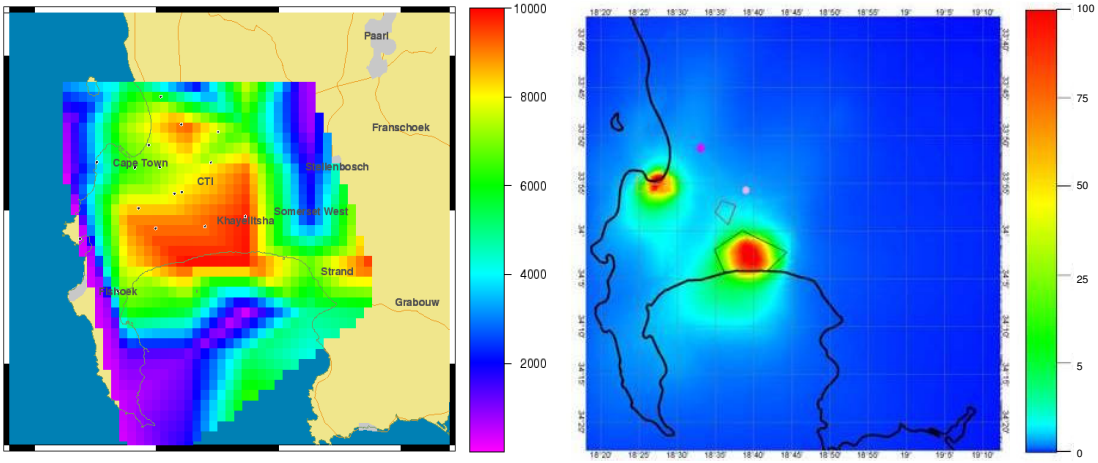

Figure 31. Spatial comparison of aircraft (left) and modelled aerosol concentrations (right) over the Cape Town region for August 2003 (Aircraft data is measured in $n.cm^{-3}$ and modelled data in $\mu g/m^3$).

Spatial distribution of concentrations

The spatial distribution of modelled NO_x, SO_2 and PM10 concentrations over the CCT for 1-hour, 3-hour and 24-hour averaging periods is shown in the figures below.

Nitrogen Oxides

Nitrogen oxide concentrations on the non-haze day, 13 August, are significantly reduced compared to the haze day, 22 August, for the worst 1-hour, 3-hour and 24-hour averages. On 13 August, a strong northerly wind transported the pollutant southwards out over False Bay and the surrounding areas. Cape Town CBD was the only significant source of NO_x emissions, originating from vehicular traffic entering and leaving the area. On 22 August, variability in the wind direction promoted the stagnation of the pollutant around the region for the worst 1-hour and 3-hour averages. Over the whole day, Cape Town CBD was again the dominant source of NO_x emissions (Figure 32).

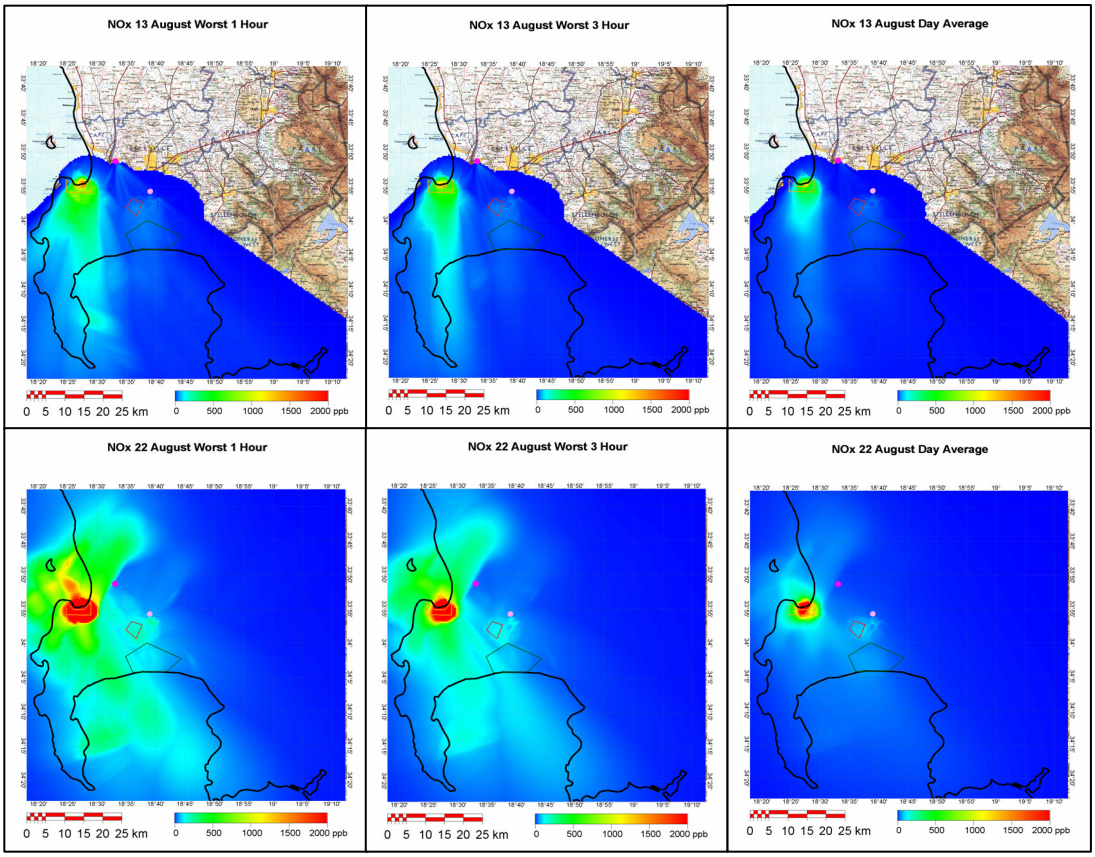

Figure 32. Spatial distribution of NO_x concentrations on 13 August (top) and 22 August (bottom) for the worst 1-hour, 3-hour and 24-hour averages.

Sulphur dioxide

The strong northerly wind that prevailed on 13 August transported SO_2 southwards out over False Bay. Caltex was the dominant source of SO_2 emissions with the contribution of diesel emissions from the CBD also important over all the averaging periods. On 22 August, higher concentrations from Caltex and the CBD were observed with a similar southerly transect out over False Bay and the Strand for the worst 1-hour and 3-hour averaging periods. The Cape Town CBD, Caltex and the townships were the dominant sources on the day of 22 August (Figure 33).

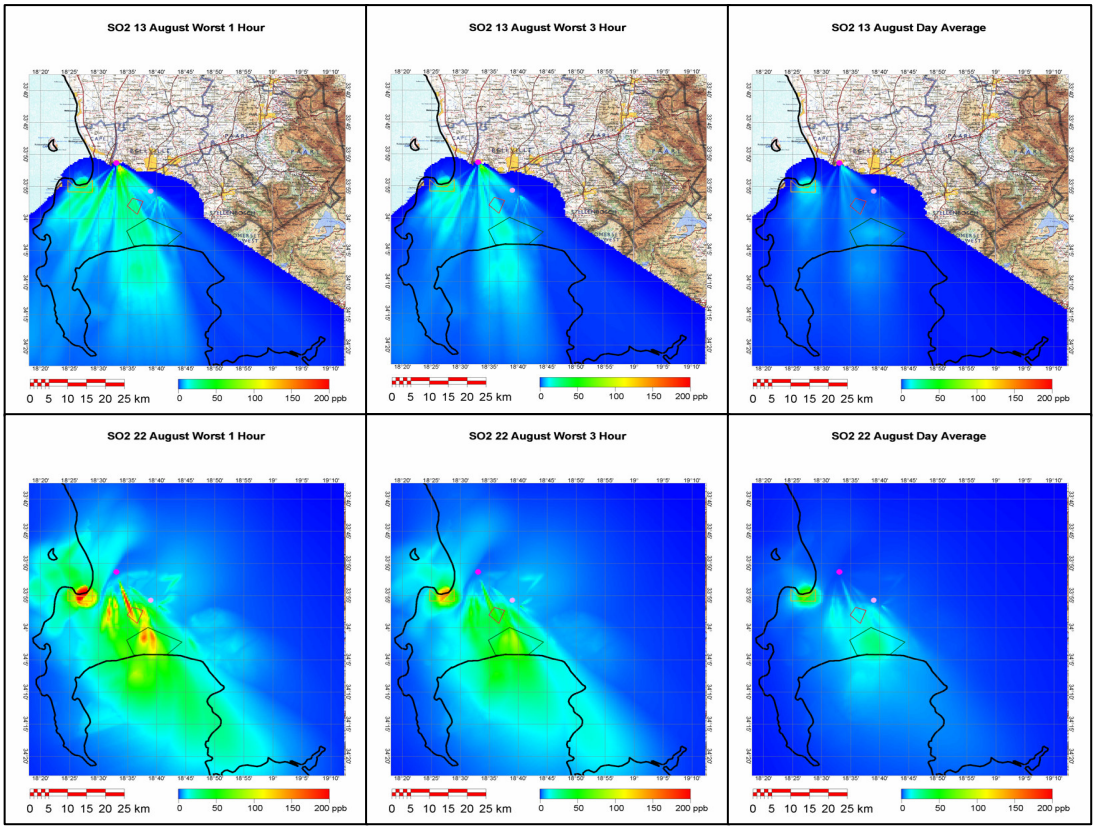

Figure 33. Spatial distribution of SO_2 concentrations on 13 August (top) and 22 August (bottom) for the worst 1-hour, 3-hour and 24-hour averages.

Aerosols (PM10)

The aerosol loading over Cape Town originates from two main sources on 13 and 22 August, namely, Cape Town CBD and Khayelitsha and Mitchell's Plain, although the impact and extent of emissions from each source is greater on the haze day than the non-haze day In the CBD, particulates are released during combustion in vehicles, particularly from diesel vehicles. Particulate emissions from the townships originate from the burning of fuels such as wood and paraffin (Figure 34).

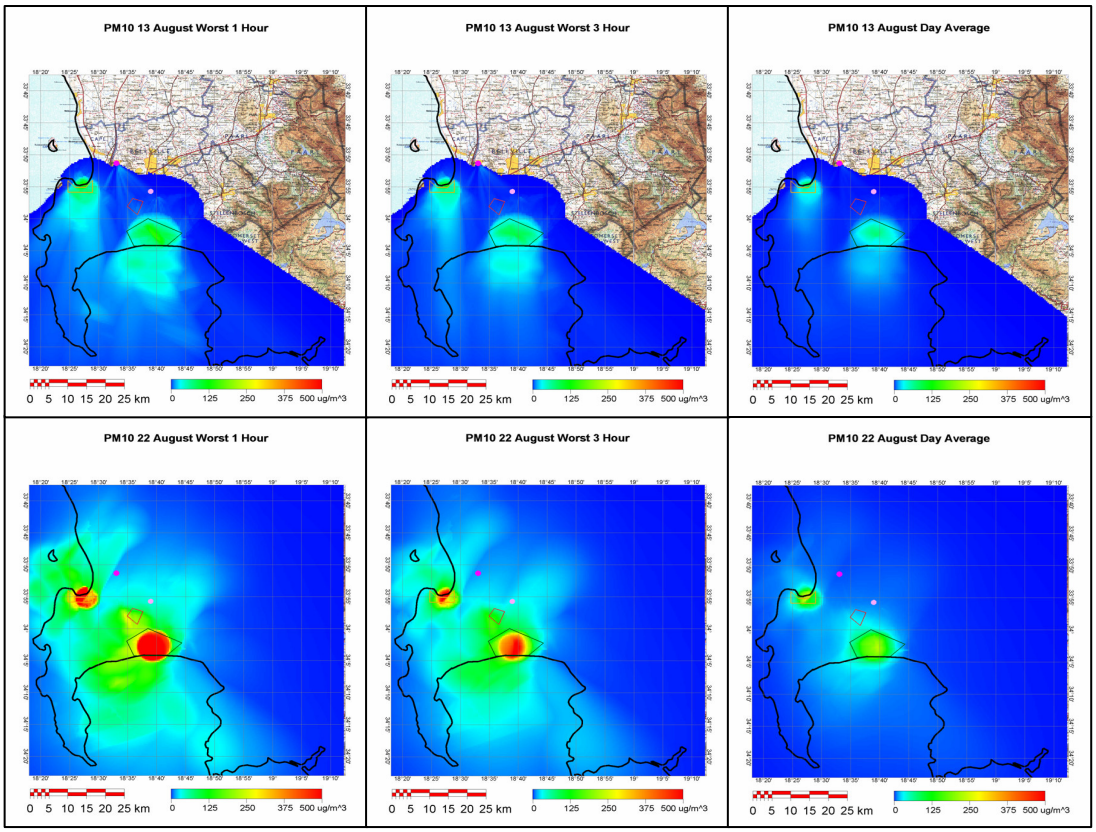

Figure 34. Spatial distribution of PM10 concentrations on 13 August (top) and 22 August (bottom) for the worst 1-hour, 3-hour and 24-hour averages.

Temporal variation of concentrations

The temporal variation of NO_x, SO_2 and PM10 concentrations over the CCT is shown in the figures below. Modelled hourly concentrations are based on a constant source emission rate and are therefore influenced by the meteorological conditions.

Nitrogen oxides

Nitrogen oxides concentrations on 22 August are elevated from midnight until the late morning (10 am) in the CBD due to stable conditions which prevail during the night and early morning. For the most part, winds change between south-westerly to south-easterly and north-easterly to northerly during this time. The highest NO_x concentrations are observed between 7 am and 8 am in the early morning,

corresponding with peak hour traffic. CALPUFF has modelled the peak in concentrations between 6 am and 10 am as recorded in the CBD by the CCT. After 10 am, NO_x concentrations are reduced as the inversion is eroded away by surface heating so that the pollutant is mixed with ambient air. During the afternoon, north-westerly winds transport emissions from the city centre towards False Bay. From 6 pm, NO_x concentrations start to increase in the CBD as stable conditions trap the pollutant within the lower atmosphere so that by the late evening, high NO_x concentrations are experienced (Figure 35 and 36).

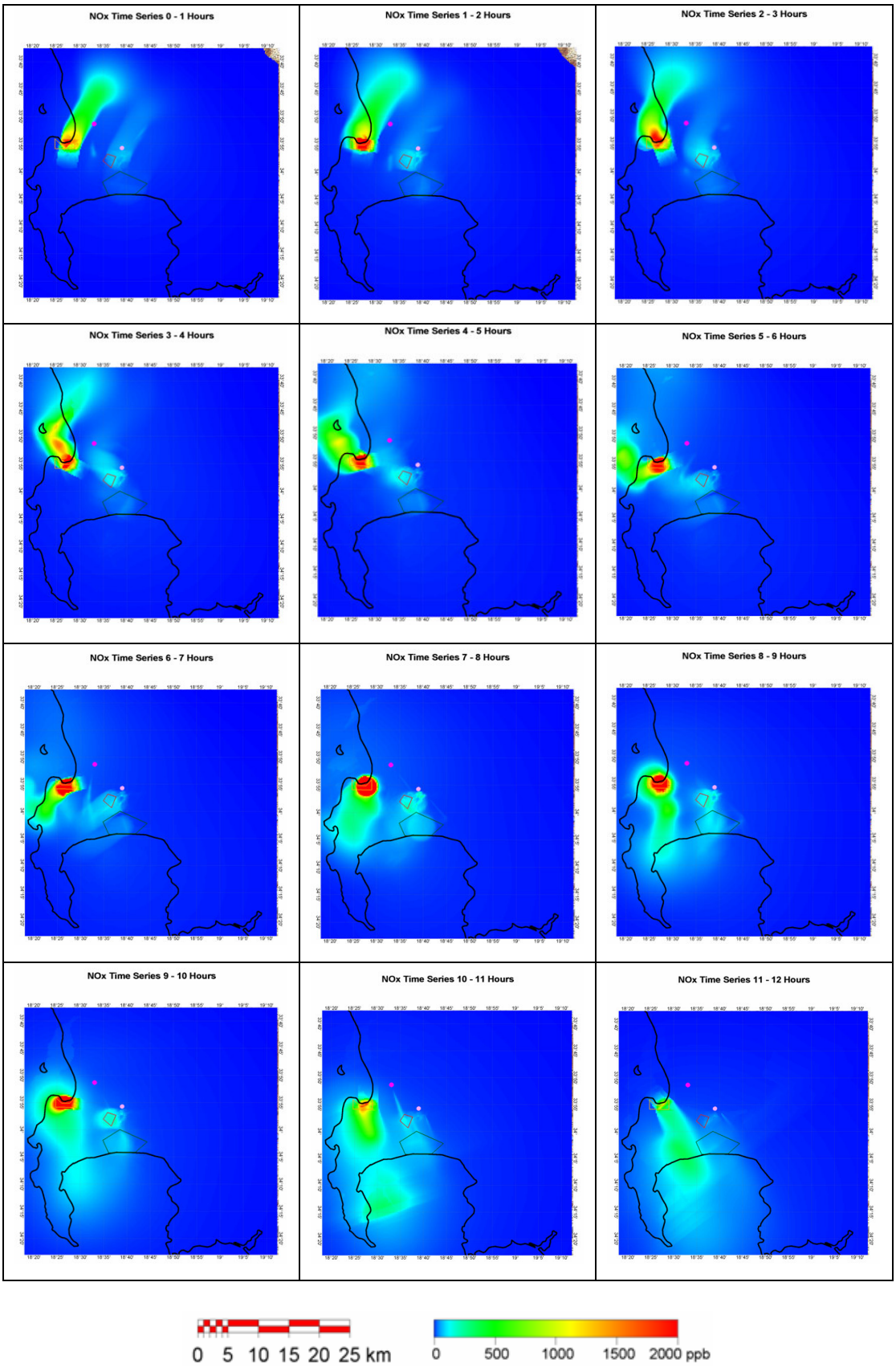

Figure 35. Nitrogen oxide concentration time series (00 – 12 hours) for 22 August 2003.

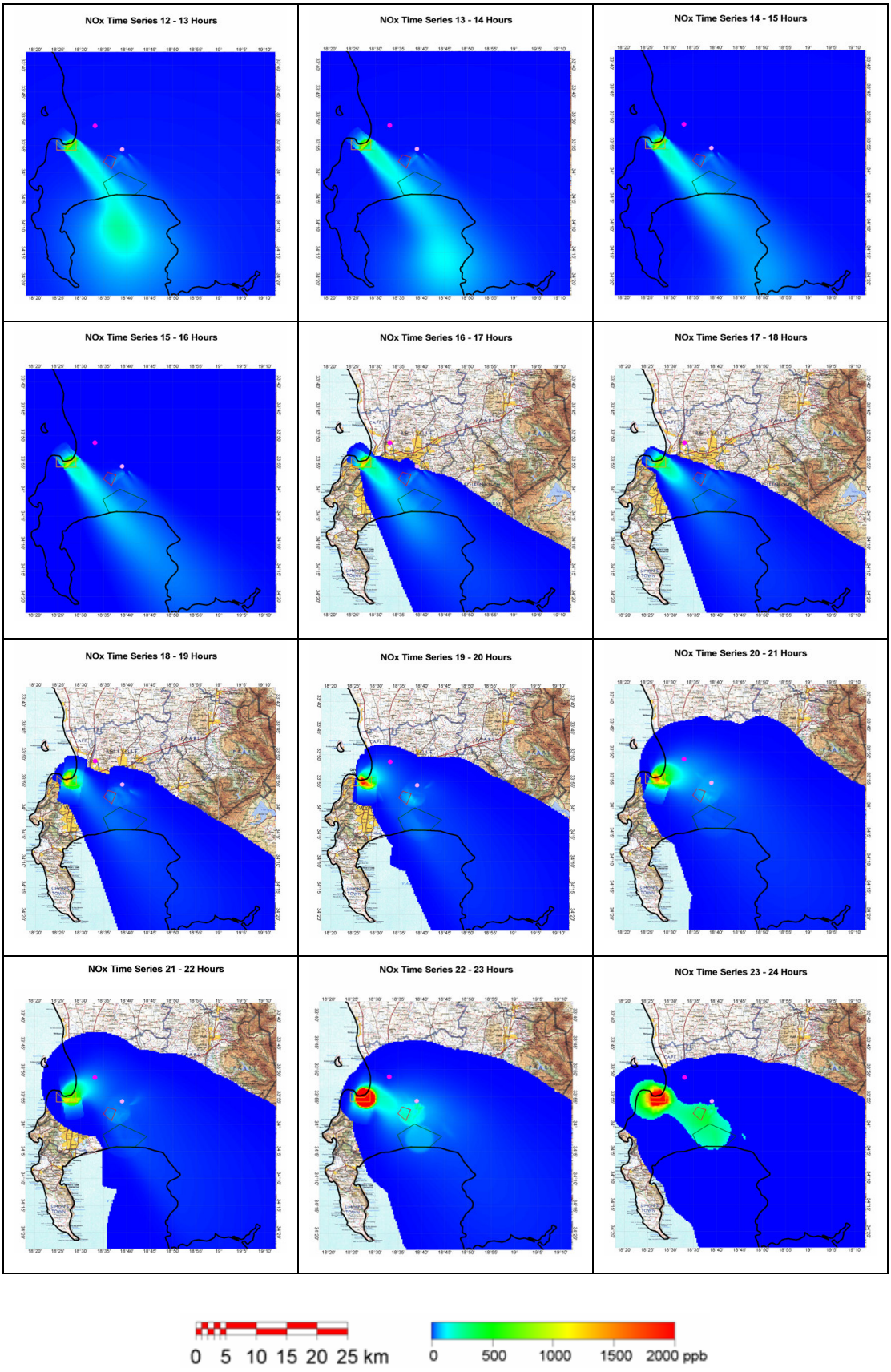

Figure 36. Nitrogen oxide concentration time series (12 – 24 hours) for 22 August 2003.

Sulphur dioxide

Sulphur dioxide concentrations on 22 August are reduced over the Cape Town region in the early morning. During the early morning, south-easterly winds transport SO_2 emissions from the CBD out towards Robben Island while emissions from the other sources accumulate directly above in the atmosphere. The highest SO_2 concentrations are observed in the Cape Town CBD from 7 am – 8 am due to the influx of vehicles into this area. The CCT recorded peak in concentrations in the CBD has also been modelled between 6 am and 10 am. Emissions from Caltex remain elevated until the late morning. As the surface inversion is eroded away, the SO_2 emissions that have accumulated over Cape Town are transported out over False Bay by north-westerly winds. After 12 pm, SO_2 levels are significantly reduced with Caltex, the CBD and Consol Glass, being the only sources. The observed peak in SO_2 concentrations in the afternoon in the CBD has not been modelled by CALPUFF. North-westerly winds associated with the passage of a cold front dominate the wind field during the most part during 22 August. Sulphur dioxide concentrations remain low until 10 pm when increased levels are observed in the CBD and over the townships as stable conditions dominate the atmosphere (Figure 37 and 38).

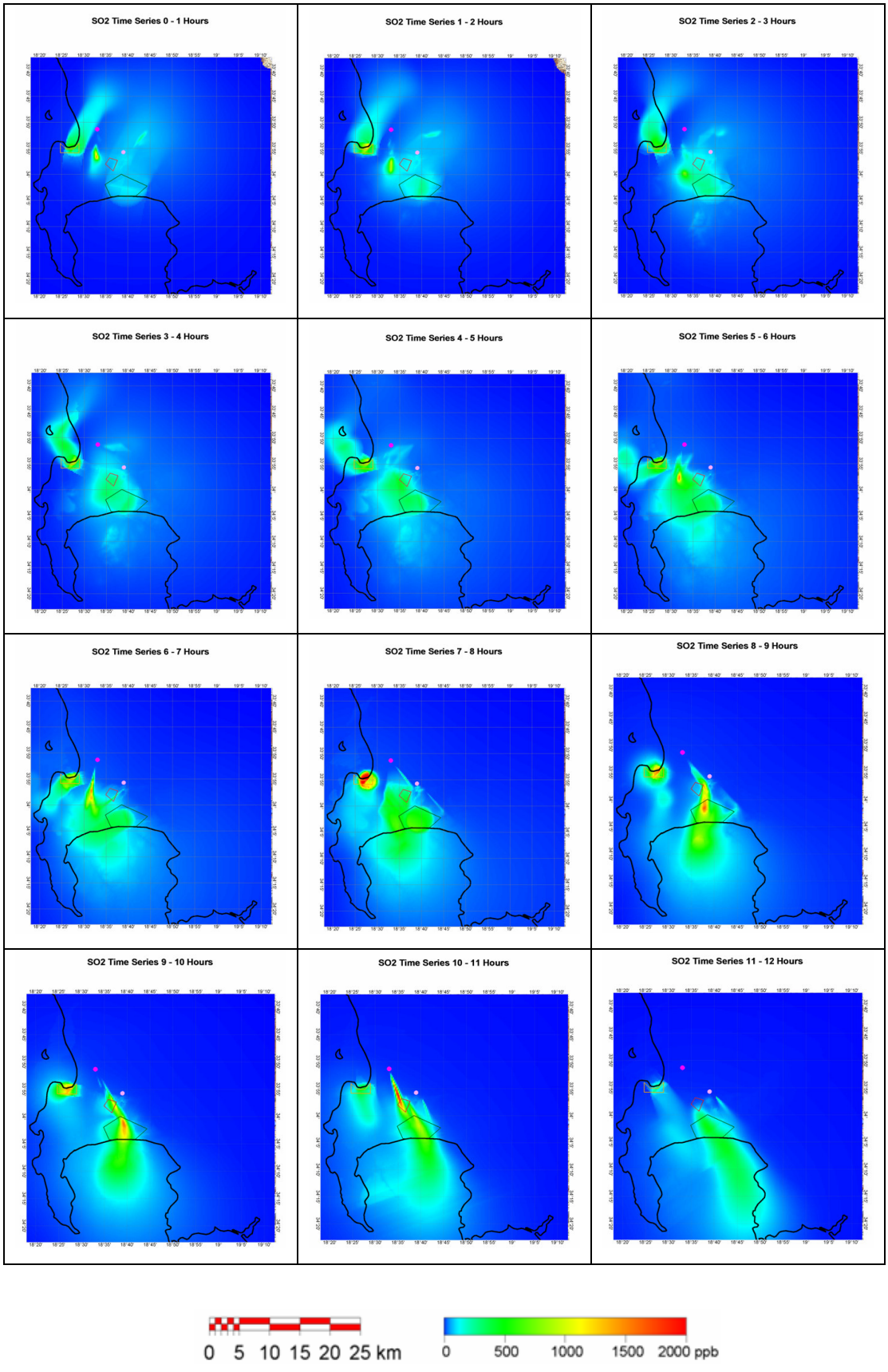

Figure 37. Sulphur dioxide concentration time series (00 – 12 hours) for 22 August 2003.

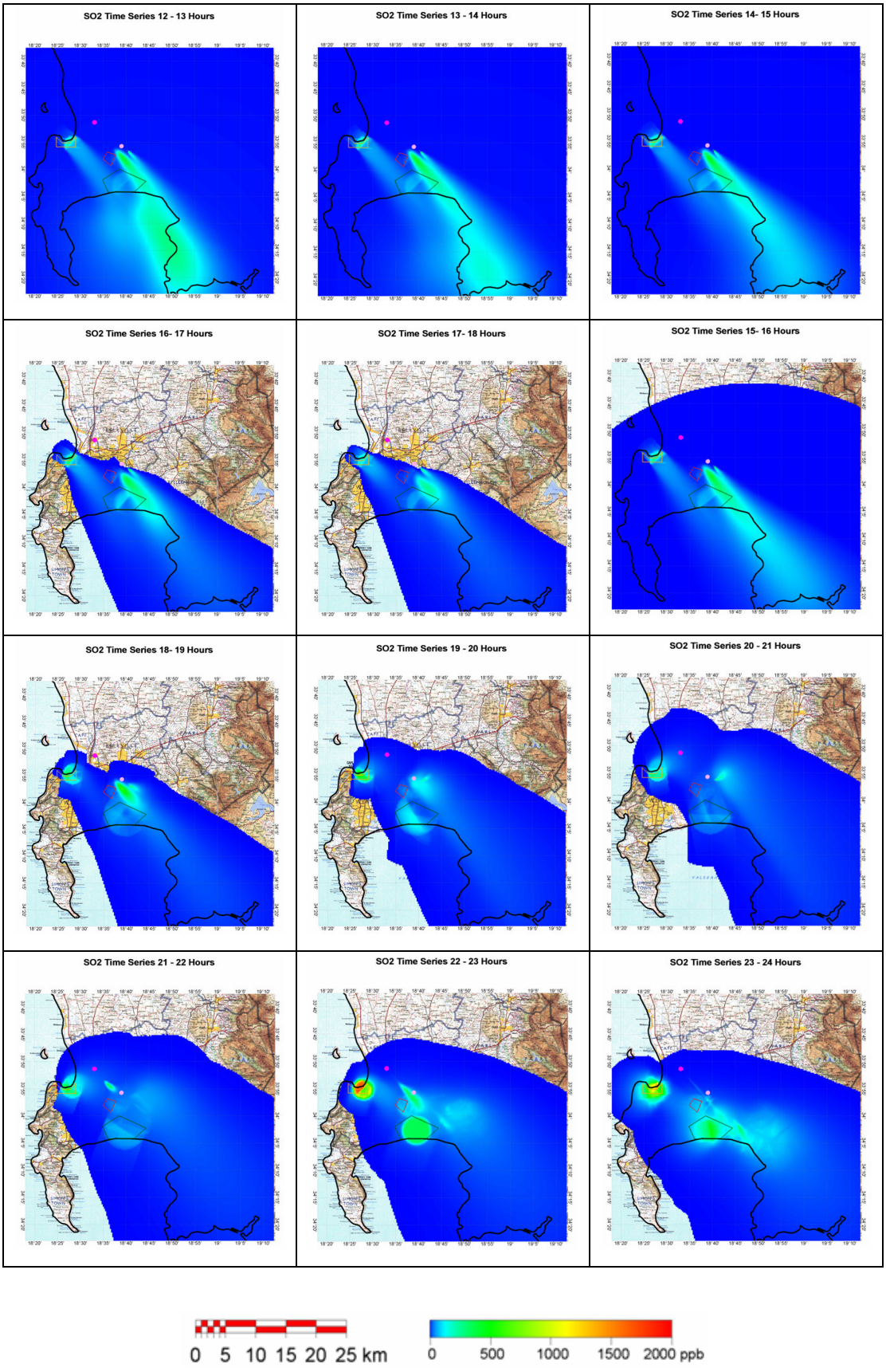

Figure 38. Sulphur dioxide concentration time series (12 – 24 hours) for 22 August 2003.

Aerosols (PM10)

Particulate concentrations are elevated in the early morning of 22 August. Cape Town CBD and the townships are the only source of particulate emissions with the highest concentrations observed over these sources between 7 am and 8 am. Elevated concentrations over the townships are attributed to wood and paraffin burning during this time while particulate emissions from the CBD are due to vehicular activity. The peak in PM10 concentrations, as modelled by CALPUFF, correlates with the peak recorded in the CBD by the CCT. At Khayelitsha, the recorded peak in the early morning between 3 am and 9 am has been modelled accurately. As the morning progresses, PM10 emissions from the townships accumulate in a pool over False Bay. Over the course of the day, PM10 levels are significantly reduced over the Cape Town area. The recorded peak in concentrations between 5 am and 12 am in the CBD and Khayelitsha has not been modelled by CALPUFF. It is only in the late evening, between 10 pm and 12 pm, that elevated concentrations are observed over these areas due to increased atmospheric stability (Figure 39 and 40).

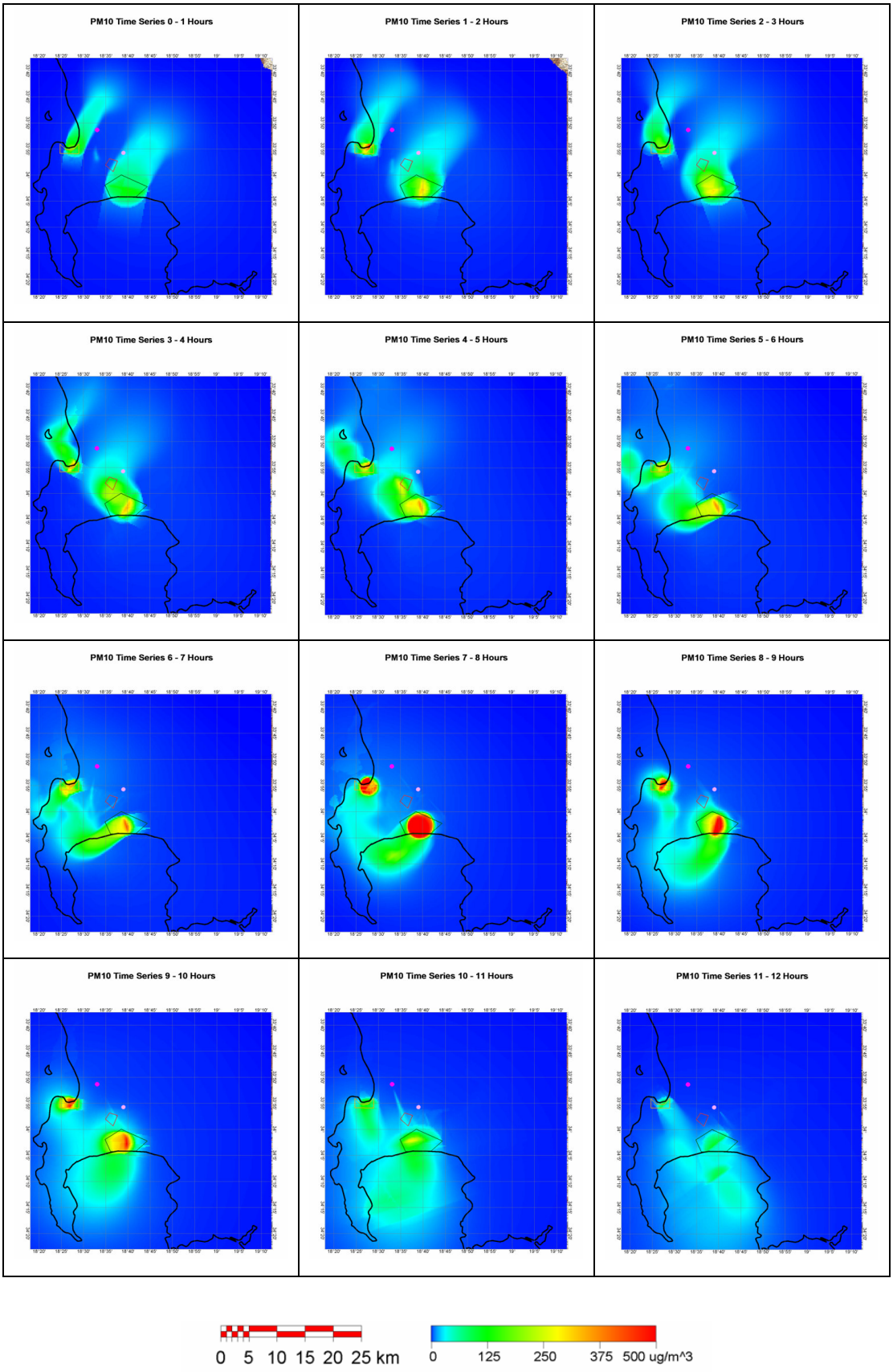

Figure 39. Aerosol concentration time series (00 – 12 hours) for 22 August 2003.

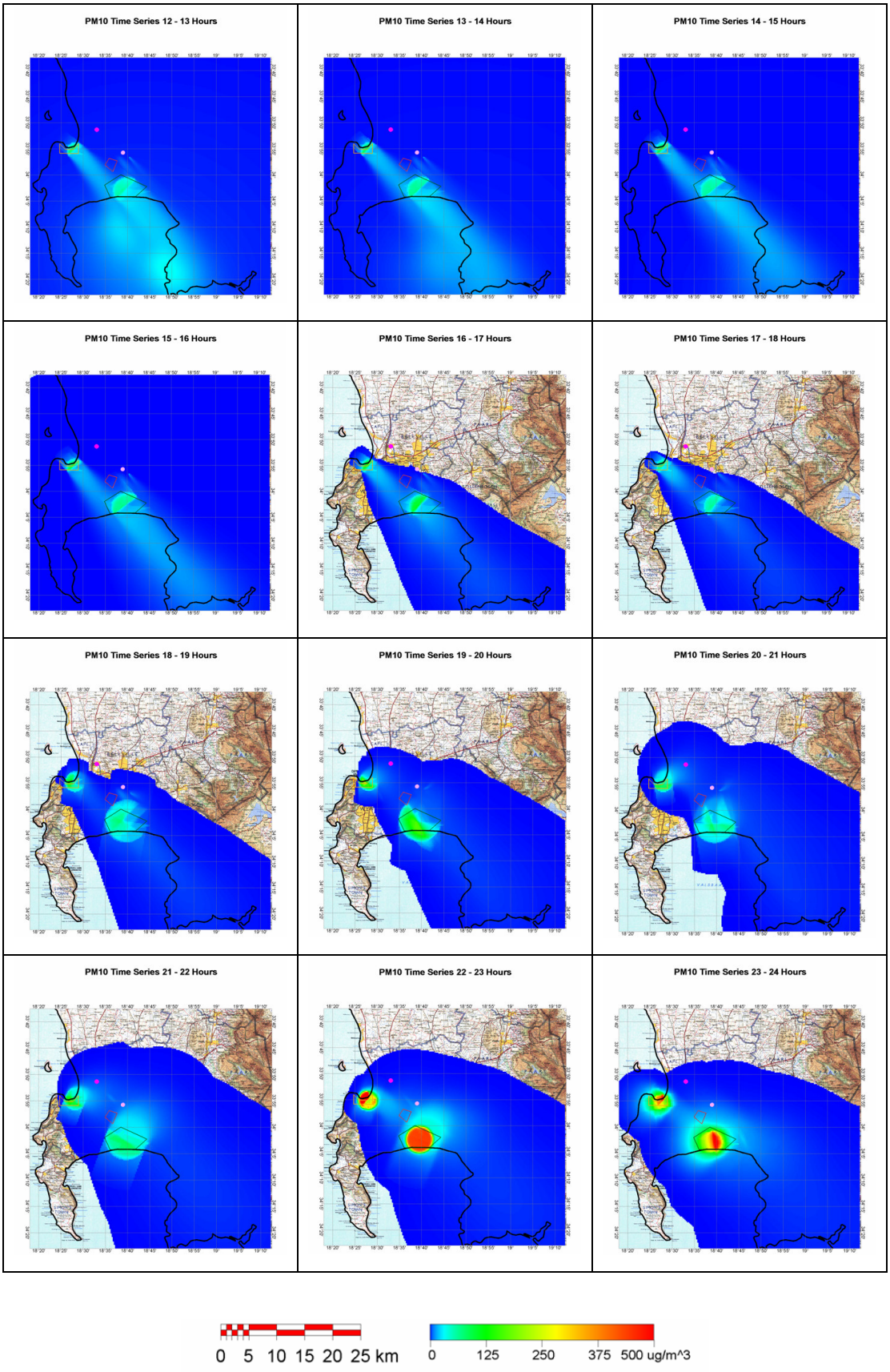

Figure 40. Aerosol concentration time series (12 – 24 hours) for 22 August 2003.

Visibility

Due to overestimated NO_x, SO_2 and PM10 concentrations, the magnitude and extent of visibility degradation over Cape Town has been overpredicted. Visibility degradation is determined by the light extinction coefficient, b_{ext}, and is expressed in inverse megameters (Mm^{-1}). As a reference, the light extinction from Rayleigh scattering is approximately 10 Mm^{-1} and corresponds to a pristine environment. An extinction value of 1000 Mm^{-1} corresponds to a 4 km visual range (Malm, 1999). A background light extinction of 78 Mm^{-1} has been calculated for the Cape Town region based on the Koschmieder equation. However, this equation has a number of assumptions which include 1) sky brightness at the observer is similar to the sky brightness at the observed object; 2) a homogenous distribution of pollutants; 3) a horizontal viewing distance; 4) earth curvatures are ignored; 5) a large black object and 6) a threshold contrast of 0.02 (Charlson *et al*., 1978; Malm, 1979).

No significant change in visibility is observed on 13 August. Visibility degradation on 22 August is evident over all the averaging periods. The worst 1-hour and 3-hour averages show extreme visibility degradation over the Cape Town CBD and areas northwards towards Table View. Over the course of the day, visibility degradation is observed in Cape Town and over the townships (Figure 41). The pattern of visibility impairment is similar to the spatial distribution of NO_x and PM10 concentrations over the CCT, indicating the importance of these components to visibility impairment of the brown haze.

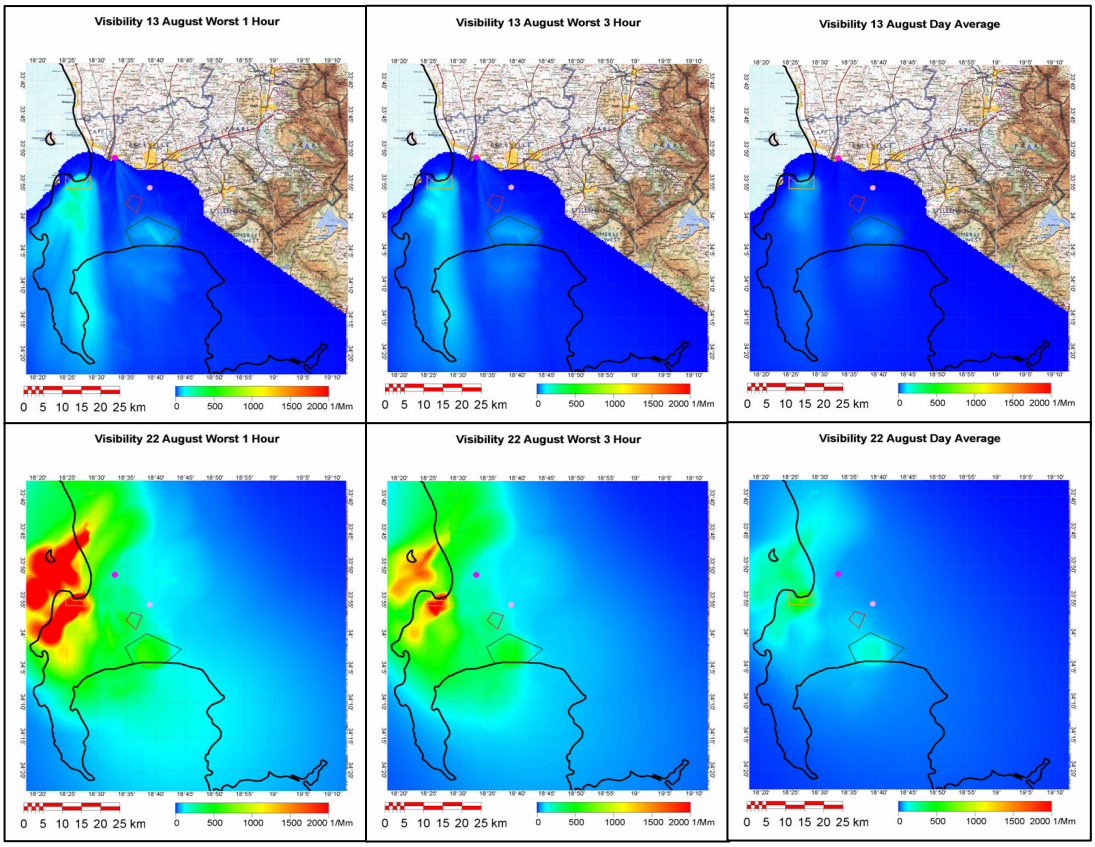

Figure 41. Visibility on 13 August (top) and 22 August (bottom) for the worst 1-hour, 3-hour and 24-hour averages.

Visibility time series

The greatest visibility reduction on 22 August is apparent between 3 am and 9 am in the morning as a consequence of stability. In the early hours of the morning, southerly to south-easterly winds transport emissions northwards, so that the greatest visibility reduction is observed northwards of Cape Town and over the Table View area. By the early morning, a shift in wind direction transports pollutants over the Cape Town region so that the greatest visibility reduction is observed in these areas. By 9 am, pollutants are able to disperse into the upper atmosphere so that visibility is only reduced directly over the area sources of the CBD and the townships. During the afternoon and evening, no visibility reduction is evident over the Cape Town region as the pollutants have dispersed during the morning (Figure 42 and 43).

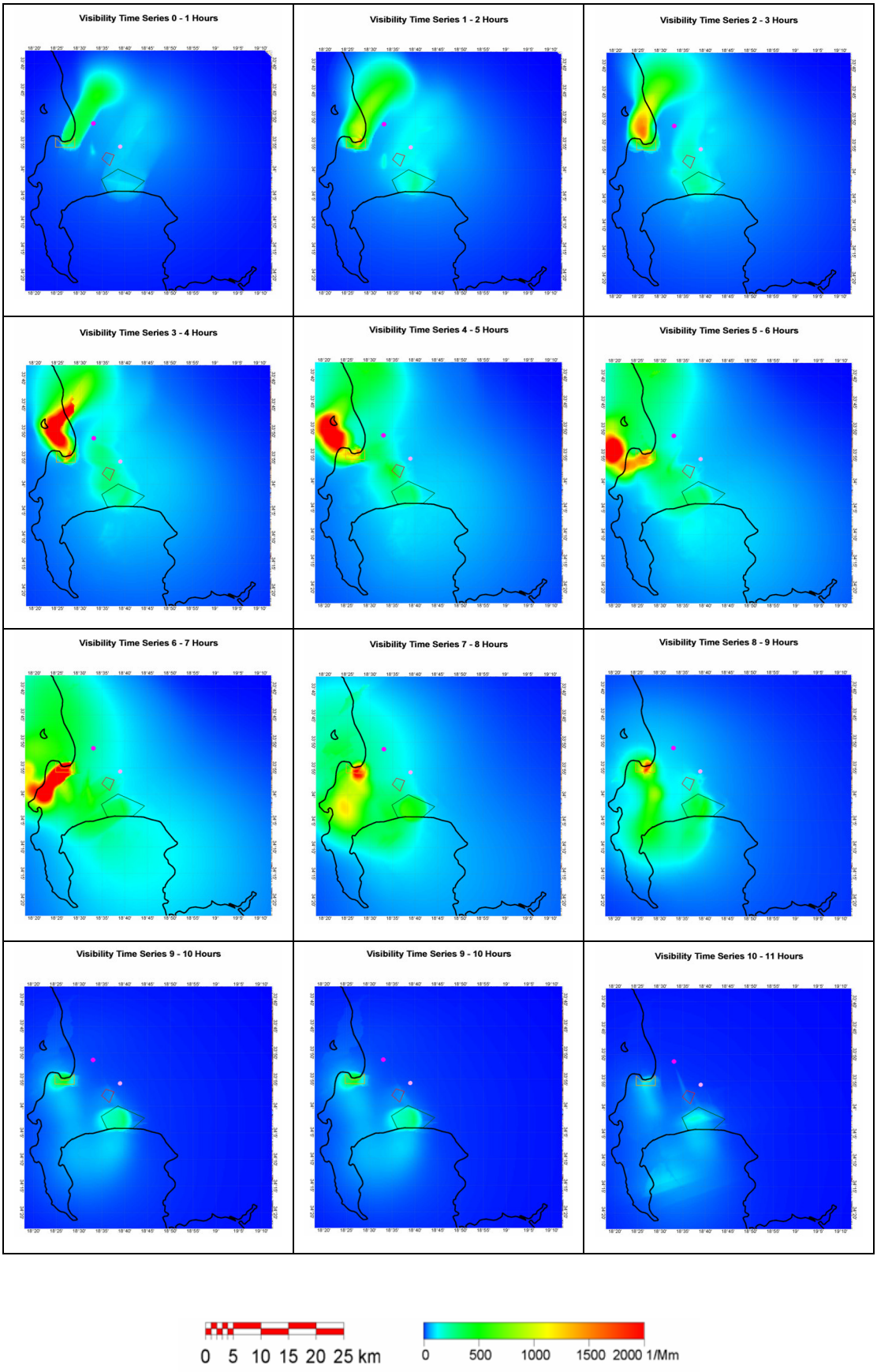

Figure 42. Visibility time series (00 – 12 hours) for 22 August 2003.

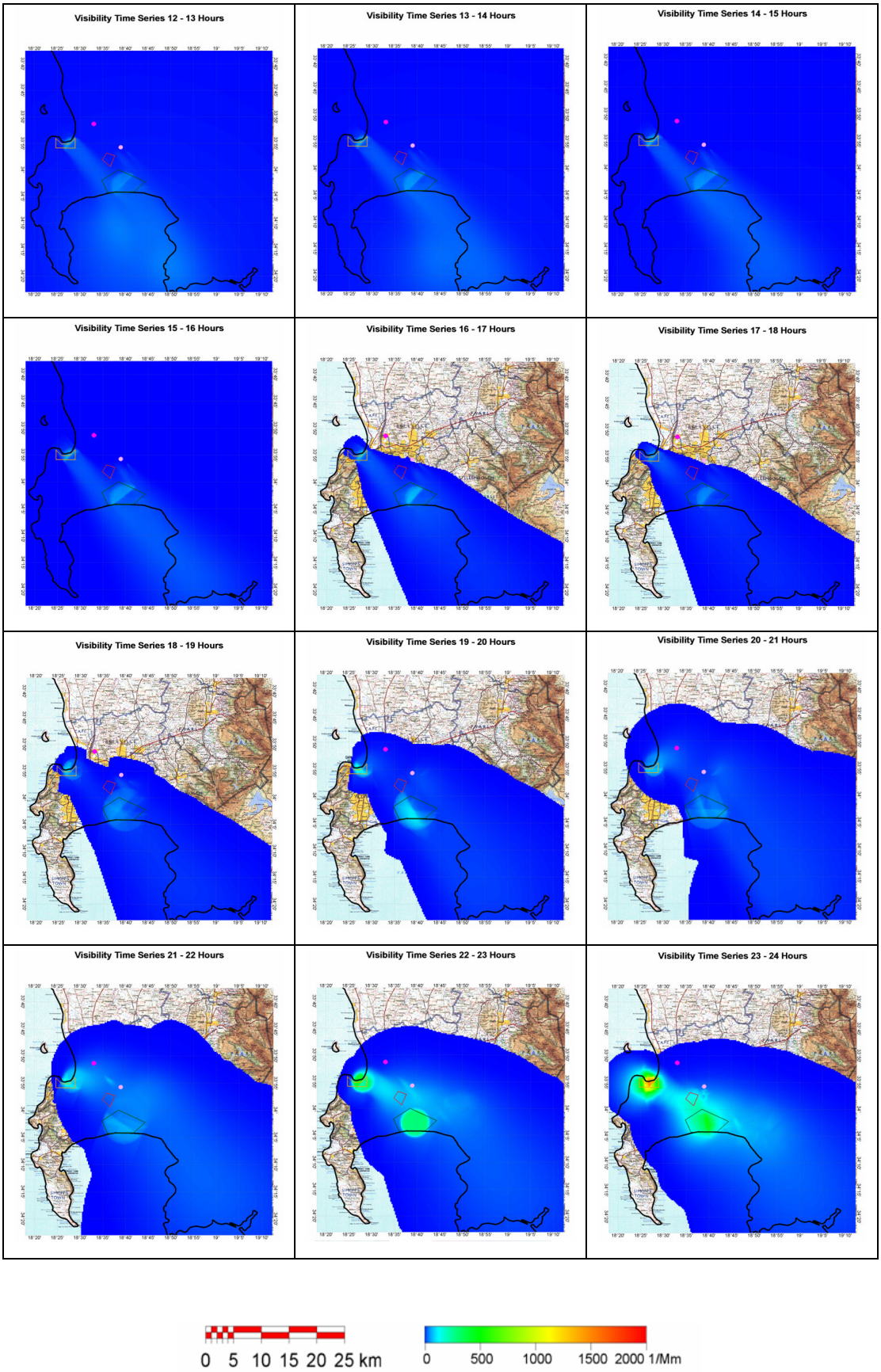

Figure 43. Visibility time series (12 – 24 hours) for 22 August 2003.

A time series analysis of the main pollutants has indicated that early morning concentrations are elevated as source emissions are trapped below a surface inversion that has developed with night-time cooling. For the most part, the highest concentrations are observed between 7 am and 8 am in the morning and are associated with increased traffic volumes and human activity during this period. CALPUFF has accurately modelled the morning peak in pollutant concentrations as recorded by the CCT's air quality monitoring network. With surface heating during the morning, the inversion is eroded away and the pollutants that have accumulated in the lower atmosphere are able to be effectively diluted and dispersed. Afternoon and early evening concentrations are generally low with a sharp increase observed between 10 pm and 12 am as pollutants that have been emitted into the atmosphere during the early evening are trapped below an inversion. The recorded evening peak in concentrations has not been modelled by CALPUFF for all the pollutants. With regard to visibility, a similar pattern is observed over the course of 22 August. The main emission sources contributing to elevated concentrations over the Cape Town region are the area sources of the Cape Town CBD and the townships of Khayelitsha and Mitchell's Plain.

Chemical relationships

PM10 to SO_2

Comparison of the relationships between measured and modelled concentrations of individual pollutant species is made at Khayelitsha due to data availability at this site. The measured concentrations of PM10 and SO_2 show only a weak linear relationship (R^2 = 0.3246) while the modelled concentrations show a distinct linear relationship (R^2 = 0.6599) (Figure 44). The linear relationship indicates that no chemical transformation has occurred. This suggests that the model has not accurately modelled the relationship between the two variables.

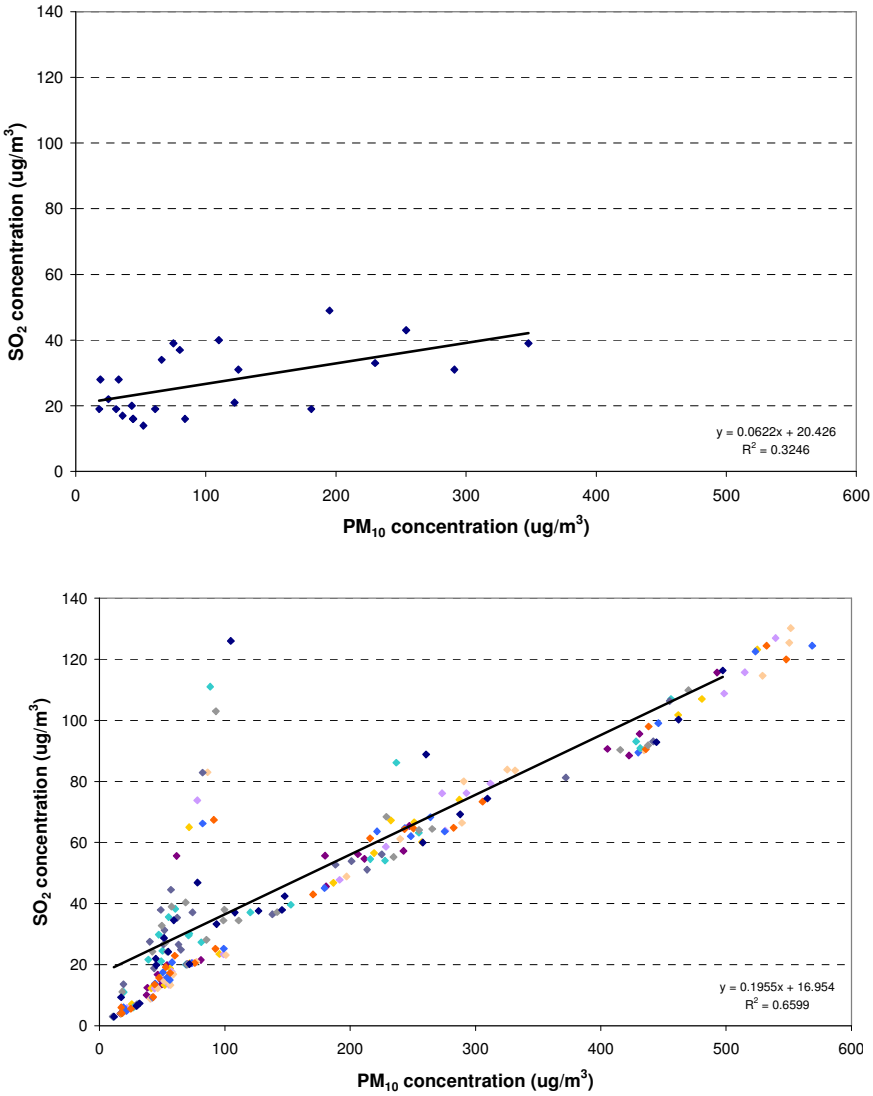

Figure 44. PM10 versus SO_2 at Khayelitsha for measured (top) and modelled (bottom) concentrations.

PM10 to NO_x

Comparison of the measured concentrations and modelled concentrations is made at Cape Town CBD due to data availability at this site. Compared to the SO_2 relationship, a stronger linear relationship exists between the measured PM10 and NO_x concentrations (R^2 = 0.6407) while the modelled concentrations have a strong linear relationship (R^2 = 0.9843) between the two variables (Figure 45). The source of both PM10 and NO_x at this site is likely to be from motor vehicles as a primary emission. The good relationship between the two atmospheric components in the observed and modelled data reflects this relationship.

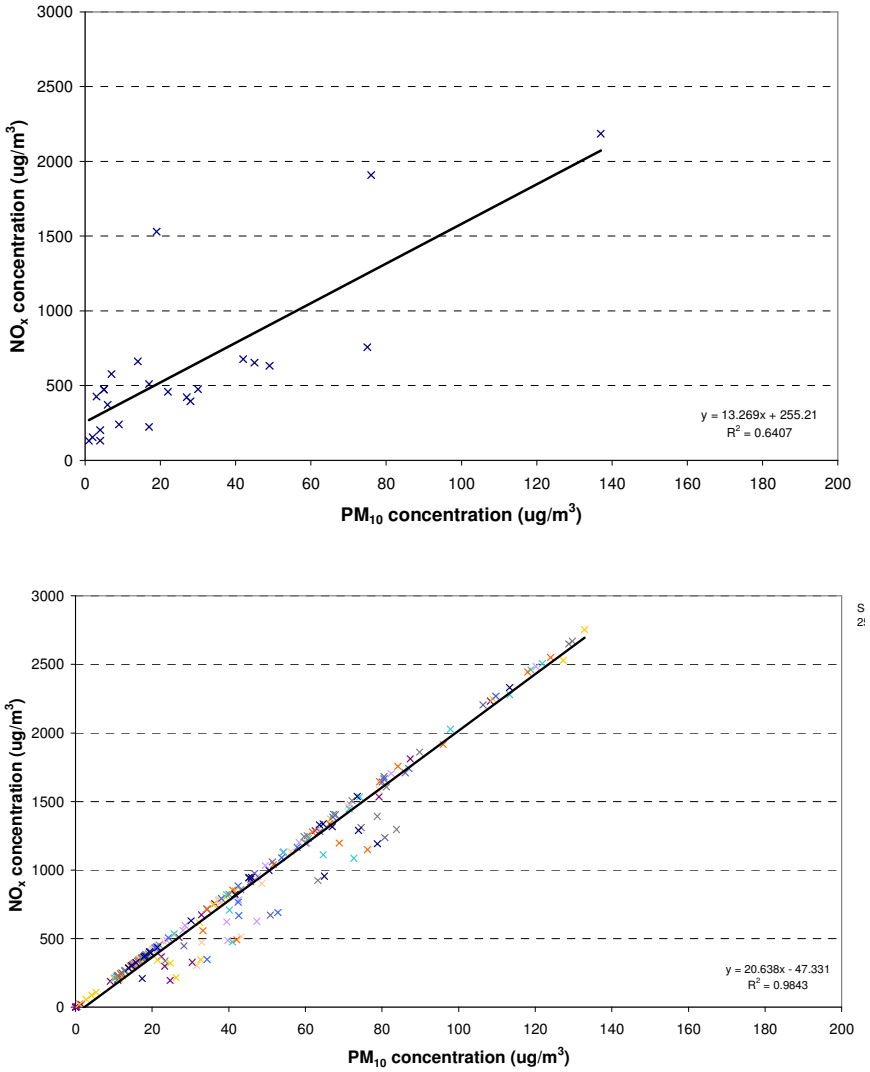

Figure 45. PM10 versus NO_x at Cape Town CBD for measured (top) and modelled (bottom) concentrations.

****

Chapter 3 described the modelling output from VISCREEN, PLUVUE II and CALPUFF. PLUVUE II modelled the visual impact of individual plumes from each source. CALPUFF addressed the spatial and temporal distribution of pollutants and the associated visibility over the Cape Town area.

CHAPTER 4 SUMMARY AND CONCLUSIONS

This chapter concludes the main findings of the research, indicating the ability of PLUVUE II and CALPUFF to model pollutant concentrations and visibility over Cape Town.

****

The main aim of this research was to determine the contribution of pollutants to visibility impairment of the brown haze through modelling of major atmospheric pollution sources. The following conclusions are based on five pollution sources that were identified in the City of Cape Town for modelling, namely, Cape Town Central Business District, Cape Town International Airport, Caltex Oil Refinery, Consol Glass and the townships of Khayelitsha and Mitchell's Plain. A non-brown haze day (13 August 2003) and a brown haze day (22 August 2003) were selected for modelling purposes. The screening model, VISCREEN and the plume visibility model, PLUVUE II are used to model the potential visual impact of emissions from sources. The CALPUFF Modelling System was employed to model the spatial and temporal distribution of NO_x, SO_2 and PM10 concentrations and the associated visibility impairment over the Cape Town area.

Initial screening analysis of plumes from Caltex and Consol Glass showed them to have visual impact indicating the need for a more detailed plume visual impact analysis. Modelling using PLUVUE II showed the two area sources of Cape Town CBD and Khayelitsha and Mitchell's Plain to be the significant contributors to visibility impairment over Cape Town. This is in agreement with CALPUFF which identified the Cape Town CBD as a major source of NO_x, SO_2 and PM10 emissions due to the large volumes of traffic that enter and leave the area. Visibility was generally poor over the CBD and immediate surrounding areas in the early morning. The townships of Khayelitsha and Mitchell's Plain were an important aerosol source with reduced visibility in the early morning due to the burning of wood for space heating and cooking purposes. The Caltex Oil Refinery was a significant source of SO_2 emissions as a result of the refining processes. Cape Town International Airport

and Consol Glass were not recognized to be major pollution sources and did not contribute to the reduced visibility experienced over Cape Town.

The influence of particulate and NO_x emissions to plume perceptibility and atmospheric colouration was undertaken using PLUVUE II. Sensitivity simulations with reduced NO_x and PM10 concentrations indicated that particulates are the dominant control on plume perceptibility. Nitrogen oxides result in a yellow-brown discolouration of the atmosphere.

The contribution of primary and secondary particles to the development of the brown haze was assessed by PLUVUE II. Modelled sulphate and nitrate conversion rates indicated that emissions of primary particles and not secondary particles are responsible for visibility impairment over the Cape Town region. However, these conversion rates were underestimated as the model does not accurately model the oxidation rates in an urban atmosphere and therefore slightly higher conversion rates can be expected.

The meteorological conditions necessary for the accumulation of pollutants in the atmosphere and subsequent formation of the brown haze was investigated. Wind roses for the non-haze day and haze day were drawn up and modelling was undertaken using CALPUFF. With the passage of a cold front over the Cape Town region, pollutant concentrations were reduced on the non-haze day compared to the haze day. Higher wind speeds were experienced on the non-haze day preventing the stagnation of pollutants. The frequent passage of cold fronts over the area brings rain and results in a cleansing of the atmosphere. On brown haze days, a prevailing dominant anticyclone promotes stable conditions and the formation of surface inversion during the night. Slower wind speeds promoted the accumulation of pollutants and the subsequent brown haze episode. On the haze day, CALPUFF identified the late evening and early morning periods (10 pm and 10 am) to have high pollutant concentrations and as a consequence, the greatest visibility degradation. This can be attributed to the prevailing night-time stable conditions and subsequent surface inversion formation. The highest NO_x, SO_2 and PM10 concentrations were observed between 7 am and 8 am which coincides with increased traffic volumes and human activity during this period. CALPUFF accurately modelled the morning peak in

pollutant concentrations as measured by the City of Cape Town. With surface heating during the morning, the inversion is eroded away so that accumulated pollutants are able to disperse into the atmosphere. After noon, afternoon concentrations are considerably lower and no visibility impairment is experienced. The False Bay and the Strand were shown to be important receptor regions of the pollutants particularly when northerly and north-westerly winds prevailed.

The VISCREEN model provides an initial screening analysis of the potential impact of emissions from a source at a specified receptor point. The PLUVUE II model can be used to model the visual impact of individual plumes from a source. The CALPUFF Modelling System is a useful tool for modelling the spatial distribution and transport of emissions from a number of sources on a regional scale. However, the ability to accurately model source contributions to pollutant concentrations and visibility impairment over the Cape Town region is strongly dependant upon the model input data, in particular, the emission rates for each pollutant. A detailed emissions inventory of the major sources around the City of Cape Town needs to be established so that future modelling can be undertaken accurately. Future modelling of the Cape Town region should include all source contributions to the pollutant levels in Cape Town.

****

REFERENCES

Airports Company South Africa (ACSA), 2004, <http://www.acsa.co.za> (10 August 2004).

Atkinson, B.W., 1981: *Meso-scale atmospheric circulations*, Academic Press, London.

Burr, M.L., 1997: Health effects of indoor combustion products, *Journal of the Royal Society of Health*, 117, 348 – 350.

Briggs, G.A., 1975: Plume rise predictions, *Lectures on air pollution and Environmental Impact Analysis*, American Meteorological Society, Boston, Massachusetts.

Caltex Oil Refinery, 2003, <http://www.caltex.co.za>, (8 January 2005).

Calvert, J.G and Stockwell, W.R., 1983: Acid generation in the troposphere by gas-phase chemistry, *Environmental Science and Technology*, 17: 430A.

Calvert, J.G., Lazrus, A., Kok, G.L., Heikes, B.G., Walega, J.G., Lind, J and Cantrell, C.A., 1985: Chemical mechanisms of acid generation in the troposphere, *Nature*, 317, 27 - 39.

Cass, G.R., 1981: Sulphate Air Quality Control Strategy Design, *Atmospheric Environment*, 15, 1227 - 1249.

Charlson, R.J., Waggoner, A.P and Thielke, J.F., 1978: Visibility protection for Class I areas: The Technical Basis, Report to Council of Environmental Quality, Washington, D.C.

City of Cape Town (CCT)., 2002: *State of the Environment Report for the City of Cape Town: Year Five 2002*, Cape Town.

City of Cape Town (CCT), 2005, < http://www.capetown.gov>, (21 February 2005).

Clean Air Act., 1990: 42 U.S.C § 7401 *et seq*, <http://www.epa.gov/oar/caa/>, (10 September 2005).

Comrie, A., 1988: *Growth, Structure and Prediction of the Thermal Internal Boundary Layer*, M.Sc. Thesis, Environmental and Geographical Science Department, University of Cape Town.

Consol Glass, 2004, <http://www.consol.co.za>, (19 February 2005).

Country Analysis Briefs, "South Africa: Environmental Issues", 2002 <http://www.eia.doe.gov/emeu/cabs/safrenv.html>, (24 March 2005).

De Wind, J., 2004: Personal communication, Consol Glass.

Department of Provincial and Local Government (DPLG), 2004, <http://www.dplg.gov>, (3 December 2004).

Derwent, R.G and Hertel, O., 1998: Transformation of air pollutants, In J. Fenger., O. Hertel and F. Palmgren (eds), *Urban air pollution – European Aspects*, Kluwer Academic Publishers, Environmental Pollution, Volume 1, 137 - 159.

Dewar, N., 2004: 'Stemming the tide': Revitalizing the Central Business District of Cape Town, *South African Geographical Journal*, 86, 91 - 103.

Diab, R.D., Jury, M.R., Combrink, J and Sokolic, F., 1996a: A comparison of anticyclone and trough influences on the vertical distribution of ozone and meteorological conditions during SAFARI-92, *Journal of Geophysical Research*, 101 (D19), 23 809 – 23 821.

Diab, R.D., Thompson, A.M., Zunckel, M., Coetzee, G.J.R., Combrink, J., Bodeker, G.E, Fishman, J., Sokolic, F., McNamara, D.P., Archer, C.B and Nganga, D., 1996b: Vertical ozone distribution *over southern Africa and adjacent oceans during SAFARI-92, Journal* of Geophysical Research, 101, D19, 23 823 – 23 833.

Dittenhoefer, A.C., 1984: *Evidence of aqueous phase oxidation in power plant plumes*, Proceedings of the 77th Annual meeting of APCA, San Francisco, 25 June 1984.

Dracoulides, D., 2002: Air quality impact assessment and monitoring plan for the Cape Town International Airport, prepared for ACSA, Cape Town.

Durban Metro, "Air Quality Guidelines", 1999 <http://www.ceroi.net/reports/durban/issues/air/guidelin.htm> (5 September 2003).

Dyantyi, R and Frater, W., 1998: Local Economic Development Initiatives in Khayelitsha, Unpublished report for the Isandla Institute, Cape Town.

Eatough, D.J., Caka, F.M and Farber, R.J., 1994: The conversion of SO_2 to sulphate in the atmosphere, *Israel Journal of Chemistry*, 34, 301 - 314.

Edgerton, S.A., Arriaga, J.L., Archuleta, J., Bian, X., Bossert, J.E., Chow, J.C., Coulter, R.L., Doran, J.C., Doskey, P.V., Elliot, S., Fast, J.D., Gaffney, J.S., Guzman, D., Hubbe, J.M., Lee, J.T., Malone, E.L., Marley, N.A., NcNair, L.A., Neff, W., Ortiz, E., Petty, R., Ruiz, M., Shaw, W.J., Gosa, G., Vega, E., Watson, J.G., Whiteman, C.D and Zhong, S., 1999: Particulate air pollution in Mexico City: A collaborative research project, *Journal of Air and Waste Management Association*, 49, 1221 – 1229.

Elsom, D., 1987: *Atmospheric pollution: Causes, effects and control policies*, Basil Blackwell Ltd, Oxford, United Kingdom.

Elsom, D., 1996: *Smog Alert: Managing urban air quality*, Earthscan Publications Ltd, London.

ENPAT (Environmental Potential Atlas), 2000: Department of Environmental Affairs and Tourism, University of Pretoria, GISBS.

FAA (Federal Aviation Administration), "Aviation and emissions, A Primer", Office of Energy and Environment, Washington, DC, 2005, <http://www.aee.faa.gov/emissions/>, (17 January 2005).

Fenger, J., 2002: Urban air quality, In J. Austin, P. Brimblecombe and W. Sturges (eds), *Air pollution science for the 21st century*, Elsevier, Oxford.

FLAG (Federal Land Managers' Air Quality Related Values Workgroup)., 2000: *Phase I report* , U.S Forest Service, National Park Service and U.S Fish and Wildlife Service.

Frampton, M.W., Morrow, P.E., Cox, C., Gibb, F.R., Speers, D.M and Utell, M.J., 1991: Effects of nitrogen dioxide exposure on pulmonary function and airway reactivity in normal humans, *American Review of Respiratory Disorders*, 143 (3), 522 - 527.

Gartrell, G., Jr. and Friedlander, S.K., 1975: Relating particulate pollution to sources: The 1972 California aerosol characterization study, *Atmospheric Environment*, 9, 279 - 299.

Gillani, N.V and Wilson, W.E., 1983: Gas-to-particle conversion of sulfur in power plant plumes – II. Observations of liquid-phase conversion, *Atmospheric Environment*, 17, 1739 – 1752.

Haas, P.J and Fabrick, A.J., 1981: The effects of NO_2-aerosol interaction on indices of perceived visibility impairment, *Atmospheric Environment*, 18, 10/11, 2171 - 2177.

Harrison, R.M. and R.E. van Grieken, 1998: *Atmospheric Aerosols*. John Wiley: Great Britain.

Hegg, D.A and Hobbs, P.V., 1982: Measurements of sulphate production in natural clouds, *Atmospheric Environment*, 16, 2663 - 2668.

Heisler, S.L, Friedlander, S.K and Husar, R.B., 1973: The relationship of smog aerosol size and chemical element distributions to source characteristics, *Atmospheric Environment*, 7, 633 - 649,

Hewitt, C.N., 2002: The atmospheric chemistry of sulphur and nitrogen, In J. Austin, E. Brimblecombe and W. Sturges (eds), *Air pollution science for the 21st Century*, Elsevier, Oxford,

Hidy, G.M *et al*., 1974: Characterization of aerosols in California (ACHEX), Science Center, Rockwell International, prepared under California Air Resources Board Contract No. 358.

Hidy, G.M and Friedlander, S.K., 1971: The nature of the Los Angeles aerosol, In H.M Eglund and W.T Berry (eds), *Proceedings of the Second International Clean Air Congress*, Academic Press, New York.

Husain, L., Dutkiewicz, V.A., Husain, M.M., Khwaja, H.A., Burkhard, E.G., Mehmood, G., Parekh, P.P., Canelli, E., 1991: Oxidation of SO_2 in summer clouds, *Journal of Geophysical Research*, 96, 18789 - 18805.

Husar, R.B., Patterson, D.E., Husar, J.D., Gillani, N.V and Wilson, W.E., 1978: Sulphur budget of a power plant plume, *Atmospheric Environment*, 12, 549 - 568.

Husar, R.B and White, W.H., 1976: On the colour of the Los Angeles smog, *Atmospheric Environment*, 10, 199 – 204.

IPCC, 2001: Climate Change 2001: The Scientific Basis, Contribution of Working Group I to the Third Assessment Report of the Intergovernmental Panel on Climate Change, J.T. Houghton, Y. Ding, D.J. Griggs, M. Noguer, P.J. van der Linden, D.K. Maskell, C.A. Johnson (eds), *The Climate System: An Overview*, Cambridge University Press, Cambridge, 288 - 348.

Isaksen, I., Hesstredt, A and Hov, O., 1978: A Chemical Model for Urban Plumes: Test for Ozone and Particulate Sulfur Formation in St. Louis Urban Plume, *Atmospheric. Environment,* 12, 599 - 604.

Islam, M.S and Ulmer, W.T., 1979: Threshold concentrations of SO_2 for patients with oversensitivity of the bronchial system, *Wissenschaft and Umwelt*, 1 (1), 41 - 47.

Jackson, S.P and Tyson, P.D., 1971: Aspects of weather and climate over Southern Africa, *Environmental Studies Occasional Paper No.6*, Department of Geography and Environmental Studies, University of Witwatersrand, Johannesburg.

Jury, M.R., 1987: Aircraft observations of meteorological conditions along the west coast of South Africa, 30-35°S, *Journal of Climate and Applied Meteorology,* 11, 1540 - 1552.

Jury, M.R and Spencer-Smith, G., 1988: Doppler Sounder Observations of Trade Winds and Sea Breezes along the African West Coast Near 34°S, 19°E, *Boundary Layer Meteorology*, 44, 373 – 405.

Jury, M., Tegen, A., Ngeleza, E and Du Toit, M., 1990: Winter air pollution episodes over Cape Town, *Boundary Layer Meteorology*, 53, 1 - 20.

Keen, C.S., 1979: Meteorological aspects of pollution transport over the southwestern Cape, Report to Cape Town Council, *Geography Department Technical Report 4*, University of Cape Town.

Klemm, O., Talbot, R.W., Klemm, K.I., 1992: Sulfur dioxide in coastal New England fog, *Atmospheric Environment,* 26A, 2063 - 2075.

Kumar, P and Mohan, D., 2002: Photochemical smog: mechanism, ill-effects, and control, *TERI Information Digest on Energy and Environment*, 1(3), 445 - 456.

Latimer, D.A., Bergstrom, R.W., Hayes, S.R., Lui, M.K., Seinfeld, J.H, Whitten, G.Z., Wojcik, M.A and Hillyer, M.J., 1978: *The Development of Mathematical Models for the Prediction of Anthropogenic Visibility Impairment*, EPA/450/4-78-110. U.S. Environmental Protection Agency, Research Triangle Park, N.C.

Latimer, D.A and Samuelsen, G.S., 1978: Visual impact of plumes from power plants: A theoretical model, *Atmospheric Environment*, 12, 1455 - 1465.

Levey, K.M., 1996: Interannual temperature variability and associated synoptic climatology at Cape Town, *International Journal of Climatology*, 16, 293 - 306.

Li, Y., Powers, T.E and Roth, H.D,. 1994: Random effects linear regression meta-analysis models with application to nitrogen dioxide health effects studies, *Journal of the Air and Waste Management Association*, 44 (3), 261 - 270.

Linde, H and Ravenscroft, G, "Air quality management in the City of Cape Town", 2002, City of Cape Town, <http://www.cemsa.org/contents%/%Cfullpapers/Air%20Quality%Management/G74-Linde.pdf> (7 April 2004)

Manahan, S.E., 1991: *Environmental Chemistry*, Lewis Publishers Inc, United States of America.

Malm, W.C., 1979: Visibility: A physical perspective, In D, Fox., R.J, Loomis., T.C Greene (technical co-ordinators), *Proceedings of the Workshop in Visibility Values*, Fort Collins, Colorado, U.S Department of Agriculture, 56 – 58.

Malm, W.C., 1999: *Introduction to visibility*, Cooperative Institute for Research in the Atmosphere, Colorado State University, Fort Collins, CO.

Maroni, M., Seifert, B., Lindvall, T., 1995: *Indoor air quality – a comprehensive reference book*, Elsevier, Amsterdam.

McKinley, G., Zuk, M., Höjer, M., Avalos, M., González, I., Iniestra, R., Laguna, I., Martínez, M., Osnaya, P., Reynales, L., Valdés, R and Martínez, J., 2005: Quantification of local and global benefits from air pollution control in Mexico City, *Environmental Science and Technology*, 39, 1954 – 1961.

McMurray, P.H and Wilson, J.C., 1983: Droplet phase (heterogenous) and gas phase (homogenous) contributions to secondary ambient aerosol formation as a function of relative humidity, *Journal of Geophysical Research*, 88C, 5101 - 5108.

Meagher, J.F, Bailey, E.M and Luria, M., 1983: The seasonal variations of the atmospheric SO_2 to $SO_4^{=}$ conversion rate, *Journal of Geophysical Research*, 88, 1525 – 1527.

Mert, J., 2004: Personal communication, Pentech University.

Miller, M.S., Friedlander, S.K and Hidy, G.M., 1972: A chemical element balance for the Pasadena aerosol, *Journal of Colloid and Interface Science,* 39, 165 – 176.

Miller D.F, 1978: Precursor effects of SO_2 oxidation, *Atmospheric Environment*, 12, 273 - 280.

Ministry for the Environment, "Good practice guide for monitoring and management of visibility in New Zealand", Wellington, New Zealand, 2002, <http://www.mfe.govt.nz>
(10 January 2005)

Monn, C., 2002: Exposure assessment of air pollutants: a review on spatial heterogeneity and indoor/outdoor/personal exposure to suspended particulate matter, nitrogen dioxide and ozone, In J. Austin, P. Brimblecombe and W. Sturges (eds), *Air Pollution Science for the 21st Century*, Elsevier, Oxford.

Muzondo, I.F., Barry, M., Dewar, D and Whittal, J., 2004: *Land conflict resolution: A case study of Khayelitsha settlement in Cape Town*, Cape Town, Presented at 'The Commons in an Age of Global Transition: Challenges, Risks and Opportunities', 10th Conference of the International Association for the Study of Common Property, Oaxaca, Mexico, August 9 – 13.

NAPAP (National Acid Precipitation Assessment Program)., 1990: Office of the Director, *Acid Deposition, State of Science and Technology*, Report 24, Visibility: Existing and Historical Conditions – Causes and Effects, Washington, DC.

Piketh, S.J., Otter, L.B., Burger, R.P., Walton, N., van Nierop, M.A., Bigala, T., Chiloane, K.E and Gwaze, P., 2004: Cape Town Brown Haze II Project – Final Report.

Piketh, S.J., Swap, R.J., Anderson, C.A., Freiman, M.T., Zunckel, M and Held, G., 1999: The Ben Macdhui high altitude trace gas and aerosol transport experiment, *South African Journal of Science*, 95, 35 – 43.

Pienaar, J.J and Helas, G., 1996: The kinetics of chemical processes affecting acidity in the atmosphere, *South African Journal of Science*, 92, 128 – 132.

Pitchford, M.L and Malm, W.C., 1994: Development and application of a standard visual index, *Atmospheric Environment*, 28, 1049 – 1054.

Postlethwait, E.M and Bidani, A., 1990: Reactive uptake governs the pulmonary air space removal of inhales nitrogen dioxide, *Journal of Applied Physiology*, 68 (2), 594 - 603.

Redding, S., Norden, C and VanAs, D., 1982: The relationship between synoptic scale airflow and local wind fields over Duynefontein, *Report PIN-629*, Atomic Energy Board, Pelindaba.

Samaras, Z and Sorensen, S.C., 1999: Mobile sources, In J. Fenger, O. Hertel and F. Palmgren (eds), *Urban air pollution – European aspects*, Kluwer Academic Publishers, Denmark.

Saxena, P and Seigneur, C., 1987: On the oxidation of SO_2 to sulphate in atmospheric aerosols, *Atmospheric Environment*, 21, 807 – 812.

Schwartz, S.E and Newman, L., 1983: Measurements of sulphate production in natural clouds, *Atmospheric Environment*, 17, 2629 - 2633.

Scire, J.S., Strimaitis, D.G and Yamartino, R.J., 2000: A User's Guide for the CALPUFF Dispersion Model, Earth Tech Inc, Concord, MA.

Scorgie, Y., 2003: Socio-Economic impact of air pollution reduction measures – Task 1: Definition of air pollutants, Airshed Planning Professionals (Pty) Ltd.

Seigneur, C., Bergstrom, R.W and Johnson, C.D., 1984: Measurements and simulations of the visual effects of particulate plumes, *Atmospheric Environment*, 18, 2231 - 2244.

Seigneur, C and Saxena, P., 1988: A theoretical investigation of sulphate formation in clouds, *Atmospheric Environment*, 22, 101 - 115.

Seinfeld, J.H and Pandis., S. N., 1998: *Atmospheric chemistry and physics: From air pollution to climate change*, John Wiley and Sons, Inc, United States of America.

Seinfeld, J.H., 1986: *Atmospheric Chemistry and Physics of Air Pollution*, John Wiley, New York.

Spengler, J.D., 1993: Nitrogen dioxide and respiratory illnesses in infants, *American Review of Respiratory Disorders*, 148 (5), 1258 – 1265.

Stedman, J.R., Espenhahn, S.E and Willis, P.G., 1998: *Air pollution forecasting in the United Kingdom: 1997*, Report AEA/20008001/008, Culham: AEA Technology, National Environmental Technology Centre.

Stevens, C.S., 1987: Ozone formation in the Greater Johannesburg Region, *Atmospheric Environment*, 21, 523 – 530.

Tyson, P.D., Preston-Whyte, R.A and Diab, R.D., 1977: Towards an inversion climatology of southern Africa: Part 1, Surface inversions, *The South African Geographical Journal*, 58 (2), 151 – 163.

Tyson, P.D., Kruger, F.J and Louw, C.W., 1988: *Atmospheric pollution and its implications in the Eastern Transvaal Highveld, South African National Scientific Programmes*, Report, 150, Foundation for Research and Development, Pretoria.

Tyson, P.D., Garstang, M and Swap, R., 1996: Large-Scale Recirculation of Air over Southern Africa, *Journal of Applied Meteorology*, 35, 2218 – 2234.

Tyson, P.D and Preston-Whyte, R.A., 2000: *The Weather and Atmosphere of Southern Africa*, Oxford University Press, Cape Town.

USEPA., 1979: Protecting Visibility, An EPA report to Congress, U.S. Environmental Protection Agency, Office of Air, Noise and Radiation, Office of Air Quality Planning and Standards, Research Triangle Park, N.C.

USEPA., 1992a: Tutorial package for the VISCREEN model, U.S. Environmental Protection Agency, Research Triangle Park, N.C.

USEPA., 1992b: User's Manual for the Plume Visibility Model (PLUVUE II) (Revised), EPA Publication No. EPA-454/B-92-008, Office of Air Quality Planning and Standards, U.S. Environmental Protection Agency, Research Triangle Park, N.C.

USEPA., 1995: *Compilation of air pollutant emission factors, AP-42, Fifth Edition Volume 1: Stationary point and area sources*, U.S Environmental Protection Agency, Research Triangle Park, N.C.

USEPA., 1998: Interagency Workgroup on Air Quality Modelling (IWAQM), Phase 2 summary report and recommendations for modelling long range transport impacts, EPA-454/R-98-019, U.S. Environmental Protection Agency, Research Triangle Park, N.C.

USEPA., 1999: Ozone and your health, EPA Publication No. EPA-452/F-99-003, Office of Air and Radiation, U.S Environmental Protection Agency, Washington, DC.

USEPA, 2005, <http://www.epa.gov>, (10 March 2005).

Van Niekerk, W., 2001: *Technical Background Document for the Development of a National Ambient Air Quality Standard for Sulphur Dioxide*, Department of Environmental Affairs and Tourism, Pretoria.

Vega, E., Reyes, E., Sánchez, G., Ortiz, E., Ruiz, M., Chow, J., Watson, J and Edgerton, S., 2002: Basic statistics of $PM_{2.5}$ and PM_{10} in the atmosphere of Mexico City, *The Science of the Total Environment*, 287, 167 – 176.

Wagner, D. M., Osmundson, M., Biggs, G and Twaroski, C.J, "Class 1 Areas Impacts Analyses for a Proposed Expansion of a Taconite Processing Facility in Northeast Minnestota", Barr Engineering Company, Minnesota, 2004, <www.barr.com/PDFs/Papers/Class_1_impacts/pdf> (8 March 2005)

Warneck, P., 1988: Chemistry of the Natural Atmosphere, International Geophysics Series, Volume 41, Academic Press, San Diego, CA.

Watson, J.G., Chow, J.C., Richards, L.W., Haase, D.L., McDade, C., Dietrich, D.L., Moon, D., Chinkin, L and Sloane, C., 1990: The 1989 - 1990 Phoenix Urban Haze Study, Volume 1: Program Plan, DRI Document No. 8931.1F, prepared for Arizona Department of Environmental Quality, Phoenix, AZ, by Desert Research Institute, Reno, NV.

Watson, J.G., Chow, J.C, Lurmann, F.W and Musarra, S.P., 1994: Ammonium nitrate, nitric acid and ammonium equilibrium in wintertime Phoenix, Arizona, *Journal of Air and Waste Management Association*, 44, 405 - 412.

White, W.H and Roberts, P.T., 1977: On the nature and origins of visibility-reducing aerosols in the Los Angeles air basin, *Atmospheric Environment*, 11, 803 - 812.

Wicking-Baird, M.C., de Villiers, M.G and Dutkiewicz R.K., 1997: *Cape Town Brown Haze Study*, Report No. Gen 182, Energy Research Institute, Cape Town.

Wilson, W.E., 1978: Sulphates in the atmosphere: A progress report on project MISTT, *Atmospheric Environment*, 12, 537 - 547.

Wilson, W.E., 1981: Sulphate formation in point source plumes: A review of recent field studies, *Atmospheric Environment*, 15, 2573 - 2581.

World Health Organization, WHO Air Quality Guidelines for Europe, 2nd edition, WHO Regional Office for Europe, 2000, Copenhagen, Denmark. (WHO Regional Publications, European Series, No 91).